Università degli Studi di Siena

SCUOLA DI DOTTORATO DI RICERCA IN SCIENZE POLARI

XX CICLO

EFFECTS OF ENERGETIC SOLAR PARTICLES ON OZONE AND MINOR ATMOSPHERIC COMPONENTS INSIDE THE POLAR REGIONS

Candidato: DAMIANI ALESSANDRO
CNR-IDAC – Area di Ricerca Roma - Tor Vergata

Tutore: Dott.ssa STORINI MARISA
INAF-IFSI – Area di Ricerca Roma - Tor Vergata

Co-tutore: Ing. RAFANELLI CLAUDIO
CNR-IDAC – Area di Ricerca Roma - Tor Vergata

Università degli Studi di Siena
SCUOLA DI DOTTORATO DI RICERCA IN SCIENZE POLARI
XX CICLO

Collegio dei docenti
Carlo Baroni
Riccardo Cattaneo-Vietti
Mariachiara Chiantore
Simonetta Corsolini
Silvano Focardi
Luigi Folco
Francesco M. Faranda
Roberto Frache
Francesco Francioni
Giovanna Giorgetti
Marcello Mellini
Rosaria Palmeri
Paolo Povero
Carlo Alberto Ricci (Coordinatore)
Giancarlo Spezie
Franco M. Talarico
Sergio Tucci
Patrizia Vigni

Data dell'esame finale
20 Dicembre 2007

Commissione giudicatrice
Prof. Giorgio Fiocco
Prof.ssa Patrizia Francia
Prof. Mario Parisi

Esperto
Prof. Sandro Fuzzi

Supplente
Prof. Carlo Alberto Ricci

Abstract

Solar activity influences the Earth's environment, in particular the atmospheric ozone, by the direct output of the e.m. radiation or through the variability of the incoming cosmic ray flux (solar and galactic particles). Especially energetic particles, arising from huge explosions on the Sun's surface, travel in the interplanetary medium and, if the circumstances were favorable, they could enter the terrestrial atmosphere (driven by the geomagnetic field lines of our planet) and reach the polar cap regions (geomagnetic latitude > 60°). There, they provide additional external energy and are able to produce ionizations, dissociations, dissociative ionizations and excitations phenomena by interacting with the minor constituents. The induced changes are not confined to the ion chemistry but also to the neutral components. In this way a rise of the concentration of HO_x and NO_x species and the triggering of catalytic cycles which lead to short (hours) and medium (days) term ozone destruction occur. Finally, also no-reactive reservoir species (e.g., HNO_3, HCl, HOCl) are involved in these processes and endure large variations.

The present thesis highlights the chemical variability of the middle atmosphere during and after some Solar Energetic Particle (SEP) events recorded during the current solar cycle. Special attention has been paid to the relationship between ozone and HO_x data (retrieved from the Microwave Limb Sounder of EOS AURA satellite) for four events referred to 2005. The HO_x data, recorded for the first time during the intense ionization caused by the SEP flux, have pointed out some features related to these phenomena not wholly captured by the current theoretical models. In addition, they have highlighted that the HO_x rise is able to destroy the so-called third ozone peak at the polar latitudes of the winter hemisphere and it occurs also during medium intensity events. Besides, the analyses of January 2005 SEP events have shown that the changes on the hydrogen species leaded to variability in the concentration and partitioning of chlorine family, not discernible in the summer hemisphere. Further, the use of data coming from the HALOE instrument, referred to SEP events occurred in July 2000 and April 2002, has in short confirmed past experimental results. Finally, the study of a little SEP event occurred during May 2003 has pointed out that SEP events are not the unique ionization source inside the polar latitudes during the winter.

Riassunto

L'attività solare influenza l'ambiente terrestre ed in particolare l'ozono atmosferico mediante la diretta emissione della radiazione elettromagnetica o attraverso variazioni indotte nel flusso dei raggi cosmici (particelle solari o galattiche). In particolare, le particelle energetiche, correlate alle grandi esplosioni che avvengono sulla superficie del sole, viaggiano nel mezzo interplanetario e, se le circostanze sono favorevoli (guidate dalle linee del campo geomagnetico del nostro pianeta) possono entrare nell'atmosfera terrestre delle regioni polari (latitudine geomagnetica > 60°). Qui non solo forniscono un'energia addizionale esterna ma anche interagiscono direttamente con i costituenti minoritari producendo fenomeni di ionizzazione, dissociazione, ionizzazione dissociativa ed eccitazioni. Questi cambiamenti non sono limitati solo alla chimica ionica ma anche a quella dei componenti neutri. Si verificano quindi incrementi nella concentrazione delle specie HO_x e NO_x e l'innesco di cicli catalitici che inducono a distruzioni di ozono a breve (ore) e medio (giorni) termine. Infine, anche componenti non reattivi (es. HNO_3, HCl, HOCl) sono coinvolti in questi processi e subiscono ingenti variazioni.

La presente tesi evidenzia la variabilità chimica dell'atmosfera media durante e dopo alcuni eventi di particelle solari energetiche (SEP) registrati nell'ultimo ciclo solare.

Speciale attenzione è stata posta sulla connessione tra dati di ozono e dati di HO_x (ricavati dallo strumento Microwave Limb Sounder del satellite EOS AURA) per quattro eventi avvenuti nel 2005. I dati di HO_x, registrati per la prima volta durante un'intensa ionizzazione causata dal flusso di particelle solari energetiche, hanno evidenziato caratteristiche connesse a questi fenomeni non del tutto descritte dai modelli teorici in uso. Inoltre, hanno mostrato che la distruzione del cosiddetto terzo picco di ozono alle latitudini polari dell'emisfero invernale dipende dall'incremento di HO_x ed accade anche durante eventi di media intensità.

Ulteriori analisi sugli eventi del Gennaio 2005 hanno indicato che variazioni nelle specie HO_x hanno indotto una variabilità, non evidenziabile nell'emisfero illuminato dal sole, nella concentrazione e nella partizione della famiglia dei cloruri.

L'ulteriore utilizzo di dati provenienti dallo strumento HALOE e riferiti ad eventi accaduti nel Luglio 2000 e Aprile 2002 ha in pratica confermato i precedenti risultati sperimentali. Infine lo studio di un piccolo evento SEP avvenuto nel Maggio 2003 ha evidenziato come questi eventi non siano l'unica sorgente di ionizzazione durante l'inverno all'interno delle latitudini polari.

EFFECTS OF ENERGETIC SOLAR PARTICLES ON OZONE AND MINOR ATMOSPHERIC COMPONENTS INSIDE THE POLAR REGIONS

CONTENTS

Acknowledgments

I would like to express my gratitude to my supervisors, Marisa Storini and Claudio Rafanelli, for their guidance over the years.

I thank the National Program of Antarctic Research to introduce me into the field of the polar research.

Finally I am deeply indebted to my family and my wife Mariko for their loving support and to my son Yuji for being born just now.

This work has been hosted by the Italian Institute of Atmospheric Sciences and Climate and by the Institute of Acoustics "O. M. Corbino" of the National Research Council and by the Institute for Interplanetary Space Physics of the National Institute of Astrophysics.

Publication list

I. Damiani A., P. Diego, M. Laurenza, M. Storini, C. Rafanelli, Search for the ozone variability related to SEP events occurring during the current solar cycle, Advances in Space Research, submitted, Ms. Ref. No.: C21-0038-06.

II. Rafanelli C., Damiani A., Benedetti E., Di Menno M., Anav A., Di Menno I., La concentrazione di O_3 e dei gas serra nell'atmosfera polare, Clima e cambiamenti climatici, ed. by CNR, 487-491, 2007.

III. Storini M., Damiani A., Effects of the January 2005 GLE/SEP Events on Minor Atmospheric Components, Proceedings of 30th ICRC, 2007.

IV. Damiani A., Storini M., Laurenza M., Rafanelli C., Solar Particles effects on minor components of the Polar atmosphere, Annales Geophysicae, 2007 (in press).

V. Damiani A., Benedetti E., Storini M. and Rafanelli C., Italian polar data center for capacity building associated with the IHY, Advances in Space Research, doi:10.1016/j.asr.2007.01.046, 2007.

VI. Damiani A., Storini M., Laurenza M., Rafanelli C., Piervitali E. and. Cordaro E.G, Southern ozone variations induced by solar particle events during 15 January–5 February 2005, Journal of Atmospheric and Solar-Terrestrial Physics, 68, 2042–2052, 2006.

VII. Piervitali E., Benedetti E., Damiani A., Rafanelli C., Di Menno I., Casu G., Malaspina F., Anav A., Di Menno M., Evaluation of environmental UV doses by empirical WL4UV model and multi-channel radiometer, Proceedings of SPIEE, 251-259, 2005.

The papers above are entirely reported in Appendix. Publications I, III, IV and VI hereinafter referred to as DAM-S, SD07, DAM07, DAM06 respectively.

Introduction

The importance of the ozone layer for the terrestrial life against the harmful UV radiation is known from many years; the ozone is also an important proxy for the evaluation of the environmental quality of our planet.

After the discovery of Farman et al. (1985) of a dramatic decrease of ozone concentration during Antarctic springs, the international research community increased the interest on the issue. The so–called “ozone hole” (see Solomon, 1999 for an extensive review) became the symbol of the human pollution on the Earth and the media has enormity increased the significance of this phenomenon, half natural and half man made. The first important consequence was the consciousness that human actions are really able to influence the global climate. The rise of the greenhouse gases and its human contribute are an incontrovertible datum. We can discuss on the effectiveness of these variations on the global change taking effect during the on-going time, but not about the existence of these abrupt changes induced by our behavior. Anyway the chemistry of the atmosphere depends not only on human activities. Different natural phenomena are able to change it: volcanic eruptions, El Niño and La Niña, solar cycle activity and so on. A careful evaluation of their influences on the atmosphere should be done in order to better understand the impact of the man made behavior. Among the natural phenomena, transient events of energetic particles coming from the Sun are able to produce/add ionization inside the Earth’s atmosphere and start catalytic cycles of ozone destruction involving NO_x and HO_x species. The intensity of the changes induced on the minor atmospheric components depends on different parameters related to the characteristic features of the incoming Solar Energetic Particles (SEPs) and to the dynamics of the middle atmosphere. The SEP impact on a well defined atmospheric layer is joined to particle energy, flux, fluence, etc. On the other hand, the life of NO_x and HO_x molecules depends on the solar illumination. The NO_x species are long lasting during the winter. If the polar vortex is particularly stable they can reach the lower atmosphere and contribute to reduce the O_3 concentration also for many months. The HO_x components develop its effects mainly on the mesospheric ozone till the end of the particles flux.

The influence of the SEP events on the atmospheric chemistry is an issue known from the seventeen (see Crutzen at al., 1975; Heath et al., 1977; McPeters et al., 1981 and references therein) but it became again matter of study in the last years. The reason is related to the increased number and quality of satellites instruments, which are monitoring the Earth’s atmosphere and are leading innovative analyses. The possibility to compare these phenomena with the available chemical models and

to better define the natural variability of the minor atmospheric components are the most important advantages taken from this kind of studies.

In conclusion, the main goals of the present work are to check the accuracy of the large part of the reactions which are dominant in the middle/upper stratosphere and the mesosphere by the careful evaluation of the short time SEPs effects on the minor atmospheric components and to quantify their influence on the polar atmospheric chemistry. For this reason some of the major SEPs of the current solar activity cycle have been investigated.

The thesis is divided into 6 chapters. Chapter 1 is devoted to a briefly description of the Sun-Earth system and SEPs. Chapter 2 shows the main features of the middle atmospheric ozone. Chapter 3 regards the ionosphere and the chemical variability induced by SEPs. The event analyses are reported in Chapter 4. Finally Chapter 5 and 6 give us the main attained results and conclusions.

Chapter 1

SUN-EARTH SYSTEM AND SOLAR ENERGETIC PARTICLE EVENTS

1.1 - The Sun-Earth system

The Sun-Earth system is characterized by the solar radiation emissions, i.e. the electromagnetic and the corpuscular radiations. The later is formed by plasma and suprathermal particles.

The solar plasma is called solar wind. It continuously evaporates from the corona, expands inside the heliosphere and is responsible of the planetary magnetosphere dynamics. The solar wind is organized in interplanetary macrostructures, traveling towards the outer solar system. The solar wind/Earth's magnetosphere coupling produces the geomagnetic storms (lasting few days) and substorms (few hours), both visible as auroras at elevated latitudes.

1.2 - The Sun and the SMF

The Sun is composed by hydrogen (75 %), helium (23 %) and heavier elements (2 %). The internal structure of the Sun can be drawn as a series of concentric layers. The core is the site where the nuclear reactions come up (as the pp1 chain regarding the transformation of hydrogen to helium). The produced energy goes outside the core by radiative and convective transfer processes. Particularly, in the radiative zone the temperatures are high enough to detach electrons from the atomic nuclei (ionized

gas) and the photons are able to diffuse towards the surface (very slow process). On the convective zone the atoms are still able to keep some of their electrons, therefore the gas is opaque to photons and the energy is transported by convection. The convective cells rise to the surface and produce the granulation of the photosphere, where the temperatures are similar to the ones of the black body (about 5770 K). Outward, the thin layer of rarefied gas with temperature of 10^5 K is called chromosphere. Beyond, a huge wrapping gas expanding millions of km and with temperatures between 1 and 2 millions of K exists (the corona).

The solar plasma or solar wind is mainly composed by ionized hydrogen and a very small quantity of He, C and O. Its density decreases as the inverse of the square of its distance from the Sun; at 1 A.U. the density is 10 cm^{-3}, the temperature is 10^5 K and the velocity is about 400 km/sec. These conditions are typical of the quiet solar wind (or low-speed solar wind) and the lines of the magnetic field of the sun are frozen in plasma having the shape of the Archimedean spiral.

The magnetic field of the sun, called Solar Magnetic Field (SMF), is roughly similar to a dipolar magnetic field. However, superimposed on this basic field, there exist complex series of local fields, varying in time. These fields are vertical to the photospheric surface and the convention of matter occurs only along the filed lines (there is not heat transfer among adjacent columns). In this way the cooling can occur only by the radiative transfer towards the outside. The complex field process makes the sunspots which are often associated to closed field lines in the photosphere.

The classic butterfly diagram shows that the regions involved by sunspots (active regions) are concentrated mainly between 40° N and 40° S during the solar cycles. Inside the active regions, the flares, the most striking phenomena connected to solar activity, occur. They are violent explosions releasing giant amount of energy and occur on the Sun's atmosphere. The flares take place in the chromosphere and solar corona, heating plasma to tens of millions of K and accelerating electrons, protons and heavier ions to near the speed of light, able to escape from the Sun and travel in the interplanetary medium. Associated with the flare phenomena, there is electromagnetic radiation production at all wavelengths, from long-wave radio to the shortest wavelength gamma rays.

The interplanetary medium is not a quiet region but it is dominated by the solar activity in time. Changes in the solar wind velocity are induced by temperature variations in the corona. If the ejected plasma has enough velocity, it can reach the previous plasma and push it, making up discontinuities in the interplanetary medium. The final result is the generation of the shock waves, followed by magnetic clouds.

This is the typical behavior of transient solar activity i.e., solar flares often associated with the Coronal Mass Ejections (CMEs).

The CMEs are large clouds composed by particles and frozen magnetic field (plasma) coming from the corona. They can interact with the terrestrial magnetic field and provoke geomagnetic storms. The CMEs take a couple of days to reach the Earth (it depends on its velocity, generally between 400 and 1200 km/h), so it is possible to avoid problems at satellites, communications and astronaut's health by a good space weather forecast.

The most dramatic solar flares can be also accompanied by the emission of energetic protons with energies till about 20 GeV. The solar flare occurrence is able to influence the terrestrial atmosphere because of the huge increase of solar radiation at short wavelengths (EUV and X ray) and the elevated flux of energetic particles. These charged particles can enter inside the geomagnetic field along its magnetic lines and penetrate into the ionosphere, where the added ionization triggers catalytic cycles involving nitrogen and hydrogen species.

1.3 - The Earth magnetic field

The Earth's magnetic field is similar to that of a bar magnet tilted 11 degrees from the spin axis of the Earth. It is attributed to a dynamo effect of circulating electric currents, but it is not constant in direction. Although the details of the dynamo effect are not known in detail, the rotation of the Earth plays a part in generating the currents, which are presumed to be the source of the magnetic field. In addition, the solar events influence the geomagnetic field, via transient and recurrent solar perturbations impinging the Earth and causing geomagnetic storms able to influence the composition, dynamic and temperature of the upper terrestrial atmosphere by means joule heating, auroral particles precipitation and ion drag.

The area of space, around the Earth, that is controlled by the Earth's magnetic field is called magnetosphere (see Cowley, 1998). Its structure is dominated by the solar wind that constricts it inside a region compressed toward the sun (the boundary of the magnetosphere is at about 10-12 terrestrial radii) and extended in the opposite side (hundred radii). The region toward the sun of the magnetosphere is called magnetopause and is in equilibrium between the magnetic pressure of Earth and the dynamic pressure of the solar wind.

The Interplanetary Magnetic Field (IMF) and the magnetosphere are aligned in the same direction (northward) and remain closed to one another. However when the IMF has a southward component the magnetic field lines are jointed and the magnetosphere becomes open. In this way it is possible to transfer the energy from

the solar wind to the magnetosphere.

The CMEs and the solar wind control the geomagnetic activity because their intensity and frequency is causing the variability of the terrestrial magnetosphere. Therefore, potentially they can influence the Earth's ionosphere under such circumstances.

The magnetosphere prevents the incoming of most of the particles carried in the solar wind, from hitting the Earth. Anyway, some particles from the solar wind or associated with flares can enter the magnetosphere. They enter from the magnetotail and travel toward the Earth until the polar caps where the low geomagnetic field intensity allows them to penetrate inward. The involved energetic particles are called cosmic rays.

1.4 - The Cosmic Rays

The Cosmic Rays (CR) [see Mursula and Usoskin, 2003 for an introduction] are not rays but particles. They are ionized atoms ranging from hydrogen to heavy metals.

Their sources are inside (like those coming from the Sun) or outside (e.g. supernovae) the solar system. The terrestrial atmosphere and the geomagnetic field shield the life on the Earth and prevent the excessive exposure to these particles. When an energetic particle enters the Earth's atmosphere hits the neutral molecules (mainly N_2 and O_2) and disintegrates into a shower of particles (the so-called cosmic ray shower). By detecting these secondary particles with ground-based cosmic ray detectors, the energy of the original cosmic ray can be reconstructed. Mainly, there are two different types of CRs:

- the Galactic Cosmic Rays (GCRs)
- the Solar Cosmic Rays (SCRs)

1.4.1 Galactic Cosmic Rays

The GCRs have their sources outside our solar system. They are for the most part composed by protons (90%), then alfa-particles and other elements. They are particles strongly accelerated so this acceleration snatches their electrons from the atoms and leaves only protons. The energetic spectrum of GCRs ranges from ~ 1 GeV (10^9 eV) to ~ 10^{21} eV. The flux is inversely related with the energy of particles, therefore the most energetic particles are detected only few times per years.

Particles with energy minor of ~ 150 GeV are subjected to the solar modulation processes. As pointed out by Forbush (1954), the intensity of GCRs varied synchronously with the 11-year cycle of solar activity and it is anti-correlated with the sunspots numbers. During the maximum solar activity the solar wind is stronger and

more effective to protect the Earth's atmosphere among the CR flux, whereas the behavior is opposite during the activity minimum. In addition, in a short paper by Forbush (1937), the relationship between the occurrence of magnetic storms and contemporary CR variability was highlighted; later on, the impulsive decreases of the CR intensity (few hours), after the geomagnetic sudden commencements, and the successive slow recovery were called "Forbush decreases".

1.4.2 Solar Cosmic Rays

The Solar Cosmic Rays (or Solar Energetic Particles) are associated to the huge particles emission of solar origin (see Reames, 1999 for a review). High energy particles were fist observed as a sudden increase in the intensity registered by ground level ion chambers during the event of February 1942 (Forbush, 1946). SCRs with relativistic energies also affect neutron monitor records and, in this case, they are called Ground Level Enhancements (GLEs) [see Storini et al., 2005]. Non relativistic solar particles are registred with balloons, satellites and spacecraft. Traditionally we define a proton enhancement as a SEP event when the proton flux at energies > 10 MeV is greater than 10 particle/($cm^2 \cdot s \cdot sr$). SCR events (with relativistic and non relativistic energies) last from minutes to few days.

Most solar flares associated with GLEs are located on the western sector of the Sun, where the IMF is well connected to the Earth. The geometry of the field line is quite variable, depending on the strength of the solar wind that varies considerably, but its average structure is well represented by the so called "garden hose" field line (see Fig. 1.1).

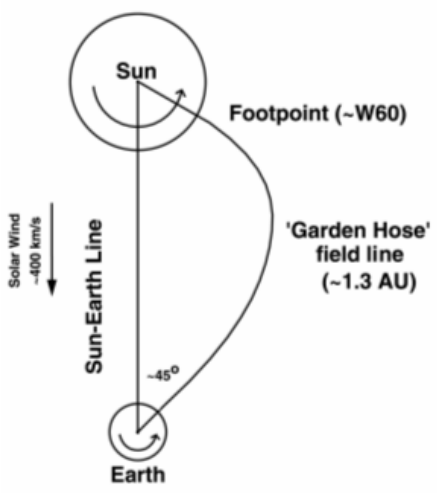

Fig. 1.1 - *Schematic representation of the "garden hose" field line connecting the Sun and the Earth. From Duldig et al., 2000.*

Solar Energetic Particles (SEPs) associated with flares located near to the

footpoint of the garden hose field line usually arrive promptly and have very sharp onsets. Conversely, SEPs associated with flares far from the garden hose field line are usually delayed in their arrival at Earth and have more gradual increases to the maximum intensity. On the other hand, it is very rare to observe GLEs associated with flares to the east of the central meridian of the Sun.

Anyway, the energy of SCR is well below the GCR energy and rarely can reach 5 GeV. In addition, the GCR flux is almost continuous whereas the SCR flux not. The CRs are charge particles, therefore they are driven by the geomagnetic field lines toward the polar cap regions where they can enter the Earth's atmosphere and interact with its chemical components. For this reason the best regions to record SEP events are the high latitudes, being elevated the geomagnetic cutoff rigidity of equatorial areas (Fig. 1.2).

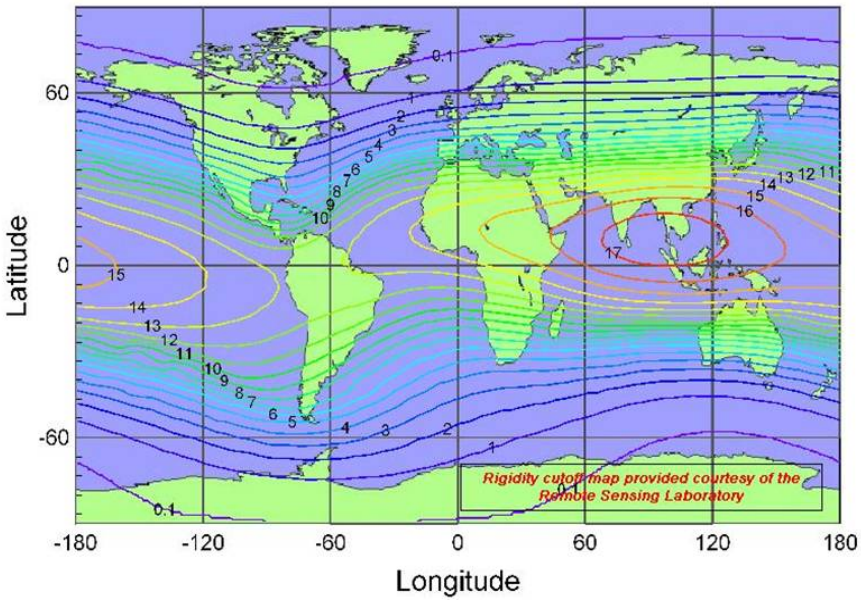

Fig. 1.2 – *Geomagnetic rigidity cutoff map.*

Different counters can recorder in different way the same event and sometime instruments located at low latitudes can absolutely lost its occurrence.

Traditionally it has been supposed that all SEP events originate from solar flares, but recently also the acceleration by CMEs, that involves bigger amount of coronal mass compared to flares, has been pointed out. In addition, their impulsive and gradual behavior can be recognized in the acquired data.

1.5 - Short history of the SEP-Ozone relationship

The proton flux coming from the Sun is able to produce ionization at different altitudes of the terrestrial environment and to start catalytic cycles of the ozone

depletion, involving NO_x (N, NO, NO_2) and HO_x (H, OH, HO_2) components (see Crutzen et al., 1975 and Solomon et al., 1981a).

Many past works have been devoted to investigate the effects of intense solar proton events on the terrestrial atmosphere (Krivolutsky, 2003 for a review). The main solar proton events of the last solar cycles have been investigated in detail: the November 1969 (Weeks at al., 1972; Solomon et al., 1981a) the August 1972 (Maeda and Heath, 1980; Reagan et al., 1981; Solomon et al., 1981b), July 1982 (Solomon et al., 1983), October 1989 (Reid et al., 1991; Jackman et al., 1995) and so on. In these works the atmospheric ozone depletion after the solar proton flux was explained and described by models and satellite data; whereas, the increase of odd nitrogen and hydrogen species during and after a SEP event was essentially studied by models.

On the other hand, almost all of the past instruments were not able to retrieve the ozone concentration without the solar light and that lacked of the possibility to check the goodness of the models on the night hemisphere.

Nevertheless, only during the last decade it was possible to check the chemical models involving other components with satellite data. During the solar proton event of July 2000 (see Krivolutsky et al., 2006 for a recent review) for the first time the contemporary availability of ozone and NO_x data, coming from different satellites, has shown the goodness of the employed models (Jackman et al., 2001).

Afterwards, when in late October 2003 a new intense SEP event occurred and an elevated number of new instruments were aboard satellites, novel and interesting features related to the influence of SEPs in the terrestrial atmosphere were pointed out (Jackman et al., 2005; Seppälä et al., 2004; Rohen et al., 2005; López-Puertas et al., 2005a; Verronen et al., 2005; Degenstein et al., 2005b; Fadel et al., 2006 and references therein). Moreover, by the new instruments the analyses were extended also to others retrieved chemical parameters, i.e. HNO_3, N_2O_5, $ClONO_2$, HOCl and ClO (López-Puertas et al., 2005b; Orsolini et al., 2005; von Clarmann et al., 2005). Until 2005 the principal lack of chemical data in the Earth's atmosphere, connected to SEP effects, was related to odd hydrogen species. Later on, different SEPs were observed during the 2005 i.e., 17 and 20 January, 15 May and 11 September.

Particularly, the study of January 2005 SEP events is very important since for the first time a satellite instrument was able to record the rise of HO_x during the proton flux that was hitting the Earth' atmosphere during 17 and 20 January. Verronen et al. (2006a) showed that the OH rise measured by MLS EOS instrument on the AURA satellite and the ozone depletion measured by Gomos instrument on the Envisat satellite, on 18 and 20 January at 69º-70º N at twilight condition, are in good

agreement with the models. In addition, a work by DAM-S, highlights that MLS OH values, averaged at 81° N and 0.1 hPa (~64 km) with the same solar zenith angle (SZA) to avoid the daily variability (LST: 7.67 hr/SZA: ~ 108°), increase of hundreds % on 18 January (less on 20 January), but the same outstanding rise does not appear in the equivalent location of the southern hemisphere. The reason of this behavior is based on the concentration of OH in the mesosphere. On the night hemisphere the weak background concentration of HO_x makes easier to point out the abrupt rise due to solar proton flux. Instead on the day hemisphere the high background of odd hydrogens hides the expected increase from the solar proton flux.

The SEP events occurred in 2005 constitute a unique opportunity to verify the effects of HO_x catalytic cycles on the ozone in different seasons by the same instrument.

1.6 - Analyzed SEP events

The main goal of the present work is to quantify the influence of the SEP events on the polar atmospheric chemistry. For this reason some of the major SEPs of the current Solar Cycle have been investigated. Figure 1.3 shows the monthly values of Sunspots number during Solar Cycle 23. The maximum solar activity is between 2000 and 2002.

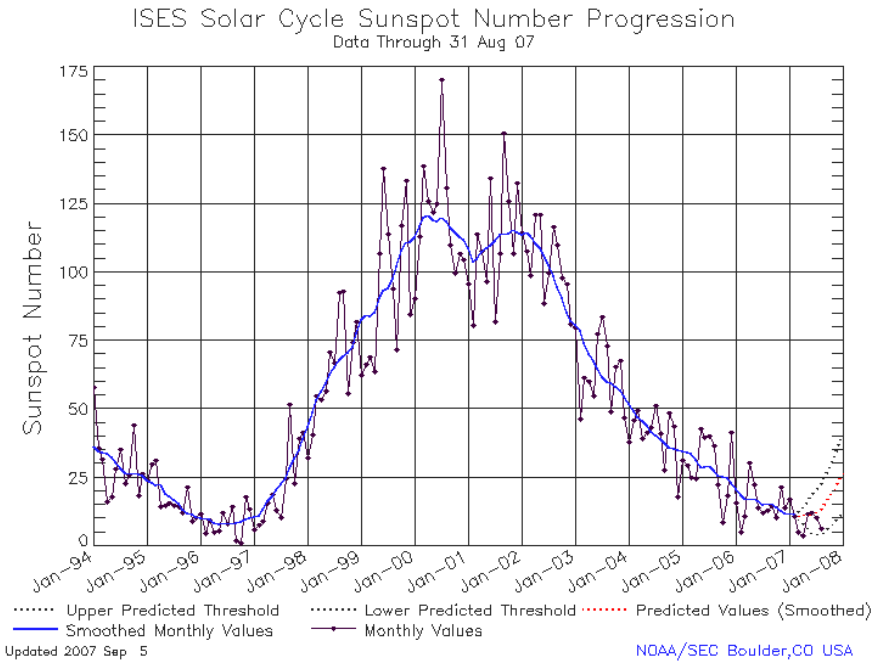

Fig. 1.3 - *Monthly values of Solar Cycle 23 Sunspots number (from NOAA/SEC Boulder).*

The maximum solar activity coincides with the maximum frequency of SEPs, even if strong events are present also during the lower phase. Table 1.1 reports the list of the largest 12 SEP events [the last one (May 2003) is negligible but it is inserted to investigate the cause of elevate NO_x values recorded in June-July 2003], documented by records of several experiments, during the last solar cycle. The Table shows the rank number (first column), the start date (second column), the time of maximum (third column), the maximum flux on 5 min. data average (fourth column) and the GLE number (fifth column), when observed by the neutron monitor network (see the present GLE list in the Appendix).

Table 1.1 – *Rank list for large SEP events (E > 10 MeV; $F_p \geq 10$ pfu) during solar cycle 23. The SEP events analyzed in this thesis are marked in yellow.*

RANK N°	Start (Year/Day/UT)	Maximum (Day/UT)	F_p (> 10 MeV) (part.cm^{-2}.s^{-1}.sr^{-1})	GLE N°
1	2001/Nov. 04/17:05	Nov. 06/02:15	31700	62
2*	2003/Oct. 28/12:15	Oct. 29/06:15	29500	65 + 66
3	2000/Jul. 14/10:45	Jul. 15/12:30	24000	59
4	2001/Nov. 22/23:20	Nov. 24/05:55	18900	
5	2000/Nov. 08/23:50	Nov. 09/16:00	14800	
6	2001/Sep. 24/12:15	Sep. 25/22:35	12900	
7*	2005/Jan. 16/ 02:10	Jan. 17/17:50	5040	68 + 69
8	2005/May 14/05:25	May 15/02:40	3140	
9	2002/Apr. 21/02:25	Apr. 21/23:20	2520	
10	2001/Oct. 01/11:45	Oct. 02/08:10	2360	
11*	2006/Dec. 06/15:55	Dec. 07/19:30	1980	70
12	2005/Sep. 08/02:15	Sep. 11/04:30	1880	
	2003/May 28/23:35	*May 29/15:30*	*121*	

**: A series of intense energetic solar eruptions were at the origin of outstanding particle storms propagating in the interplanetary medium for several days.*

The penetration depth and the ion production rate are function of the proton energies. Protons with energies of about 1 MeV reach the mesopause, 10 MeV protons reach about 65 km, and protons with 100 MeV get down to about 30–35 km (Reid, 1986).

In addition, a description of the most powerful SEP events recorded in 2005 (e.g., January, May and September) is given in the Soft X-ray measurements (1-8 Å) and proton flux data at energies >10 MeV, >50 MeV, >100 MeV from the GOES satellite series, available at the web site http://www.ngdc.noaa.gov/stp/GOES/goes.html. As mentioned above, in order to define a proton enhancement as a SEP event, the

proton flux at energies >10 MeV must be greater than the standard NOAA threshold of 10 pfu [1pfu=particle/(cm^2 s sr)]. Nevertheless, in this work this condition must be satisfied for at least one hour (see Laurenza et al., 2007). Table 1.2 summarizes key properties of the selected SEP events, which, for convenience, are referred to by number as events 1 to 4: date and time of the SEP maximum intensity, the peak flux value and fluence (both computed on hourly basis) for all the energy channels and the total duration, i.e. the time interval (Δ) between the onset time of the SEP event and its end.

Table 1.2 - *Characteristic parameters for the considered SEP events. See the text for details [from DAM07].*

SEP event							Associated flare			
Label	Date	Time [UT]	Energy [MeV]	Peak flux pfu	Fluence [part./(cm^2 sr×3600)]	Δ [d]	Date	Time [UT]	X-ray class	Hα location
1	17 Jan 2005	17:30	>10 >50 >100	4.13×10^3 3.33×10^2 2.59×10^1	5.61×10^4 3.98×10^3 2.99×10^2	2.76	17 Jan	09:52	X 4.2	N14W24
2	20 Jan 2005	08:30	>10 >50 >100	1.42×10^3 9.39×10^2 4.89×10^2	1.72×10^4 5.05×10^3 1.88×10^3	2.45	20 Jan	07:00	X 7.9	N12W58
3	15 May 2005	03:30	>10 >50 >100	1.90×10^3 0.58×10^0 0.14×10^0	7.98×10^3 1.07×10 2.11×10^0	1.05	13 May	16:57	M8.5	N12E12
4	11 Sep 2005	04:30	>10 >50 >100	1.88×10^3 5.10×10^1 7.63×10^0	4.57×10^4 2.09×10^3 3.52×10^2	4.81	7 Sep	17:40	X 17	S06E89

The maximum proton intensity and fluence were obtained from hourly averages of 5-min raw data. We considered as the start of a SEP event the first of 3 consecutive 5 minutes data points with fluxes $\geq$ 10 pfu. The end of an event is the last time the flux was $\geq$10 pfu if no new injections follow the event; otherwise, the end of the previous event is set at the point preceding the successive increase. Table 1.2 also includes the characteristics of each SEP associated flare, taken from the data base described by Laurenza et al. (2007).

The considered SEP events present very different characteristics between each other. SEP 1 has the highest flux and fluence at 10 MeV, although it has a shorter duration than the longest one, namely SEP 4 (2.76 d and 4.81 d, respectively). Moreover, it has a minor content of very high energies relative to SEP 2 that turned to be a GLE, where the rise of the three different energy ranges is also simultaneous. Finally, SEP 3 has the shortest duration (1.05 d) and smallest fluence at all energies.

The analyzed SEP events of this work are: July 2000, April 2002, May 2003, January 2005, May 2005, September 2005 and December 2006 (see Tab. 1.1). They have induced changes on the concentration of the minor atmospheric species (e.g.,

O_x, NO_x and HO_x) at terrestrial polar latitudes. The next chapter is devoted to point out the main features of the ozone which is the most important involved component and its relationship with the other species.

Chapter 2

THE MIDDLE ATMOSPHERIC OZONE

2.1 - Some features of the atmospheric ozone

As recalled in the introduction, the ozone is probably the most important minor component of the terrestrial atmosphere, at least the most famous after the discovery of the ozone hole.

We should separate the harmful tropospheric ozone from the beneficial stratospheric one. In troposphere the production of ozone happens by photolytic reaction in the UV band of polluting component due to human activities (i.e. car, heating of buildings, industries emission and so on). On the contrary, in the upper part of atmosphere, has natural origin and its primary importance is related to the absorption of bad UV of solar radiation, 200 – 320 nm (2000-3200 Å). This band produces damages into DNA chain of the cells.

The maximum ozone concentration is in stratosphere. In the tropical regions it forms a thin layer that becomes larger toward the Poles. The ozone column density [or Total Ozone Content (TOC)] is measured by the Dobson Unit [DU, in honor of prof. G.M.B. Dobson, one of the first scientists to investigate atmospheric ozone (~1920 - 1960)] and it is the thickness that the ozone column would occupy at standard temperature and pressure (T =273.2 K, P = 1 atm): 1 DU = 10^{-3} atm·cm = $2.69 \cdot 10^{16}$ molecules cm^{-2}.

The total ozone varies with season and latitude. Fig. 2.1 reports the mean annual cycle of ozone, as derived from data recorded by TOMS instrument, between November 1978 and May 1993. Even if the ozone is mainly produced in the tropical regions, the highest concentrations are in the midlatitude areas. The global circulation moves the tropical air masses pole ward and downward accumulating O_3 near the poles.

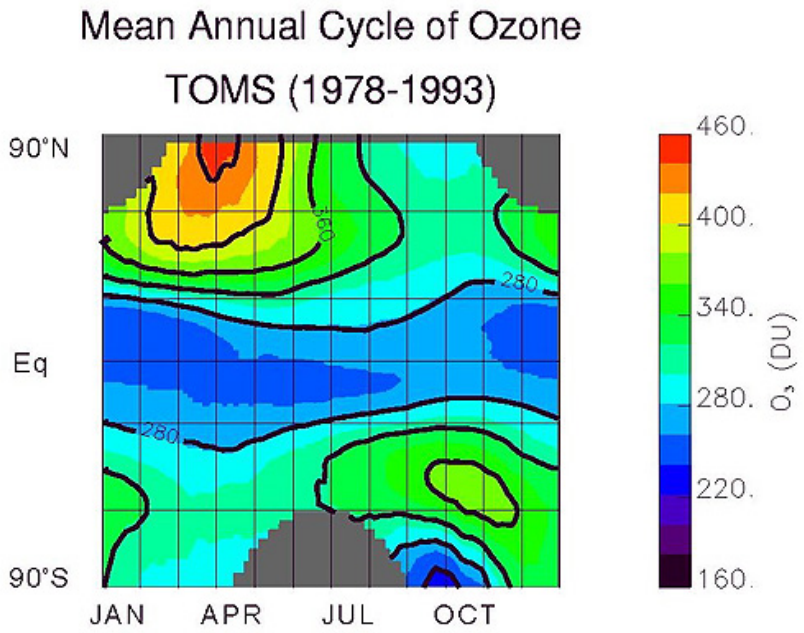

Fig. 2.1 - *Average amount of column ozone at a given latitude band as a function of time (from TOMS measurements).*

The ozone average in the Tropic is about 260 DU, even if there are large fluctuations related to the Solar Cycle, QBOs, volcanic eruptions and weather systems.

The vertical distribution of the ozone has its maximum between 20-30 km, where the ozone layer is most consistent but it depends on the measure unit adopted. Normally, it is used the “number density” (it refers to the absolute ozone concentration, i.e. the number of ozone molecules per cubic centimeter), the “partial pressure” (refers to the fraction of the atmospheric pressure at a given altitude for which ozone is responsible) and the “volume mixing ratio” (in ppmv, related to the fractional concentration of ozone which is the number of ozone molecules per million air molecules) to measure the ozone profile. The first two units are very similar and the ozone profile has its maximum between 20 and 30 Km. A slight variation is present if we utilize the volume mixing ratio since the number of molecules are distributed with the altitude in a different way and they decrease with the increase of altitude. If we utilize the ppmv for ozone the maximum concentration is slightly up, around 30-40 km (see Fig. 2.2).

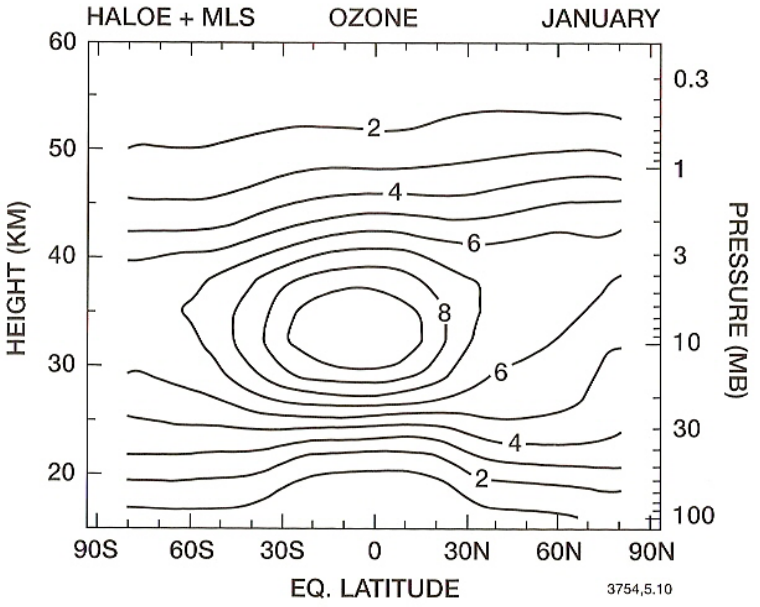

Fig. 2.2 – *Zonally averaged ozone mixing ratio (ppmv) in the stratosphere in January. Climatological values derived from HALOE and MLS instruments. From W. Randel, NCAR.*

Normally we use number density for the troposphere-stratosphere and ppmv for the upper atmosphere. Since this work is principally devoted to ozone variability at elevated altitudes we will adopt the ppmv notation if not indicated.

2.2 - The Chapman Model of pure oxygen atmosphere

The ozone concentration in the stratosphere depends on its production, loss and transport. The mean life of an O_3 molecule is very short (few minutes) in the high stratosphere and longer in the lower one (until 1 year). This different behavior induces the dominance of the chemical process in the high stratosphere and the transport in the lower one.

As pointed out by Chapman (1930) in a steady state system, where the produced ozone is equal to the destroyed ozone, the principal laws governing the process are:

$$O + O + M \rightarrow O_2 + M \quad (2.1)$$

$$O + O_2 + M \rightarrow O_3 + M \quad (2.2)$$

$$O + O_3 \rightarrow 2O_2 \quad (2.3)$$

$$O_3 + h\nu\ (2300\ \text{Å} < \lambda < 2900\ \text{Å, Hartley Band}) \rightarrow O_2 + O \quad (2.4)$$

$$2O_3 \rightarrow 3O_2 \quad (2.5)$$

$$O_2 + h\nu\ (1300\ \text{Å} < \lambda < 1800\ \text{Å}) \rightarrow O + O \quad (2.6)$$

Therefore a simple oxygen model can describe the ozone budget in the upper stratosphere. The O_3 molecule is created by Reaction (2.2) that works only with the

presence of a third body (needed for the energy balance of the reaction) and is mainly destroyed by Reaction (2.4) where the UV photolysis in the Hartley Band (2300-2900 Å) splits the O_3 in molecular and atomic oxygen. As the O atoms have short lifetime (less than 1 second in the stratosphere), they quickly reform ozone after dissociation, converting the energy of the photons at these wavelengths into the thermal energy (the thermal energy is the energy which is given to the third body). In addition it is important to point out that more energy is needed to dissociate the O_2 molecule in Reaction (2.6) [slow reaction] by UV photolysis in the 1300-1800 Å range since photon energy is $E = hc/\lambda$. Finally, we know today that it is possible to neglect the Reaction (2.5). Chapman estimates are too much high in the tropics, and too low in the Polar Regions.

There are two other mechanisms at work in addition to the Chapman cycle that reduces the equilibrium in the amount of ozone. First, reactions of O_X with other trace gases (containing chlorine, bromine, nitrogen, and hydrogen) alter the ozone budget. Second, the Brewer-Dobson (BD) Circulation transports ozone from its tropical source region into the extra-tropical areas.

Since the bonds between atoms in molecules have varying strengths, it takes different amounts of energy to break them down. The bond between the two oxygen atoms in an oxygen molecule (O_2) is really strong and can be broken down if the molecule absorbs the very high energy UV-C radiation. The bonds between the oxygen atoms in ozone are a bit weaker and can be broken down by absorption of the slightly less energetic UV-B radiation. Absorption of this highly energetic and short-wavelength radiation by O_2 and O_3 in the upper atmosphere prevents it reaching the troposphere and destroying O_2 and O_3. Less energetic radiation (with longer wavelengths) reaches the surface of the Earth (see Fig. 2.3).

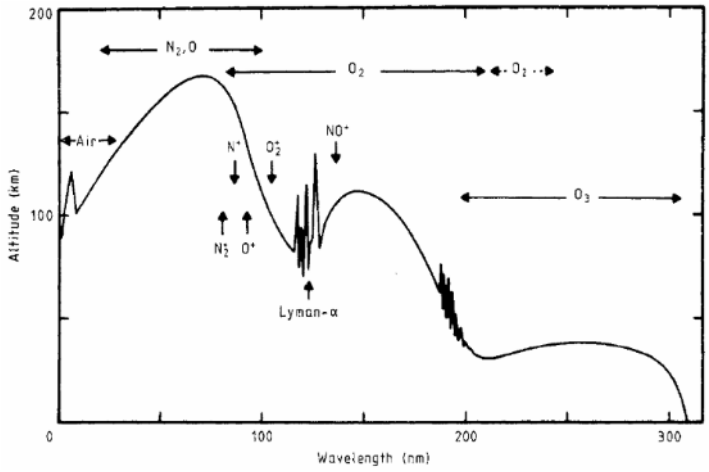

Fig. 2.3 - *Altitudes for attenuation of solar radiation to (l/e) of its initial intensity. Dominant absorbing species are given. From Brasseur and Solomon (1984).*

2.3 - Catalytic cycles of ozone destruction

The catalytic cycles of ozone destruction in the stratosphere (Fig. 2.4) have been extensively investigated in the past years by many authors (see Thrush, 1988 for a review) and the modeled profile of the ozone concentration has been remarkably improved if compared with the pure oxygen chemistry of Chapman.

These processes are most simply regarded as catalytic cycles in which a species X converts $O + O_3$, into $O_2 + O_2$ without being destroyed, and have a general form:

$$X + O_3 \rightarrow XO + O_2$$
$$XO + O \rightarrow X + O_2$$
$$\text{Net: } O_3 + O \rightarrow O_2 + O_2 \qquad (2.7)$$

However, the dominant stratospheric cycles involve only X = NO, H, HO and Cl (see Crutzen, 1971). The abundances of other potential X species in the stratosphere are either insufficient to play a significant role or they form stable molecules from which active species are not readily regenerated. Although it is convenient to discuss the ozone destruction cycles separately, it need to remind that they are linked chemically among them (see Wayne, 2000, pp. 164-174).

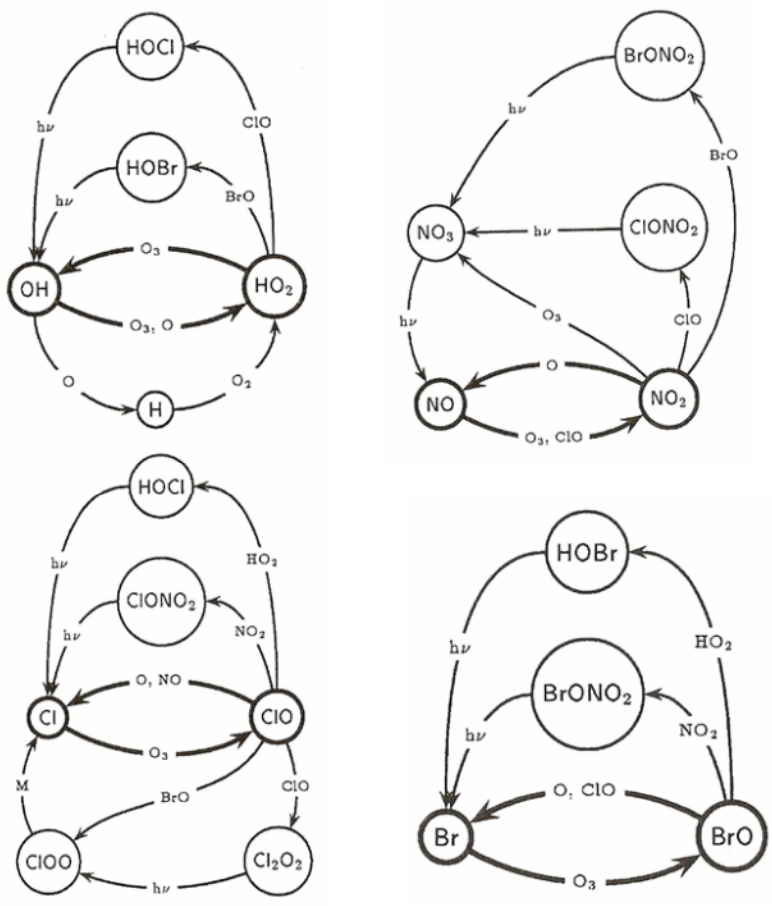

Fig. 2.4 - *Main catalytic cycles of O_x destruction. Adapted from Lary, 1997.*

2.3.1 The HO_x catalytic cycles

The importance of HO_x (H, OH, HO_2) atmospheric catalytic cycles was first recognized by Bates and Nicolet (1950). The main gas sources of HO_x active species are the water vapor and the methane which are very copious in the troposphere. The water vapor (H_2O) and the methane (CH_4) enter the stratosphere through the cold tropical tropopause. Methane is able to pass easily in stratosphere and goes up to the mesosphere, where it is oxidized and transformed in H_2O. The water vapor has a very high concentration in the troposphere but enters the stratosphere very slowly. In fact the lower stratosphere is generally dry. At elevated altitudes its concentration increases thanks to methane dissociation and the concentration of the two gases are in inverse relation to themselves (high methane concentration and low water vapor in lower atmosphere, *viceversa* in the upper atmosphere).

Above about 30 km the methane transforms in water vapor by two different paths.

By hydroxyl radical (OH) oxidation:

$$CH_4 + OH \rightarrow CH_3 + H_2O \qquad (2.8)$$

by reaction with $O(^1D)$ atoms coming from the photolysis of ozone at wavelengths shorter than 325 nm:

$$CH_4 + O(^1D) \rightarrow CH_3 + OH \qquad (2.9)$$

$$CH_3 + O_2 + M \rightarrow CH_3O_2 + M \qquad (2.10)$$

$$CH_3O_2 + NO \rightarrow CH_3O + NO_2 \qquad (2.11)$$

$$CH_3O + O_2 \rightarrow HCHO + HO_2 \qquad (2.12)$$

$$HCHO + HO \rightarrow CHO + H_2O \qquad (2.13)$$

Above 65 km the methane is photolysed.

The water vapor produces hydrogen species by (see Crutzen, 1997):

$$H_2O + O(^1D) \rightarrow 2OH \text{ (below 70 km)} \qquad (2.14)$$

$$H_2O + hf \ (\lambda = 121.6 \text{ nm, Lyman } \alpha \text{ radiation}) \rightarrow OH + H \text{ (above 70 km)} \qquad (2.15)$$

The importance of the HO_x catalytic cycle of ozone destruction is primary in the mesosphere and smaller in stratosphere. The main HO_x cycles are (see Lary, 1997):

$$HO + O_3 \rightarrow HO_2 + O_2$$

$$HO_2 + O_3 \rightarrow HO + O_2 + O_2$$

$$\text{Net: } 2O_3 \rightarrow 3O_2 \text{ (in the lower stratosphere)} \qquad (2.16)$$

$$HO + O_3 \rightarrow HO_2 + O_2$$

$$HO_2 + O \rightarrow HO + O_2$$

$$\text{Net: } O + O_3 \rightarrow 2O_2 \text{ (in the middle stratosphere)} \qquad (2.17)$$

$$H + O_2 + M \rightarrow HO_2 + M$$
$$HO_2 + O \rightarrow OH + O_2$$
$$OH + O \rightarrow H + O_2$$
$$\text{Net: } O + O \rightarrow O_2 \text{ (in the upper stratosphere)} \qquad (2.18)$$

The catalytic cycle (2.18) has the main chain effectiveness (the chain length of the cycle multiplied for the effective amount of the involved catalytic radical) of 10*9 molecules cm^{-3} s^{-1} between 50 and 70 km (see Lary, 1997).

The cycle (2.16) may be very important during the night since it does not involve the oxygen atom. In fact, since without solar illumination almost all O_x (O_3 + O) are constituted by O_3 (there are only few O molecules), it can lead catalytic cycle also during the winter season at polar latitudes.

The catalytic cycles are active until the HO_x species are lost by a different pathway which destroys them. For exemple chemical reactions are able to transforme the hydrogen molecules from active to inactive reservoir species e.g., H_2O, HNO_3, HNO_4 and also *cannibalistic* reactions contribute to destroy the odd hydrogens.

In addition, in the lower stratosphere the HO_x can partecipate to other catalytic cycles involving chlorine and bromine species.

Finally, it is important to recall that HO_x life is very short (few houres) in the stratosphere and mesosphere (roughly below 80 km) since they are easily photolized.

2.3.2 The NO_x catalytic cycles

The tropospheric nitrous oxide (N_2O) is the main source (90%) of stratospheric NO_x (NO, NO_2). It is completely inert in the lower atmosphere and it is slowly transported upwards through the tropical tropopause by the lifting of the BD circulation. In the stratosphere the 95 % of N_2O is lost by photolysis process (Thrush, 1988) to form N_2. The remainder leads to active nitrogen species formation:

$$N_2O + O(^1D) \rightarrow 2NO \qquad (2.19)$$

Other sources are the CR flux in the lower stratosphere (Nicolet, 1975), the ionization processes in the ionosphere and the occurrence of SPE events.

In the lower stratosphere the CR flux constitutes an important source of nitric oxide (NO) molecules by the ionization and dissociation of molecular nitrogen (N_2). At Polar Region during the winter time, when the lack of sun light prevents the formation of NO via reaction of nitrous oxide with atomic oxygen, the CR flux can become the main source of nitric oxide (Nicolet, 1975).

Different works (Vitt and Jackman, 1996; Jackman et al., 1999) examined the sources of NO_y (N, NO, NO_2, NO_3, N_2O_5, HNO_3, HO_2NO_2, $ClONO_2$, $BrONO_2$) constituents at high latitudes. They pointed out as the main source at latitudes > 50° N

is the horizontal transport of NO_y, primarly as result of oxidation of N_2O at lower latitude (about an order off magnitude than any other sources). Then, there is the "*in situ*" oxidation, the GCRs and finally the NO_y production by SPEs. Only in two time periods the SPE production is comparable with "in situ" production between 1965 and 1995 (see Fig. 2.5).

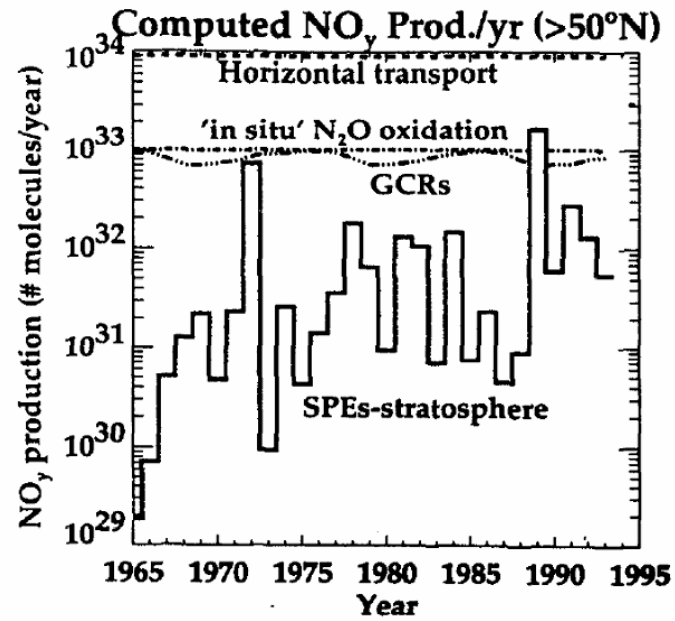

Fig. 2.5 - *Total number of NO, molecules produced per year in the northern polar stratosphere (>5O°N) by SPEs (histogram), GCRs (dash-dot-dot-dot line), 'in situ' oxidation of N_2O (dash-dot line), and horizontal transport of NO, from lower latitudes into this region (dashed line). From Jackman et al. (1999).*

The NO_x catalytic cycle of ozone destruction has the following pathway:

$$NO + O_3 \rightarrow NO_2 + O_2$$
$$NO_2 + O \rightarrow NO + O_2$$
$$\text{Net: } O + O3 \rightarrow 2O_2 \qquad (2.20)$$

The catalytic cycle IV has the main chain effectiveness elevated throughout the stratosphere and a peak of greater then 10*9 molecules cm^{-3} s^{-1} at 45 km (see Lary, 1997).

The main loss process for stratospheric nitrogen oxides is the formation of nitric acid (HNO_3) by:

$$NO_2 + OH + M \rightarrow HNO_3 + M \qquad (2.21)$$

Other loss processes lead to formation of HNO_4 and N_2O_5 reservoir gas. Particularly, the reaction of creation of nitric pentoxide (N_2O_5) i.e.,

$$NO_2 + NO_3 + M \rightarrow N_2O_5 + M \qquad (2.22)$$

which is particularly active during the night, leads to different concentration of stratospheric NO_x ($NO + NO_2$) in night and day with $NO_{x\ (day)} > NO_{x\ (night)}$. For this

reason it need actention when solar occulatation NO_x data (e.g., coming from HALOE instrument) retrievied at SS (sun set) and SR (sun rise) are utilized together since the $NO_{x\ (ss)} > NO_{x\ (sr)}$ (see Nevison et al., 1996).

Moreover the following pathway gives a null-cycle in which the odd oxygen is destroyed and then regenerated:

$$NO + O_3 \rightarrow NO_2 + O_2$$
$$NO_2 + hf\ (\lambda<395\ nm) \rightarrow NO + O$$
$$O + O_2 + M \rightarrow O_3 + M$$
$$\text{Net: Null} \qquad (2.23)$$

In the lower stratosphere HNO_3 can be photolysed by UV radiation ($\lambda < 280$ nm) and NO_x radicals are regenerated.

In addition the reaction of hydroxyl radical with HNO_3 takes to NO_3 formation. Then the radiation in the visible band can lead fast photolysis of the NO_3 and creation of NO_2 molecule (and atomic oxygen).

It is important to keep in mind that all reactions are temperature dependent and for the NO_x species that is particularly true. The reaction $NO + O_3 \rightarrow NO_2 + O_2$ is called as bimolecular reaction. When the temperature increases the two molecules in the left side are moving faster and there are greater probabilities that they meet each other and react (the reaction rate increases). So, the higher the temperature is the more ozone is depleted (see also next chapter).

In contrast to this bimolecular behavior, the termolecular (three molecules) reaction rate decreases with the temperature rise (i.e., $O + O_2 + M \rightarrow O_3 + M$).

It is also interesting to examine the NO_x production and loss in the thermosphere where elevated amount of nitrogen species are produced by photoionization processes. In fact the photoionization by solar X rays and EUV (Extreme UV), during geomagnetically quiet conditions, is the main NO_x source in the thermosphere. Moreover, Lyman α ionization is the major source between 90 and 60 km (Solomon et al., 1982b).

The path of NO_x production in the thermosphere is (see Solomon et al., 1982a):

$$x + hf \rightarrow x^+ + e^* \qquad (2.24)$$
$$e^* + N_2 \rightarrow 2N + e^* \text{ [with N } (^4S, {}^2D)] \qquad (2.25)$$
$$N + O_2 \rightarrow NO + O \qquad (2.26)$$

or

$$N + OH \rightarrow NO + H \qquad (2.27)$$
$$N^2 + hf \rightarrow NO + N_2^+ + N \qquad (2.28)$$
$$N_2^+ + O \rightarrow NO^+ + N \qquad (2.29)$$
$$N_2 + hf \rightarrow N^+ + N + e \qquad (2.30)$$

$$N_2 + hf \rightarrow 2N \quad (2.31)$$

With e* = secondary electron formed by photoionization of molecules.

Whereas the following path gives NO_x loss in the mesosphere (see Solomon et al., 1982b):

$$NO + hf \rightarrow N(^4S) + O \ (\lambda<191 \text{ nm}) \quad (2.32)$$

$$N(^4S) + NO \rightarrow N_2 + O \quad (2.33)$$

In addition at elevate geomagnetic latitudes also energetic particles (e.g., Auroral Proton and Electron Precipitations) are able to increase the ionization in the Mesosphere and Lower Thermosphere (MLT) zone with large NO production peaking at about 110 km (see S.C. Solomon et al., 1999; Barth et al., 2001 and references therein).

If only a little portion of thermospheric NO_x production could reach the upper stratosphere, the total nitrogen rate could remarkably change.

2.3.3 The ClO_x and BrO_x catalytic cycles

The importance of the reactive chlorine radicals was pointed out for the first time by Molina and Rowland (1974). They showed that the manmade tropospheric chlorofluoromethanes reaching the stratosphere are there photolysed and its reactive radicals are able to destroy ozone. In the same year Stolarsky and Cicerone (1974) highlight also the ClO_x (Cl + ClO) of different origin (i.e., from volcanic eruption or solid fuel rocket) are involved in extremely active catalytic cycles of O_x destruction.

The most important ClO_x catalytic cycle between 35 and 45 km is:

$$Cl + O_3 \rightarrow ClO + O_2$$

$$ClO + O(^3P) \rightarrow Cl + O_2$$

$$\text{Net: } O + O3 \rightarrow 2O_2 \quad (2.34)$$

with $O(^3P)$ coming from the photodissociation of O_2 in the Herzberg bands (300–500 nm).

Also the cycle involving Cl_2O_2 (ClO dimer) may have relevance in the lower stratosphere (mostly at polar latitudes).

Several reactions transform reactive chlorine into reservoir species. The result is a formation of hydrochloric acid (HCl), hypochlorous acid (HOCl) and chlorine nitrate ($ClONO_2$). The chlorine nitrate is very important because, if photolysed, can destroy the O_3 both by NO and Cl active radicals.

Also BrO_x (Br + BrO) reactive radicals coming from bromine compounds are important in the O_x catalytic cycles even if its abundance is not too large. In addition, they develop the most important cycle in the lower stratosphere of high latitudes, involving the ClO_x radicals:

$$BrO + ClO \rightarrow Br + Cl + O_2$$
$$Cl + O_3 \rightarrow ClO + O_2$$
$$Br + O_3 \rightarrow BrO + O_2$$
$$\text{Net: } 2O_3 \rightarrow 3O_2 \qquad (2.35)$$

1.4 - The ozone variability

Since this work is devoted to investigate the ozone changes in the high atmosphere connected to transient solar activity phenomena, it is important to point out the main factors causing the variability on the stratospheric ozone (see Wayne, 2000, pp. 191-198), roughly above and below 40 km. In this way it will be possible to compare different phenomena and better understand the right importance of the examined matter inside the atmospheric ozone budget.

Generally we must point out that the low stratospheric ozone is mainly governed by transport phenomena whereas the high stratosphere one is driven by chemistry. The explanation of this behavior resides on the long lasting life of ozone molecules (and other minor components) in the low stratosphere relative to the higher one (see Fig. 2.6).

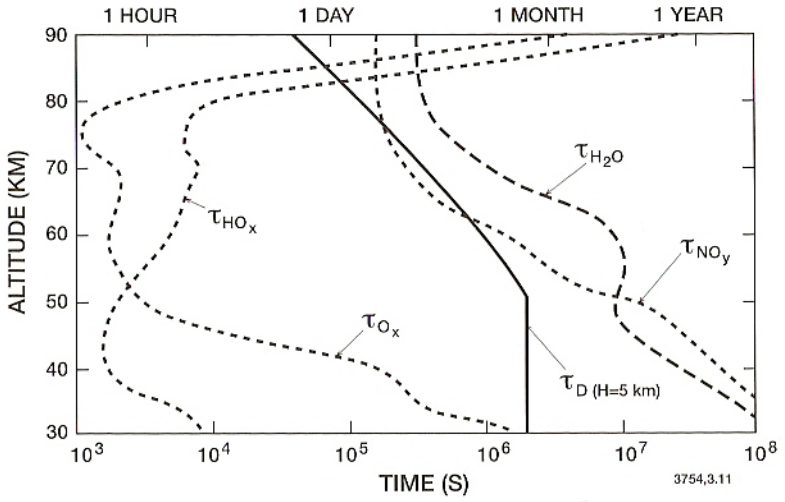

Fig. 2.6 – *Vertical profiles of the chemical lifetimes of O_x, HO_x, H_2O and NO_y. In addition typical constants for vertical exchanges are shown. From Brasseur and Solomon, 2005.*

We can subdivide the ozone variability according to temporal scales. In this way we have: short term variability, seasonal variability, interannual variability and long term variability.

2.4.1 Variability in the upper stratosphere

The ozone amount in the high stratosphere has a negligible influence inside of the total ozone budget (few percents) but its variability is essential for the understanding of this thesis.

A. Short term variability

We can start our analysis from the diurnal ozone variability. In the steady state system where the ozone produced is equal to the ozone destroyed (without transport), the principal laws governing the process are (see Sect. 2.2):

$$O_2 + hf\,(\lambda < 240\ \text{nm}) \rightarrow O + O \qquad (2.6)$$

$$O + O_2 + M \rightarrow O_3 + M \qquad (2.2)$$

$$O_3 + hf\,(\lambda < 310\ \text{nm}) \rightarrow O_2 + O \qquad (2.4)$$

$$O + O_3 \rightarrow O_2 + O_2 \qquad (2.3)$$

The UV radiation with λ < 240 nm hits an oxygen molecule and splits it into two atoms of oxygen. In presence of an third body the atomic oxygen reacts with the molecular oxygen and forms an ozone molecule. In addition, the UV radiation with λ < 310 nm can destroy the ozone and form atomic and molecular oxygen. The O_3 can be destroyed also by combination with a free oxygen atom.

During the night the photolysis is not effective and the Reactions (2.6) and (2.4) do not work. On the contrary, Reaction (2.2) is very fast (few seconds) and active also without solar radiation. Almost all free oxygen atoms are converted to ozone in this way and this process is not balanced by the Reaction (2.3) since it is very slow (1 day). The result is an high atmospheric ozone rise during the nigh until the sunrise when the excess of O_3 molecules are quickly destroyed (in few minutes) by Reaction (2.4) till the balance condition [the Reaction (2.6) is slow] is established (see Fig. 2.7).

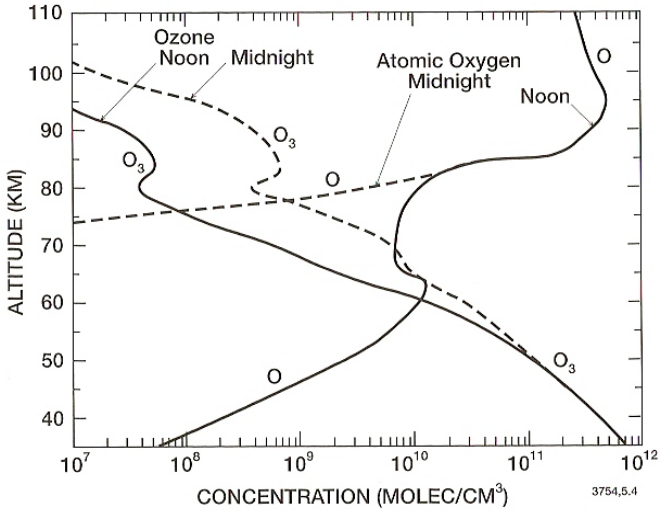

Fig. 2.7 – *Calculated vertical distribution of ozone and atomic oxygen at noon and midnight. From the model of Garcia and Solomon (1983).*

For example the ratio O/O_3 is about 0.1 at 50 km. This means during the night the ozone concentration increases up to 10%.

The second short term variability factor is the UV solar radiation. A change of ultraviolet output from the Sun induces to ozone variation. The output of the solar UV radiation is influenced by the presence of sunspots because of stronger magnetic field in these active regions. When an active region is present on the solar disk, we can identify a cycle of 27 day in the stratospheric ozone concentration. Both the production and loss rate of ozone [see Reactions (2.6) and (2.4)] are able to undergo variations. As pointed out by Dessler et al. (1998) the solar radiation changes from solar maximum (more sunspots) to solar minimum (less sunspots) in different percents depending on wavelength. Particularly for the UV irradiance they calculated a rise of 8-4 % for wavelengths below 240 nm and a rise less of 1% for the wavelengths below 300 nm. This behavior leads to a little ozone rise since the Reaction (2.6) [O_3 production] is incremented more then Reaction (2.4) [O_3 loss]. The effect on the TOC has been evaluated by Chandra (1991), who finds 1.5% of ozone variability over a solar cycle for a 6% change in solar UV flux near 200 nm. On the contrary, the total irradiance does not range much (about 0.1%, Foukal, 1998).

Also the temperature affects the ozone concentration in the upper stratosphere. Principally if the temperature increases, the ozone concentration decreases. For example the upper stratospheric ozone is subjected to fall down during the winter when the planetary wave activity is most intense. The propagation of the waves toward the upper atmosphere induces the temperature raise. The result is an increase of the rate of ozone loss [see Reaction (2.3)] and the higher the temperature is the more ozone loss is observed.

The last one element that can stimulate short term ozone variability in the upper atmosphere is exactly the main topic of this paper: the presence of solar energetic particle fluxes, able to trigger catalytic cycle of the ozone destruction. For an extensive discussion on this issue see the following chapters.

B. Seasonal variability

The not so strong seasonal variability associated to upper stratospheric ozone is totally caused by the differences of temperature depending on the elevation angle of the sun. The maximum UV radiation (summer solstice) causes the maximum temperature in the upper stratosphere. This is the reason for which the ozone concentration falls down. The minimum UV radiation (winter solstice) induces to minor temperature and ozone increase in the stratosphere.

2.4.2 Variability in the lower stratosphere

Even if the solar influence does not reach directly the lower stratosphere, we inspect the main sources of ozone variability.

A. Short term variability

In the lower stratosphere the life of O_3 molecules is very long, therefore it is not expected a dominance of chemistry on the trace gas composition. In fact, the only short term variability in the lower atmosphere is connected to the passage of the weather system. In this way ozone is not created or destroyed, but the transport simply redistributes ozone concentration from place to place.

B. Seasonal variability

The seasonal variability of ozone is related to the large scale circulation. We can find out a maximum O_3 at midlatitude in late winter-early spring. The raison arises from the Brewer-Dobson circulation that transports the air mass from the tropical area, where much more O_3 is produced, to polar region during winter. The low sun angle prevents the O_3 photolysis, therefore the ozone is stored at elevated latitudes until late winter.

C. Interannual variability

The most important processes triggering the interannual variability are: the Quasi Biennial Oscillations (QBOs), the El Niño-Southern Oscillation (ENSO) and the volcanic eruptions.

The Quasi-Biennial Oscillation is an oscillation in the average zonal winds in the tropical stratosphere. Roughly every 27-30 months, the tropical stratospheric winds in the 10 mb to 100 mb altitude range are observed to shift from westerly to easterly and then back again. Weather systems in the tropical lower stratosphere reflect this shift and the O_3 concentration, in the tropic and extratropic, ranges between high and low values according to the QBO phase (see Baldwin et al., 2001 for a review).

The El Niño-Southern Oscillation is the variability of the temperature surface of the Pacific Ocean near the South America. In this area normally the water is cold since an upwelling ocean current is present and the winds are easterly. During the El Niño period the winds are quite and the warm water of west Pacific moves toward the east cost. In this way, the variation of surface temperature of water leads to the shift in the global circulation pattern and changes in the transport of ozone.

The volcanic eruptions can inject a large amount of different gas in the lower stratosphere. Sometimes the chlorine originated from volcano can directly destroy the ozone by the well known catalytic cycles. Otherwise, the sulfur dioxide given out leads to heterogeneous chlorine chemistry. The last one develops on the surface of sulfate aerosol deriving from the SO_2 (see Adriani et al., 1987 and references therein).

D. Long term variability

The most important factor correlated to long term ozone variability is the man made CFC (see Molina and Rowland, 1974) but it is not the issue of this thesis.

2.5 - The ozone vertical profile

The ozone vertical profile shows a maximum in the stratosphere around 30 km, depending on latitude, season and unit of measure adopted. The O_3 peak corresponds to maximum UVB absorption that leads to release of long wave radiation able to warm the stratosphere. The O_3 concentration is about 6-9 ppmv according to the season and latitude. Normally, this ozone maximum is only slightly influenced both by undicennal and sporadic solar activity so is not central in the present paper. Above, the ozone concentration falls down quickly.

However, the behavior of the ozone profile in MLT zone is also interesting for many reasons. Fist of all it is important to know the O_3 concentration in the whole of the atmosphere to separate natural variability from anthropogenic perturbations. Then, it is important to check the atmospheric chemical models. Finally, the MLT (and the upper stratosphere) is the atmospheric zone most influenced by the solar activity (i.e., solar wind, energetic particles, auroras).

In the MLT region is also present an interesting ozone peak called secondary maximum known since the 1970s (see Evans and Llewellyn, 1972). In fact, in the mesopause, at around 90 km there is an elevate ozone layer (different ppmv) comparable to the stratospheric peak. Fig. 2.8 shows the annual average, night-time ozone distribution from measurements of the GOMOS instrument during 2003.

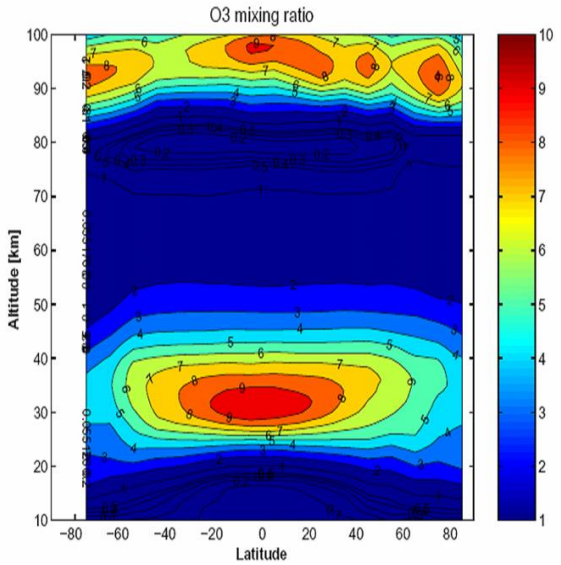

Fig. 2.8 – *Annual average, night-time ozone distribution from measurements of the GOMOS instrument during 2003. From Verronen, 2006.*

It is evident the presence of two ozone peaks of comparable volume mixing ratio (vmr) in the stratosphere and MLT. The secondary maximum is about 6-10 ppmv during the night and substantially smaller during the day (1-2 ppmv). Many factors lead to elevate ozone mixing ratio in the MLT zone. The main chemical reactions controlling the MLT ozone are shown below:

$$O + O_2 + M \rightarrow O_3 + M \quad (2.2)$$

$$O_3 + O \rightarrow O_2 + O_2 \quad (2.3)$$

$$O_3 + H \rightarrow OH + O_2 \quad (2.36)$$

$$O_3 + h\nu \rightarrow O_2 + O\ (^1D) \quad (2.4)$$

The elements influencing the presence of the secondary peak in the mesopause are (Smith and Marsh, 2005; Marsh et al., 2002):

- The large availability of atomic oxygen coming from the thermosphere by molecular diffusion.

- The longer life of ozone molecules during the night [Reaction (2.4)].

- The large diurnal variability of HO_x species. The molecular diffusion works also to move upward (out the MLT) the atomic hydrogen during the night. A minor importance has the eddy diffusion that brings hydrogen up from the mesosphere and decreases the ozone during the night.

- The very low temperature existing in the mesopause region. As expected, the low temperatures cause elevate efficiency of termolecular (three molecules) reactions and low the bimolecular ones. So, the O_3 production [Reaction (2.2)] is accelerated and the loss is decreased [Reactions (2.3) and (2.36)].

- Finally, the vertical advection of atomic oxygen by the solar diurnal tide.

To resume, the low temperatures increase the ozone production and decrease the loss. In addition, the elevated ozone mixing ratio in the mesopause region depends also on the molecular diffusion, that brings atomic oxygen from the thermosphere. Moreover the large diurnal variability results from the molecular diffusion that pushes out the MLT the hydrogen during the night and determines high ozone concentration.

Other interesting feature of the ozone profile is the existence of the so-called “third ozone maximum” (Marsh et al., 2001; Sonnemann et al., 2006) in the mesospheric winter hemisphere at high latitudes and at about 72 km of altitude (even if Degenstein et al., 2005a shows that it is not confined to polar latitudes).

In the mesosphere the ozone concentration is mainly function of the effectiveness of catalytic cycles involving HO_x components.

The main reservoir of mesospheric odd hydrogen is the water vapor that exhibits a strong seasonal cycle, with summer concentrations [~7-8 ppmv] higher than in winter [~1-2 ppmv] (Hervig et al., 2003; Seele and Hartogh, 1999).

Figure 2.9 shows the different water vapor concentration at the polar latitudes of the Northern and Southern hemisphere between 15 and 31 January 2005 (MLS instrument on AURA satellite). Note the inter-hemispheric difference above 1 hPa. There is a minor availability of HO_x species destroying O_3 in the winter mesosphere than in the summer one (Marsh and Smith, 2003).

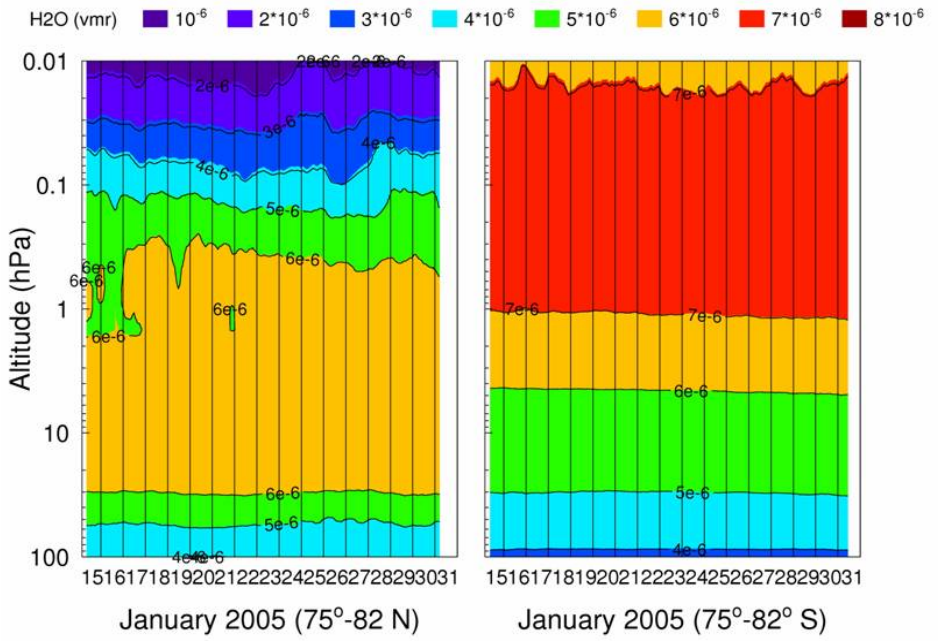

Fig. 2.9 – *Temporal evolution of averaged values (75°–82° N and S) of atmospheric water vapor volume mixing ratio between 15 and 31 January 2005. The left side reports the Northern Hemisphere and the right the Southern one.*

Typically, in the lower mesosphere and stratosphere (below to ~0.15 hPa /60 km) the main OH source is the reaction of water vapor with metastable oxygen $O(^1D)$. Moreover, above approximately 60 km the main source of odd hydrogen species is the photolysis of H_2O, especially by the absorption of the Lyman-alpha [121.6 nm] radiation (Crutzen, 1997). Therefore on the night hemisphere, the low water vapor and $O(^1D)$ content and the weak photolysis process [during the winter the solar zenit angle is close to 90°, so the large optical depth at the Lyman-alpha wavelengths prevent H_2O photolysis while the smaller optical depth at Schuman-Runge bands (175-195 nm) allows photodissociation of O_2, see Marsh et al., 2001] lead to low OH concentration (see Crutzen, 1997; Seppälä et al., 2006; Canty et al., 2006). Therefore, the low concentration of active hydrogen leads to weak O_3 loss while the feeble photolysis of molecular oxygen should lead to ozone production.

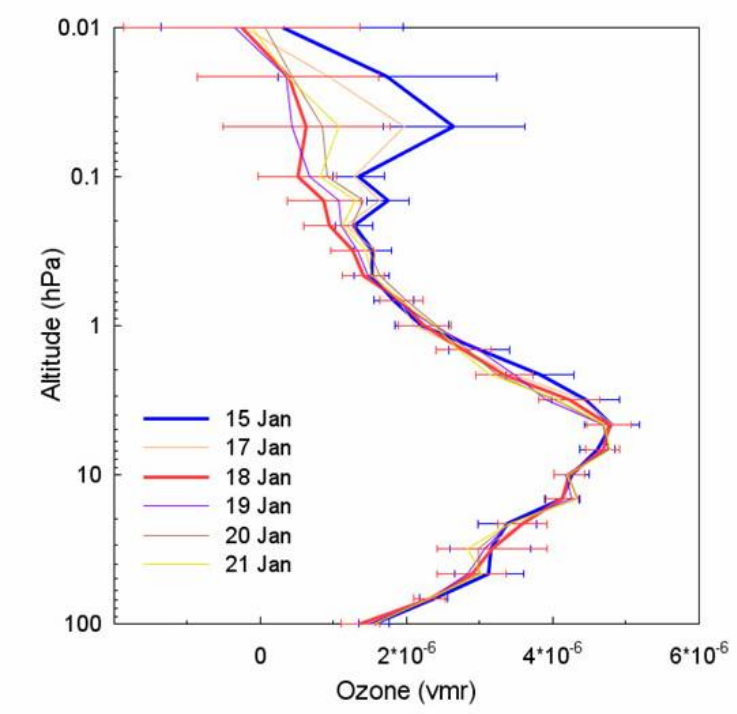

Fig. 2.10 - *Daily average ozone distribution from measurements of the MLS instrument during January 2005 at 75° – 82° N. From SD07.*

Figure 2.10 shows daily average ozone profiles from measurements of the MLS instrument during some days of January 2005 at 75° – 82° N. Note the presence of the third O_3 peak with maximum values of ~ 3 ppmv between 0.1-0.01 hPa on 15 January (before the SEPs occurrence).

2.6 - Utilized instruments

As pointed out above, the atmospheric data used in this thesis come from different instruments aboard satellites (passive remote sensing instruments). Particularly, four type of satellite instrument exist to recorder the ozone and other minor component of the atmosphere (the names of sensors utilized in this thesis are reported in the brackets):

- Backscatter Ultraviolet Technique (TOMS)
- Occultation Technique (HALOE, SAGE II, POAM III)
- Limb emission (MLS)
- Limb scattering

Figure 2.11 shows the different geometry of each sensor.

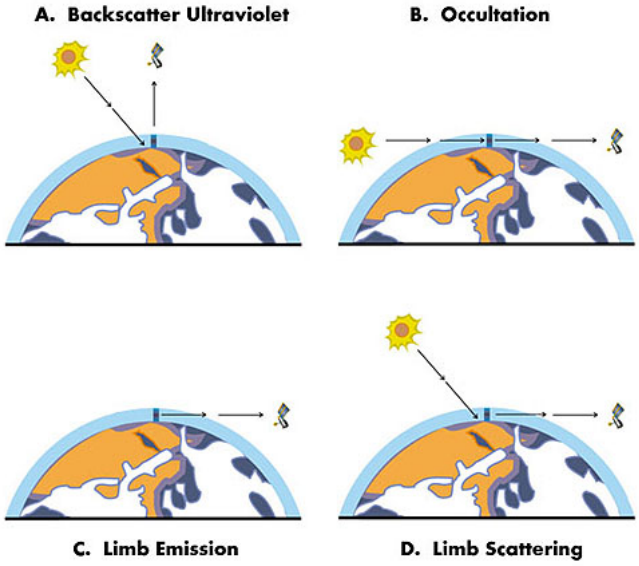

Fig. 2.11 – *Different geometry of the satellite sensors devoted to O_3 recording.*

Instruments on satellites with polar orbit are ideal for this kind of studies because they lead to investigation of both polar hemispheres at the same time. Anyway also satellites with inclined orbits have been used when the first ones were not available.

TOMS

The sensor makes measurements of total ozone in Sun-synchronous circular polar orbit. The backscatter ultraviolet technique adopted by TOMS (OMI, from 2004) instrument a board of Earth Probe (AURA, from 2004) satellite allows retrieving the ozone content by measure of incident UV irradiance from the Sun and backscattered UV radiation from the Earth.

SAGE II

The SAGE (Stratospheric Aerosol and Gas Experiment) II sensor was launched into a 57-degree inclination orbit aboard the ERBS (Earth Radiation Budget Satellite). It utilizes the solar occultation technique to measure the attenuated solar radiation. The used SAGE2_V6.20_AEROSOL_O3_NO2_H2O_BINARY data set is provided by the NASA Langley Atmospheric Sciences Data Center.

This data set, covering the latitude range from 80° N to 80° S and with a 0.5-km vertical resolution (http://eosweb.larc.nasa.gov/), includes number density profiles of ozone and nitrogen dioxide, plus molecular density and mixing ratio profiles of water vapor together with aerosol extinction profiles at 1020, 525, 453, and 385 nm.

POAM III

The POAM III is a solar occultation instrument aboard the Satellite Pour l'Observation de la Terre (SPOT) 4 with polar orbit. It measures the vertical profiles of ozone, water vapor, nitrogen dioxide, and aerosol extinction in the stratosphere and upper troposphere with a vertical resolution of 1-2 km. Data were obtained from http://eosweb.larc.nasa.gov/PRODOCS/poam3/table_poam3.html. However, POAM III made measurements in one hemisphere at a time, on alternating days during the investigated period because of technical problems.

See Fig. 2.12 for a sketch of the geometry of the instrument.

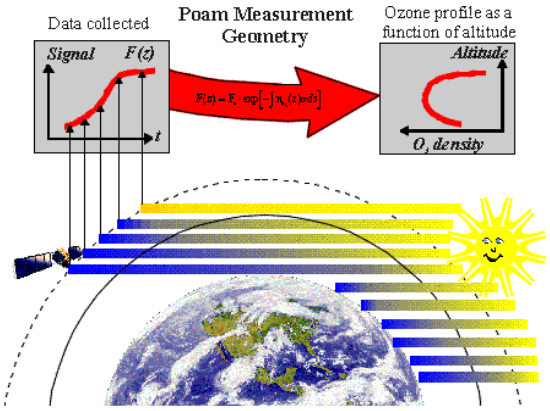

Fig. 2.12 - *Sketch of the geometry of a solar occultation instrument (i.e., POAM III).*

MLS

The data used were recorded by the Microwave Limb Sounder (MLS) instrument on the AURA satellite (Schoeberl et al., 2006). The NASA EOS (Earth Observing System) MLS (see Waters et al., 2006) is one of the four instruments of AURA launched on 15 July 2004 to a sunsynchronous near polar orbit (see Fig. 2.13).

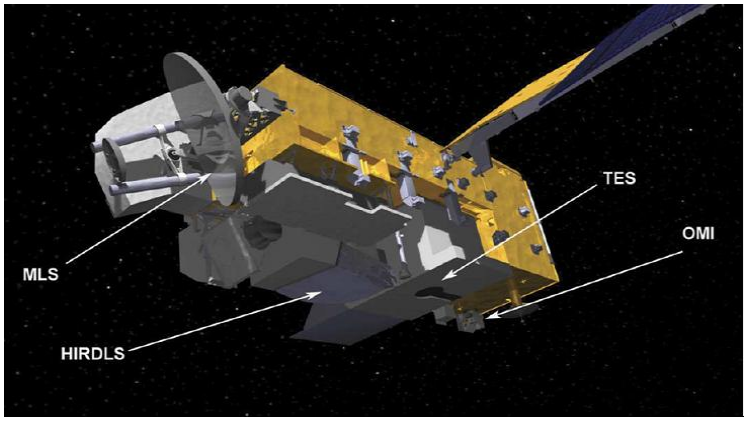

Fig. 2.13 - *Model of the Aura spacecraft showing the location of the four instruments, HIRDLS, MLS, OMI, and TES. From Schoeberl et al. (2006).*

MLS scans the Earth's limb in the forward direction of flight with a vertical resolution of about 3 km, viewing the microwave emission in different spectral regions. The measured chemical components are: O_3, H_2O, BrO, ClO, HCl, HOCl, OH, HO_2, HCN, CO, HNO_3, N_2O, and SO_2 mixing ratios (see Froidevaux et al., 2006, for early validation analyses). The MLS instrument observes in spectral bands centered near five frequencies [118 GHz (temperature and pressure); 190 GHz (H_2O, HNO_3); 240 GHz (O_3 and CO); 640 GHz (N_2O, HCl, ClO, HOCl, BrO, HO_2, and SO_2); and 2.5 THz (primarily for OH); see Schoeberl et al., 2006]. The adopted data set is the EOS MLS Version 1.5 Level 2 Data (available at http://mls.jpl.nasa.gov/data/).

The MLS instrument measures the OH mixing ratio during day and night conditions by thermal emission over the range 18–94 km. Unfortunately, Pickett et al. (2006) point out that the version 1.51 of MLS OH values can be used only between 30 and 60 km, because of a systematic error at higher altitudes which could be produced by a regular bias or an offset in the data. Nevertheless, in order to single out the SEP effects on the atmospheric components, MLS data can be used at least for the evaluation of a qualitative answer. In addition, the data quality is improved by the averaging procedure of different profiles, being the random error reduced by the mathematical approach. Moreover, the MLS ozone data version 1.51 also showed good reliability in the stratosphere but a decreased precision in the mesosphere (see Froidevaux et al., 2006).

The MLS data used in this paper were checked by their data quality and description document (Livesey et al., 2005), in order to ensure the reliability of our results. In addition, the OH data were further processed by checking their trend at each altitude level to delete a few spurious spikes that were randomly distributed in time.

HALOE

The HALOE (HALogen Occultation Experiment) is an occultation instrument on UARS (Upper Atmosphere Research Satellite) satellite with a 57° inclination orbit and a period of ~ 96 min. The HALOE (see Russell et al., 1993) measures the solar infrared radiation directly though the atmospheric limb during every satellite sunrise (SR) and sunset (SS) events. The HALOE retrieves the vertical profiles of different atmospheric constituents (O_3, HCl, HF, CH_4, H_2O, NO, NO_2) by measuring the amount of absorption of solar radiation at different wavelengths. The altitude range for measurements extends from 15 km to 60-130 km (depending on the observed atmospheric constituent) and in the course of a year covers 80° S-80° N geographic

latitudes. HALOE data coverage ranges from 11 October 1991 to 21 November 2005 (they are available at http://haloedata.larc.nasa.gov/download/index.php). In this work we will concentrate on O_3, NO_2 and NO HALOE Version 19 Data.

Chapter 3

IONOSPHERE AND VARIABILITY OF NO_X AND HO_X SPECIES

3.1 - The ionosphere

The short wave electromagnetic radiation has sufficiently energy to cause the ionization (photoionization) of the upper atmospheric gases. In addition, also precipitating energetic particles contribute to ionize (ionization by impact) this conducting layer, called ionosphere, and ranging in height from 50 km up to 1000 or 2000 km (see Hessler, 1969 for a review).

The photons come primarily from the Sun while the ionizing particles can be cosmic rays, or electrons or ions from the Sun, the magnetosphere, or a different region of the ionosphere itself.

The only requirement for the ionizing processes by photons or particles is that their energies (hf or $1/2mv^2$, respectively) must exceed the ionization potential or binding energy of the atom or molecule. The following Table 3.1 shows the ionization potentials of some important atmospheric constituents.

Table 3.1 – *Ionization potentials of some atmospherically important species together with equivalent threshold wavelengths. From Wayne, 2000, p. 109.*

Species	Ionization energy		Equivalent wavelength (nm)
	eV	kJ mol^{-1}	
Na	5.1	496	241.2
Mg	7.7	738	162.1
NO	9.3	886	135.0
NO_2	9.8	940	127.2
O_2	12.1	1165	102.7
H_2O	12.6	1214	98.7
O_3	12.8	1233	97.0
N_2O	12.9	1246	96.0
SO_2	13.1	1264	94.6
H	13.6	1312	91.2
O	13.6	1314	91.1
CO_2	13.8	1331	89.9
CO	14.0	1352	88.5
N	14.5	1403	85.2
H_2	15.4	1488	80.4
N_2	15.6	1503	79.9

Figure 3.1 reports the rates of photochemical dissociation, called ***J***, as a function of altitude for the winter solar maximum at latitude 40˚.

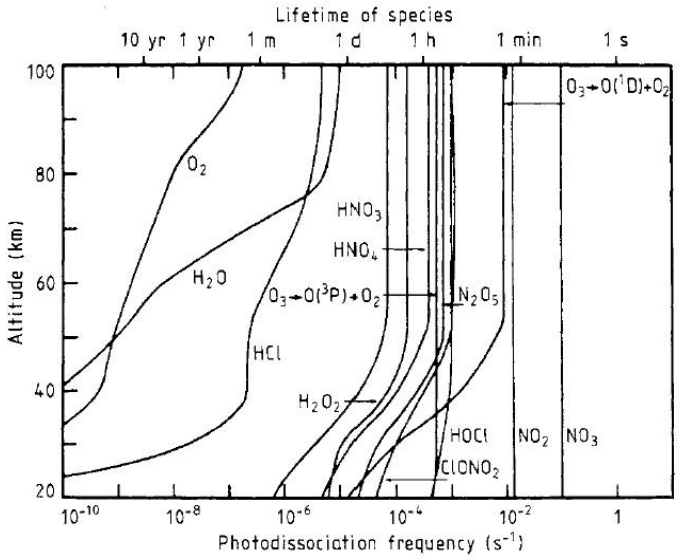

Fig. 3.1 - *Rates of photochemical dissociation (J) as a function of altitude for the winter solar maximum at latitude 40˚. From Brasseur and Solomon (1984).*

The ionosphere divides into three horizontal layers (termed D, E and F) based on distinct physical characteristics and ionization processes. Further there is subdivision of the F region. The altitude ranges of these horizontal layers are: D (60-95 km), E (95-160), F1 (140-200) and F2 (200-1000 km). The following Table 3.2 reports the main ionic processes of atmospheric importance.

Table 3.2 – *Some types of ionic process of atmospheric importance. From Wayne, (2000) p. 491.*

Charge transfer			
	$N_2^+ + O_2 \rightarrow N_2 + O_2^+$		6.3
	$H^+ + O \rightarrow O^+ + H$		6.4
Exchanges			
	$N_2 + O^+ \rightarrow N^{(*)} + NO^+$		6.5
	$O_2^+ + N_2 \rightarrow NO + NO^+$		6.6
Recombinations			
	$O^+ + e \rightarrow O + h\nu$	Radiative	6.7
	$NO^+ + e \rightarrow N^{(*)} + O$	Dissociative	6.8
	$NO^+ + NO_2^- \rightarrow NO + NO_2$	Ion–ion	6.9
Attachments			
	$e + O \rightarrow O^- + h\nu$	Radiative	6.10
	$e + O_2 + M \rightarrow O_2^- + M$	Three-body	6.11
	$e + O_3 \rightarrow O^- + O_2$	Dissociative	6.12
Detachments			
	$O_2^- + M \rightarrow O_2 + e$	Collisional	6.13
	$O_2^- + O \rightarrow O_3 + e$	Associative	6.14
	$O^- + h\nu \rightarrow O + e$	Radiative	6.15
Clustering			
	$O_2^+ + O_2 + M \rightarrow O_2^+.O_2 + M$		6.16
	$H^+(H_2O)_n + H_2O\ (+\ M) \rightarrow H^+(H_2O)_{n+1}\ (+\ M)$		6.17
	$NO_3^- + H_2O + M \rightarrow NO_3^-.H_2O + M$		6.18

The principal ions in the ionosphere derive from N_2 and O_2 since they are the main atmospheric components (99%).

The composition of positive ions in E and F regions is quite different. Gravitational separation of ionic species favours atomic over molecular ions at high levels in the heterosphere. At lower altitudes of the D region complex molecular positive ions dominate (see Fig. 3. 2).

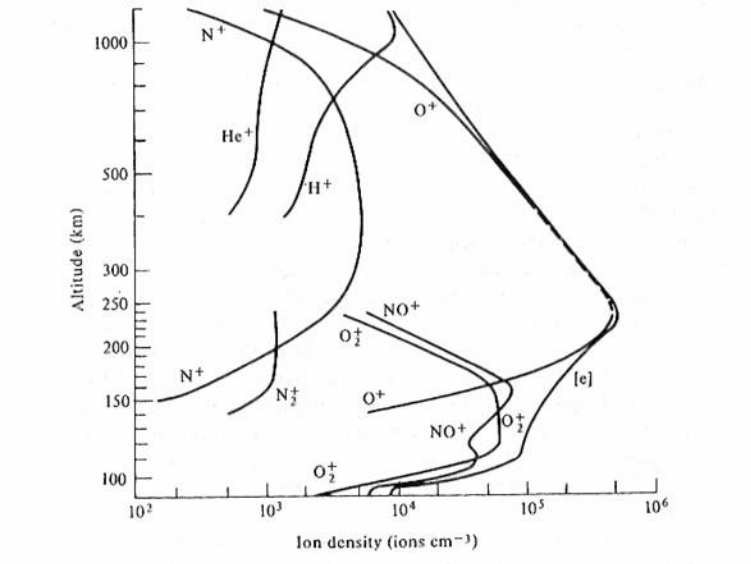

Fig. 3.2 – *Composition of positive ions in the E and F regions obtained at daytime and solar minimum. From Johnson (1966).*

The radiation of almost all wavelengths reaches the F2 region; the range 20-91 nm contributes to ionize the F1 region. The ionization of the E region comes from

EUV (80-103 nm) and X-rays (1-10 nm). In the D region the only surviving ionizing radiations are EUV > 103 nm and “hard” X rays (0.2-0.8 nm) [see Wayne, 2000, pp. 493-495].

The F region is characterized by O^+ and N^+ even if at highest altitudes the lighter H^+ and He^+ become more abundant.

The chemistry of ions in this region is quite simple since it is wholly connected to O^+ produced by photoionization of atomic oxygen. In the lower F region the following paths are essential (passage from primary ion to secondary molecular ion):

$$O^+ + O_2 \rightarrow O + O_2^+ \quad (3.1)$$

$$O_2^+ + e \rightarrow O(*) + O \quad (3.2)$$

and

$$O^+ + N_2 \rightarrow N + NO^+ \quad (3.3)$$

$$NO^+ + e \rightarrow N(*) + O \quad (3.4)$$

Because the $[N_2] >> [O_2]$ in the F region, since the O_2 molecules are almost all photodissociated, even if the rate of the first reaction of second path has an order of magnitude less than for the first one, the NO^+ path is more efficient for the neutralization.

The molecular ions N_2^+ and O_2^+ are the most important primary products in the E region but their total concentration is lower than in F region. The first one is generated by soft X rays that ionize N_2 and the second one by Lyman β (at 102.5 nm) that ionizes O_2. The O_2^+ is the principal ion of this layer, whereas the ion N_2^+ is consumed rapidly in the secondary reactions:

$$N_2^+ + O \rightarrow N(*) + NO^+ \quad (3.5)$$

and

$$N_2^+ + O_2 \rightarrow N_2 + O_2^+ \quad (3.6)$$

The first reaction is important for the elevated altitudes (large concentration of NO^+ related to N_2^+) whereas the second reaction for the lower ones of the E regions.

The quiet time ionization of the D region is provided by the short wavelengths solar radiation. Particularly the Lyman-α (121.6 nm) ionizes the NO and the Extreme UV (EUV) [102.7-111.8 nm] affects the O_2. Therefore, in quiet condition, the most abundant ion is the NO^+ and then O_2^+. The following Figure 3.3 shows the different ionization process to ion pair formation in D region.

Anyway, at elevated geomagnetic latitudes the ionization rate is more intense during high solar activity level. In addition energetic particles i.e., Relativistic Electron Precipitations from the radiation belts and Auroral Proton and Electron Precipitations in the sub-auroral latitudes which occur in the MLT zone during the winter can generate a further surplus of ionization.

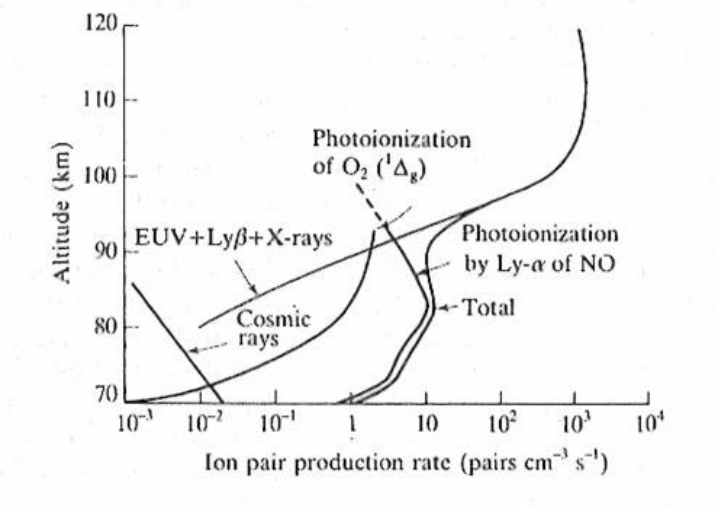

Fig. 3.3 – *Contribution of several ionization processes to ion pair formation in the "quiet" daytime E and F regions. From McEwan and Phillips (1975).*

Figure 3.4 shows that electron density is of about two order of magnitude between night and day (up to about 200 km), with larger intensity during the day and a stronger ionization during the solar maximum.

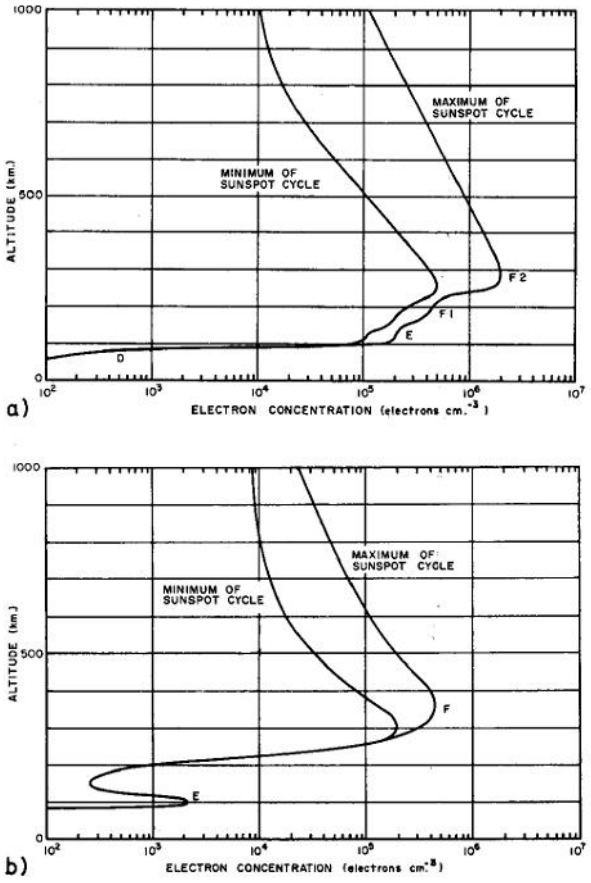

Fig. 3.4 - *Normal electron distributions at the extremes of the sunspot cycle: a. Daytime; b. Nighttime. From Johnson (1965).*

The solar radiation at shorter wavelengths has much more elevated variability during a solar cycle (see Sect. 2.4). The ratios of maximum to minimum solar intensity is of 7/1 for λ < 200 Å, 60/1 for λ < 60 Å and 600/1 for λ < 8 Å (Hessler, 1969), whereas is only of few percents for the UV radiation. Therefore, the hard X ray (λ < 1 nm) coming from solar flare phenomena and relativistic electrons from radiation belts lead to a surplus of ionization in the D region, at whole sunlight Earth and at subauroral regions. Moreover also solar energetic particle events can lead additional ionization in the stratosphere and mesosphere of the polar caps (the main issue of this work).

The ion chemistry is quite complex in the D region related to E, since different minor components are present. In fact, besides NO^+ and O_2^+ there are water cluster ions and negative ions. Below 80 km the main positive ions are the H^+ hydrates with the order of hydration ranging from 2 to 20, depending on the geophysical condition (see Fig. 3.5).

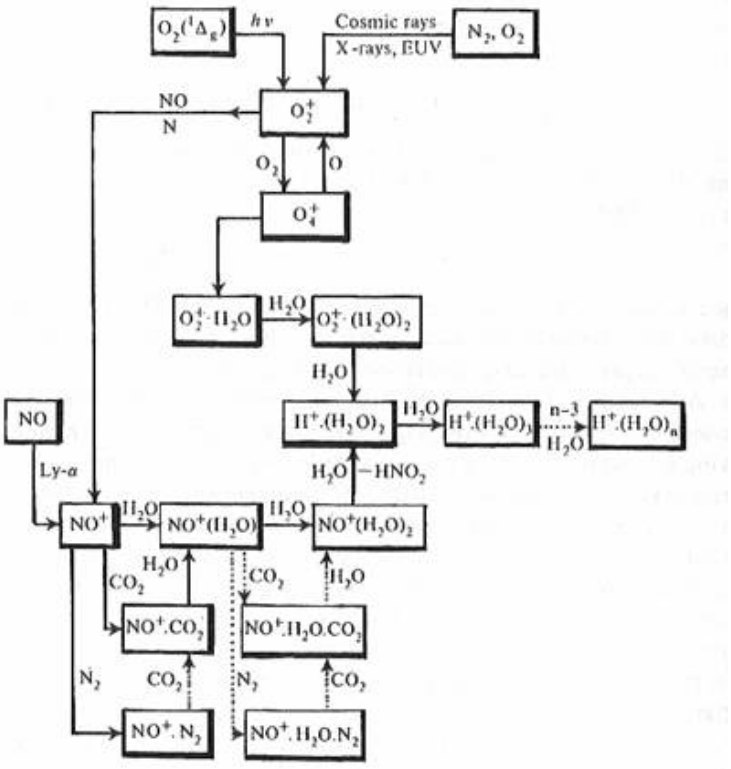

Fig. 3.5 – *Positive ion chemistry scheme in the D region. From Ferguson et al. (1979).*

Also the negative ions are important in the D region (see Fig. 3.6). They are present especially during the night time when the electron density decreases in favor of negative ions, so the following path is active:

$$O_2 + e + M \rightarrow O_2^- + M \quad (3.7)$$

whereas, during the day:

$$O_2^- + O \rightarrow O_3 + e \quad (3.8)$$

and the electron density grown up newly.

Obviously, many chemical reactions of neutralization balance the ions production, so the ionization does not overtake the 0.1% of the neutral charge (see Verronen, 2006b, pp. 20-22).

The SEPs effects on the chemistry of the middle and upper atmosphere insert in this context. The solar energetic particles add ionization and therefore are able to change the concentration and ions ratio of specific ion species.

In fact, during solar proton events the main positive ion specie is not the NO^+ but the O_2^+, because the created N_2^+ is quickly converted into O_2^+, via the following path:

$$N_2^+ + O_2 \rightarrow O_2^+ + N_2 \quad (3.6)$$

Moreover, the solar energetic particles cause elevated variability in the minor neutral constituents with large rise of odd hydrogen and nitrogen species.

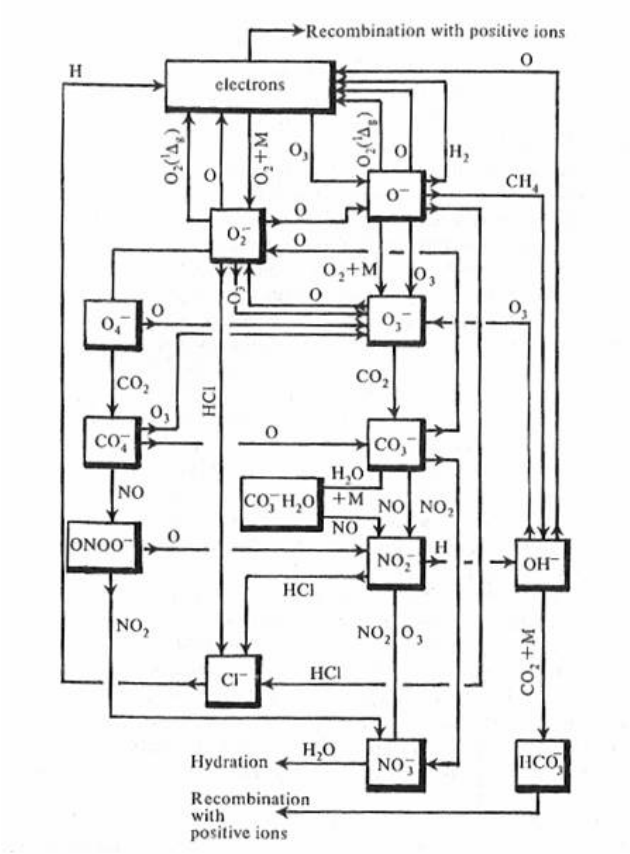

Fig. 3.6 – *Negative ion chemistry scheme in the D region. From Ferguson et al. (1979).*

3.2 Variability of HO_x and NO_x species by SEP events

As already pointed out, the main components of the terrestrial atmosphere are N_2 and O_2 molecules which endure important chemical changes during and after SEP events. The most important effect due to proton flux passage through the atmosphere is the increased ionization in the region between 20 and 90 km (see Krivolutsky et al., 2005). The solar proton hits a neutral molecule and makes a positive ion and let free an electron (called “secondary electron”) which can influence other molecules. In this way odd hydrogen and odd nitrogen components are increased. These events can change the ionization rate from its normal value of about 10 $cm^{-3}\cdot s^{-1}$ to 10^4 or 10^5 $cm^{-3}\cdot s^{-1}$ (Brasseur and Solomon, 2005, pp. 549-550).

Also reservoir species (i.e., HNO_3, $ClONO_2$, HCl, HOCl, ClO) are subjected to large variability connected to SEP events. They are not reactive but can keep inside odd components that can be released with the solar photolysis.

The ozone variability in the upper stratosphere-mesosphere is not mainly connected to air circulation motion but to chemistry. NO_x components influence the ozone variability in the stratosphere (30-45 km) and the HO_x components are more important in the mesosphere (45-80 km) [see Lary, 1997].

2.2.1 Odd hydrogen components

Two factors are very important for the development of mesospheric HO_x species during SEP events: the atomic oxygen and the electron density. Moreover also the atmospheric ion chemistry plays a fundamental role.

The additional ionization from SEPs leads to formation of N_2^+ (58.5% partitioning of total ionization), N^+ (18.5%), O^+ (15.4%) and O_2^+ (7.6%) molecules (see Rusch et al., 1981).

Particularly O_2^+ is essential for the ion chemistry of HO_x species formation. The O_2^+ forms O_4^+ (oxonium ion) by reaction with O_2 and finally the so-called water cluster ion [e.g., $O_2^+ \cdot (H_2O)$].

In addition, also NO^+, formed when N^+ and O^+ atoms react with O_2 and N_2 respectively, can produce water cluster ion (Solomon et al., 1981).

Now there are different pathways to produce HO_x by successive add of water molecules and reaction of positive ions with electrons.

The shortest path leading to HO_x productions is given by (see for exemple Jackman and McPeters, 2004):

$$O_2^+ \cdot H_2O + H_2O \rightarrow H_3O^+ \cdot OH + O_2$$
$$H_3O^+ \cdot OH + e^- \rightarrow H + OH + H_2O$$
$$\text{Net: } H_2O \rightarrow H + OH \qquad (3.9)$$

Because this kind of pathway involves recombination of positive ions with electrons, those reactions are valid above 70 km. Below 70 km the presence of electrons is very poor since there is an increase of negative ions (Solomon et al., 1981).

Anyway, different reactions come up below 70 km since the negative ions become more abundant then electrons. In this way the positive water cluster ions can react with NO_3^- to create HNO_3. At altitude between 40 and 65 km the HNO_3 should contribute to create HO_x. In fact it can be slowly photolysed and can contribute to the increase of HO_x species (Solomon et al. 1981) after a time delay (from few hours to days, depends on solar illumination). The pathway is the following:

$$O_2^+ \cdot H_2O + H_2O \rightarrow H_3O^+ \cdot OH + O_2$$
$$H_3O^+ \cdot OH + H_2O \rightarrow H^+ \cdot (H_2O)_2 + OH$$
$$H^+ \cdot (H_2O)_2 + NO_3^- \rightarrow HNO_3 + H_2O + H_2O$$
$$HNO_3 + hf \rightarrow OH + NO_2$$
$$\text{Net: } H_2O + NO_3 \rightarrow OH + OH + NO_2 \qquad (3.10)$$

The number of HO_x produced depends on the ionization rate, altitude, latitude, temperature and density of air.

Figure 3.7 shows the number of HO_x produced in polar summer condition for different levels of ionization rate. Each ion pair produces about two HO_x constituents (Solomon et al., 1981).

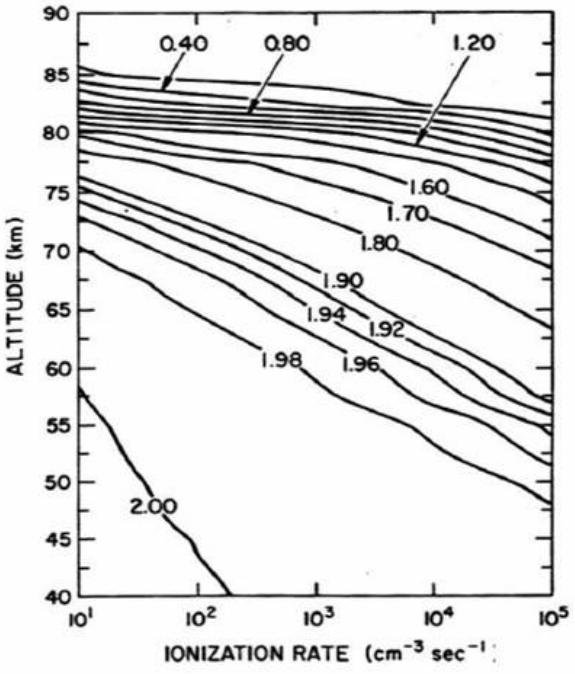

Fig. 3.7 - *Contours of odd hydrogen particles produced per ionization as a function of altitude and ionization rate for daytime summer polar conditions. From Solomon et al. (1981).*

The life of HO_x molecules is very short (few hours). In fact OH and HO_2 molecules quickly react each others to produce H_2O (*cannibalistic* reactions). Moreover they have a strong diurnal variability with several orders of magnitude lower concentration at nighttime. Anyway the effects connected to HO_x are lasting only during the protons passage.

2.2.2 Odd nitrogen components

The solar protons induce the formation of atomic nitrogen from N_2 molecules. In this way the NO_x species are produced by dissociations and dissociative ionizations.

Since Crutzen et al. (1975) the NO_x production connected to SPE, was known. There is about 1.25 (1.27) NO_x components per ion pair (see Jackman et al., 1990 and Porter et al., 1976).

NO_x species are produced by particle impact ionization, dissociation and ion chemistry (see Rusch et al., 1981):

$$N_2 + p^* \rightarrow N_2^+ + e^* + p^* \quad (3.11)$$

$$e^* + N_2 \rightarrow 2N + e^* \quad (3.12)$$

$$N + O_2 \rightarrow NO + O \quad (3.13)$$

or

$$N_2^+ + O \rightarrow NO^+ + N \quad (3.5)$$

$$NO^+ + e \rightarrow NO \quad (3.14)$$

It is important to remind that the life of NO_x molecules can be long lasting. In fact during the winter polar night the lack of sunlight prevents there the photolysis process; they can be transported towards lower altitudes by the vortex dynamics, where they can stay up to one year contributing to the decrease of the ozone concentration.

Chapter 4

ANALYSIS OF SEP EVENTS

This Chapter contains a summary of the performed analyses to investigate the relationship SEP/Minor atmospheric components. More details can be found in my published papers on the topic (see reference list).

4.1 - January 2005

4.1.1 Overview

Even if not comparable with the greatest solar proton events studied in the past, the analysis of the January 2005 SEP events is an essential part of this work, since for the first time the contemporary increase of odd hydrogen species was recorded by a satellite instrument. The atmospheric chemistry of the polar cap regions was essentially investigated by the solar occultation (SAGE II and POAM III) and the limb emission (MLS) instruments aboard of different satellites (see Sect. 1.6 for the description of the different instruments).

During the 14-22 January 2005, the active region NOAA AR 10720 displayed an interesting evolving dynamics. More than 80 X-ray flares were observed during its solar disk transit. Among them, five flares were classified as X1.2 (DD-MM/START: 15-01/0039 UTC), X2.6 (15-01/2154 UTC), X3.8 (17-01/0659 UTC), X1.3 (19-01/0803 UTC) and X7.1 (20-01/0641 UTC); see Fig. 4.1, upper panel.

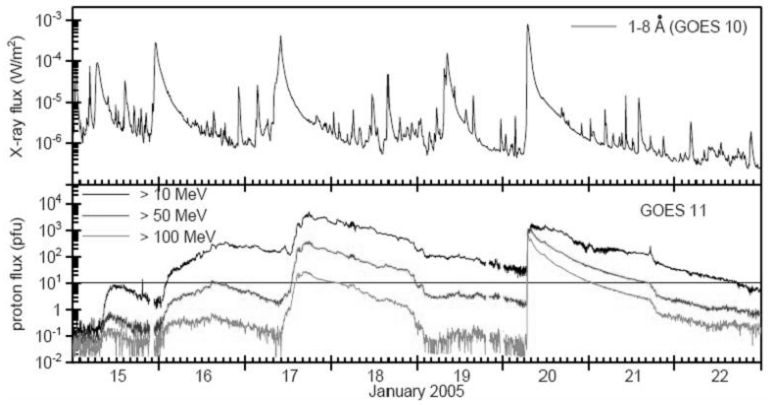

Fig. 4.1 - *Time-intensity profiles of the soft X- ray and the proton fluxes, in the three considered energy intervals, for January 2005 SEP events.*

Enhanced solar proton fluxes were observed by GOES satellites in the same period (see Fig. 4.1, second panel). In particular, the 17 January showed a big injection of solar particles peaking at 5040 pfu at the >10 MeV channel and the 20 January exhibited the hardest and most energetic particle event of the on going solar activity cycle. The peak for the >100 MeV channel was 652 pfu at 20-01/0710 UT, while the 10 MeV one was 1860 pfu at 20-01/0810 UT. Moreover, the 17 January event was characterized by near-relativistic solar particles (GLE N° 68), while the 20 January one probably contained up to about 8 GeV particles. The latter event was worldwide observed in neutron monitor records (GLE N° 69; Fig. 4.2 – upper panel as an example).

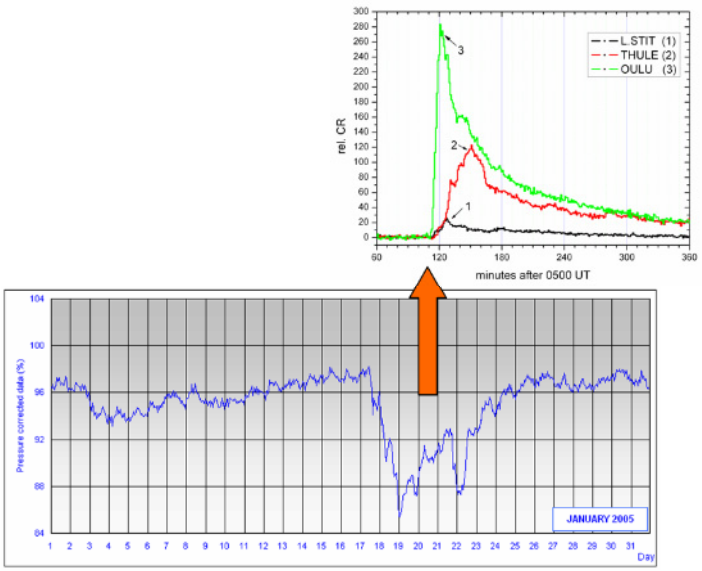

Fig. 4.2 - *Intensity profiles for GLE N° 69 for Lomnicky Stit, Thule and Oulu cosmic ray detectors (upper – after Kudela et al., 2007) and the monthly hourly intensities recorded by the Rome neutron monitor during January2005 (downloading at http://www.fis.uniroma3.it/~svirco/Dati/sm2005_file/Graf_2005_ing.htm).*

Also a huge Forbush decrease in the CR intensity was recorded (see Fig. 4.2 - lower panel).

4.1.2 Chemical variability

The investigation of the polar cap regions during the period interested by the January 2005 SEP events was carry out by the Stratospheric Aerosol and Gas Experiment (SAGE) II on Earth Radiation Budget Satellite (ERBS), the Polar Ozone and Aerosol Measurement (POAM) III on Satellite Pour l'Observation de la Terre (SPOT) 4 and the Microwave Limb Sounder (MLS) on EOS AURA.

A sudden ozone decrease at the boundary of the southern polar cap region was found by DAM06 by using POAM III and SAGE II on 17 and 20 January, respectively (see Figs. 4 and 6 of DAM06). A short term O_3 decrease (< 12 h) at different altitudes along the satellites orbit was recorded. The ozone depletion occurred in few hours after the SEPs events of January 2005 and it was of comparable magnitude in the selected altitude ranges (20-30 % at 60 km; 10-20 % at 55 km; 5-10 % at 50 km). Note that, as expected, the stronger depletion has been recorded when the spacecraft view was above the higher geomagnetic latitudes. The sudden mesospheric ozone depletion mainly arose from the rise of odd hydrogen species (see Chapter 3.2), but the adopted instruments were not able to retrieve them. However a minor contribution by odd nitrogen species should be present, especially in the stratosphere (see Lary, 1997).

POAM III and SAGE II instrument retrieved the NO_2 concentration and it has been possible to utilise such concentration as a NO_x proxy, in order to check for variabilities related to SEP events [nevertheless, it is necessary to recall that NO_2 molecules are not the best representatives of NO_x amount during the austral summertime (with sunlight condition $NO_2 + h\nu$ (λ<395 nm) $\rightarrow$ NO + O)]. Figure 8 of DAM06 shows the SAGE II NO_2 concentration of January 2005 imposed over the climatology from 1990 to 2000 at four different altitude, inside the latitude intervals between about 50° and 70° S. The NO_2 number density for January 2005 is lower than 1990–2000 at 40 km, similar at 45 km, and higher at the other two levels (47 and 49 km). This behavior could suggest that the slight increment of nitrogen composition at elevated altitudes is linked to the occurrence of the SEP events of January 2005.

As pointed out in the introduction, almost all of the past instruments were not able to retrieve the ozone concentration without the solar light and that lacked the possibility to check the goodness of the models on the night hemisphere. In fact, an

important disadvantage of the solar occultation instruments is the impossibility of recording during the night time. This is a limitation especially for the researches in which the comparison among the effects recorded in the two hemispheres is basically. For this reason also a Limb Emission Instrument (MLS) has been used.

The Microwave Limb Sounder flies a board of the polar EOS AURA satellite since 2004. This instrument is able to recorder during night and day conditions. DAM-S utilized that data to retrieve the volume mixing ratio of minor components in order to look for the difference in the response of the atmosphere to SEPs during the winter and summer condition. Verronen et al. (2005) found an enhanced ozone diurnal variability above 45 km, while they were investigating the October-November, 2003 SEP events. In order to emphasize the results DAM-S used only data at the same local solar time (LST: 7.67 hr/SZA: ~ 108° at North and 19.67 hr/SZA: ~ 72° at South) at the top of the satellite's orbit (geographic latitude 81°) to avoid ozone variability connected to the different SZAs (able to mask solar proton effects on the atmospheric ozone).

The induced ozone depletion is most pronounced and long lasting in the Northern region; at about 65 km, it was recorded the maximum depletion of 1 ppmv (over 60 % of the pre-event level) on January 18 and 0.4 ppmv on January 21-22. These results are consistent with Seppälä et al. (2006) conclusions.

In the Southern hemisphere, instead, a weaker SEP-induced modulation can be observed, with minimum values on January 17 and 20.

These findings are confirmed by Fig. 4.3 displaying MLS ozone mixing ratio at Northern and Southern Hemisphere in the second half of January 2005, evaluated in the altitude range of 20–75 km (the satellite instrument recorded data with 93˚<SZA<118˚ at North and 61˚<SZA<87˚ at South). About 250 profiles per day were available in the selected latitude intervals (75°–82°). In all the following figures the atmospheric MLS data trends are presented, as running averages of the real data, calculated on roughly 200 profiles. The standard deviation (SD) for the O_3 profiles is roughly 5–10 % for the stratosphere and 15–30 (50) % for the mesosphere in the night (day) hemisphere.

The panel on the left side shows ozone data collected in the Northern Hemisphere roughly between 75˚–82˚ geographic latitude; on the right side, the data for the South side in the same range of latitude are reported. The existence of a mesospheric ozone maximum at about 70 km, before and few days after the occurrence of the SEP events is clearly visible (left side).

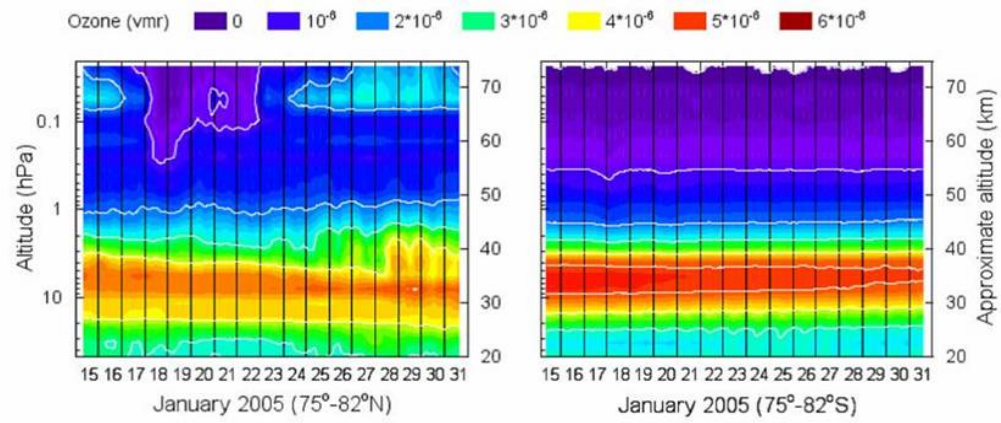

Fig. 4.3 - *Temporal evolution of averaged values (75°–82° N and S) of atmospheric O_3 volume mixing ratio (vmr) for the investigated January 2005 SEP events (North 93°<SZA<118° and South 61°<SZA<87°). Adapted from DAM07.*

In the mesosphere the ozone concentration is mainly a function of the effectiveness of catalytic cycles involving HO_x components. Moreover, above approximately 70 km the main source of odd hydrogen species is the photolysis of H_2O, especially by the absorption of Lyman-alpha radiation (Crutzen, 1997). Therefore, in the upper mesosphere-lower thermosphere (roughly above 90 km) the presence of a secondary ozone maximum can be explained by the decrease in the photolysed H_2O, which leads to the ozone rise further enhanced by thermospheric atomic oxygen. In a similar way it is possible to explain the existence of the so-called "third ozone maximum" (Marsh et al., 2001; Degenstein et al., 2005) in the mesospheric winter hemisphere at high latitudes and at about 72 km of altitude. In fact, during the night state, the reduced production of HO_x components facilitates the increase in the ozone concentration, but during the "day" such an increase is prevented. The presence of the third ozone maximum in the winter hemisphere makes it easier to highlight the ozone depletion related to solar particle events.

The mesospheric ozone depletion in the Northern Hemisphere seems to persist from 17 to 23 January with a maximum intensity and vertical extension during 18 January. A secondary maximum depletion appears roughly from the end of 20 January to the middle of 21 January. Because of minor proton fluxes at lower energies (hitting the upper Earth's atmosphere) for the 20 January SEP event in comparison to the 17, the effects on the mesosphere are more limited (however the 20 January SEP event reached relativistic energies and stratospheric effects cannot be excluded).

The theory suggests that ozone depletion is mainly related to the odd hydrogen rise until about 1 hPa, in agreement with past studies (see Lary, 1997) and observable results (Rohen et al., 2005).

At lower altitudes (stratosphere) the long lasting ozone depletion is connected to the odd nitrogen species rise (see Lary, 1997; Jackman et al., 2005). A decrease in the stratospheric ozone is present in the MLS January 2005 data but it seems to start before the 17 January SEP event (see also Fig. 4 of Seppälä et al., 2006), although an increment in the depletion appears after the 20 January GLE.

The condition of the Southern Hemisphere is very different. First of all, the poor concentration of ozone in the mesosphere makes it difficult to clearly identify an ozone decrease. Nevertheless, it is possible to note a weak ozone decrease at about 0.1 hPa, as well as in the stratosphere during the 17 and 20 January SEP events (in agreement with the short depletion [<12 h] underlined by DAM06 at the edge of the polar region of the Southern Hemisphere by using SAGE II and POAM III data).

As above pointed out, during the SEP events of January 2005 for the first time a satellite's instrument has been able to make measurements of HO_x species. The left side of Fig. 4.4 shows the OH temporal evolution for ~75°-82° N (upper panel) and S (lower panel) for 15-24 January 2005. In addition, the right side shows the OH temporal evolution at the same latitudes with OH values reported in linear scale in two different altitude ranges (~40-60 and ~60-80 km) between 15 and 31 January. The SD for the OH profiles is roughly 30% in the mesosphere and 20 (>50) % in the stratosphere on the day (night) hemisphere.

As expected, if the component concentration is low the uncertainty increases. The sudden and intense OH enhancement evidences the goodness of expectations from available models (i.e., Verronen 2006). The OH concentration raises several hundreds of % at Northern latitudes, whereas it remains almost constant at Southern ones (only a weak modulation is present).

The reason for this behavior can be explained by taking into account the OH concentration in the mesosphere. The main reservoir of mesospheric odd hydrogen species is the water vapour that exhibits a strong seasonal cycle, with summer concentrations [~8 ppmv] higher than in winter [~1 ppmv] (Hervig et al., 2003). In the lower mesosphere and stratosphere the main OH source is the reaction of water vapour with metastable oxygen $O(^1D)$. In the high mesosphere the main OH source is water photolysis. Therefore in the night hemisphere, near polar night termination, the low water vapour and $O(^1D)$ content and the weak photolysis process lead to a weak background concentration of OH (see Crutzen, 1997; Seppälä et al., 2006; Canty et al., 2006); it follows that the abrupt rise associated with the solar particle flux can be easily identified. In the day hemisphere, however, the high background of HO_x may hide the increase induced by SEP events.

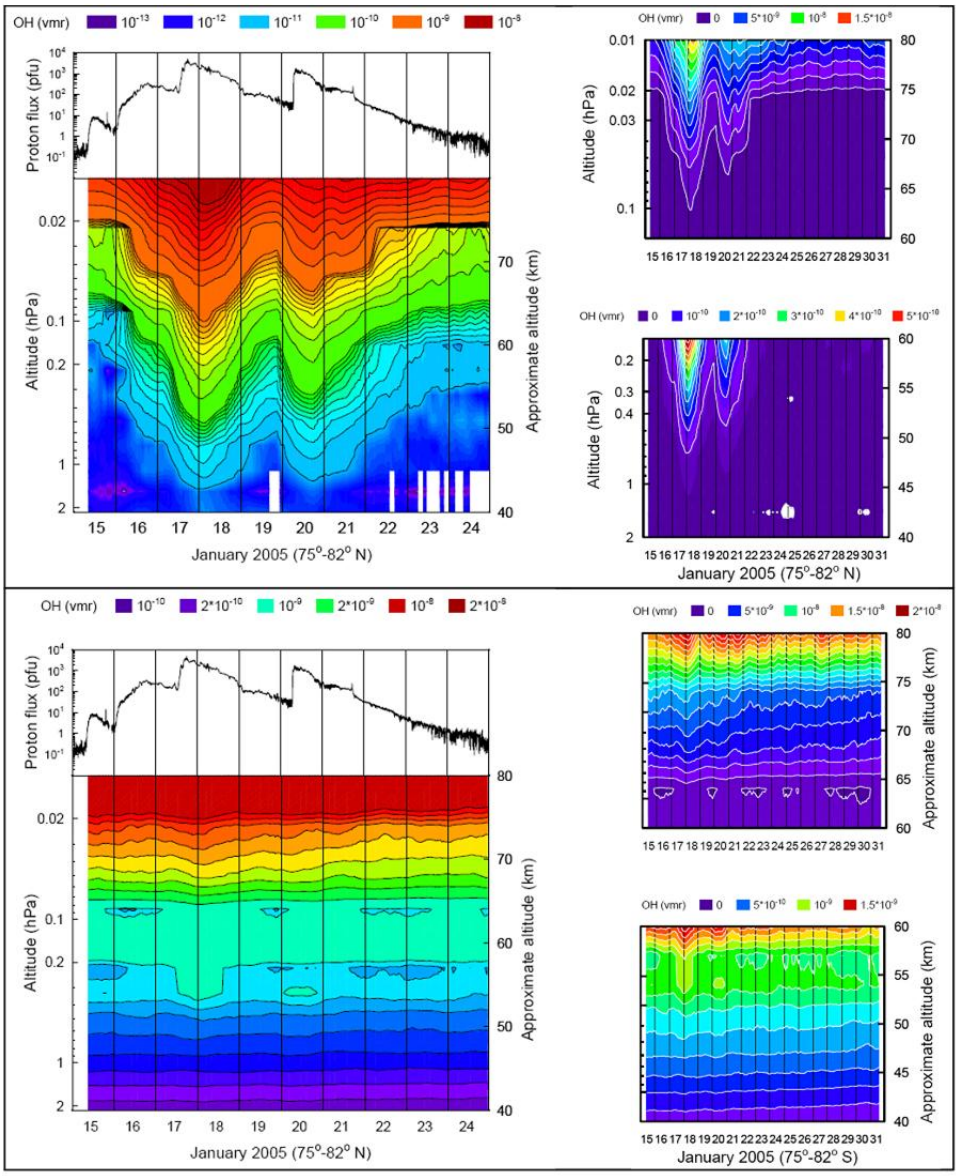

Fig. 4.4 - *Left side: solar proton flux (particle energy E > 10 MeV) from GOES 11 data and contours of OH values (volume mixing ratio) from MLS/EOS data for ~75°-82° N (upper panel) and ~75°-82° S (lower panel) between 15 and 24 January. Right side: similar at left side but the values are reported in linear scale, in two different altitude ranges and the investigated period is 15-31 January. Adapted from SD07and DAM07.*

During January the mesospheric OH background concentration is about 1 ppbv in the Northern hemisphere. When SEP events occur on 17 and 20 January a suggestive increase of OH, more intense at elevated altitudes, is recorded. It is worthwhile to note that the OH concentration reaches the maximum intensity almost at the same time as the solar proton peaks (between 17 and 18 January and in late 20 January). The OH increase in the darker hemisphere is more intense and long lasting: at about 75 km the OH mixing ratio is 10 ppbv and reaches almost 12 ppbv at

80 km (provided that data are averaged and the OH peak is smoothed). In the upper stratosphere-low mesosphere a sudden rise of the hydroxyl radical is also visible. The OH background mixing ratio is very low (between 0.01 and 0.1 ppbv). Above 55 km the OH mixing ratio is almost 0.5 ppbv during the SEP event. Overall, the hydroxyl radical mixing ratio increases by almost one order of magnitude in the upper mesosphere and 100-400 % (from lower altitudes to higher) in upper stratosphere. The impact of 20 January SEP event on the atmosphere is less intense but of the same order of magnitude both in the mesosphere and stratosphere.

In the summer hemisphere the OH background mixing ratio is noticeably higher and the variations connected to SEP event are not very impressive and have short length. In addition, the OH peak occurs also in the Southern hemisphere at the same time (Fig. 4.4).

It is interesting to observe that during the SEP events the OH mixing ratio of the dark hemisphere is almost similar to the OH background of the day hemisphere.

In the northern hemisphere the mesospheric OH rise starts on 16 January and finishes on 22 January, coinciding with the period of the strong ozone depletion. Because of the running average procedure performed on the MLS dataset it is not trivial to estimate the delay between the OH rise and ozone depletion. We estimated a delay of approximately 12 hours in the “night” hemisphere whereas it is almost contemporary in the “day” hemisphere, where the photolysis is more active.

The MLS instrument cannot measure atmospheric NO_x but it is able to retrieve nitric acid, a good proxy for NO_y (reservoir nitrogen). During January 2005 SEPs, along with stratospheric ozone depletion, an HNO_3 increase appears between 10 and 2 hPa (30-40 km), persisting till the end of the month. Figure 1 (lower panel) of SD07 shows its temporal evolution (location: ~ 75˚-82˚ N) by using derived HNO_3 (mixing ratio) contours, from 15 to 31 January 2005.

This increase of nitric acid can originate from three different processes. The former involves the most important HNO_3 production phenomenon:

$$NO_2 + OH + M \rightarrow HNO_3 + M \qquad (2.21)$$

Therefore, the HNO_3 increase can be the result of the OH and/or NO_2 raise during SEPs; this reaction is fast enough to produce the amount of nitric acid similar to that observed during October November 2003 GLE/SEP events (López-Puertas et al., 2005).

The other two processes are related to the ion chemistry (Solomon et al., 1981) and may be important since they are active also during night time (i.e., winter hemisphere at elevate latitudes). In fact through the reaction of water cluster ions with NO_3 and N_2O_5 the nitric acid is able to rise. It should be interesting to search for

the variability of NO_2, NO_3 and N_2O_5 during the investigated period to identify the right path of HNO_3 rise. Anyway the pathway involving the reaction with N_2O_5 is probably too slow (~ 2 weeks) to explain the rapid HNO_3 rise recorded.

Nevertheless, the elevate photolysis in the summer hemisphere prevents to single out the HNO_3 variability for the January GLE/SEPs. In fact in the lower stratosphere HNO_3 can be photolysed by UV radiation with $\lambda < 280$ nm and in this way the NO_x radicals are regenerated.

The raise of hydrogen species connected to SEPs was pointed out also during the event of October-November 2003 by von Clarmann et al. (2005). To reach this goal they utilized, as proxy data, ClO, HOCl and $ClONO_2$ volume mixing ratio coming from MIPAS-ENVISAT. A short term increase of all these components, proof of HO_x rise, was evidenced. For this reason also other chemical components from MLS-AURA was investigated during January 2005.

Figure 4.5 shows the contours of HCl volume mixing ratio during the second part of January 2005 at ~ 75°-82° N. The values are reported as differences from the January 15 average, between 30 and 0.15 hPa (~24-60 km). A sudden HCl decrease is clearly visible after the first SEP event with peak at about 1 hPa (~ 50 km) on 18 January. Then a second most intense drop off occurs after the GLE N° 69 event and the peak is at about 3 hPa (~ 37 km) on 21 January. Since the HCl can be destroyed by reaction with OH, $O(^1D)$ and $O(^3P)$ (in addition to photolysis process with $\lambda < 220$ nm) it is not difficult to suggest that in this case the HCl decrease (see Fig. 4.4) can be explained by the following path:

$$OH + HCl \rightarrow H_2O + Cl \qquad (4.1)$$

essentially caused by the OH rise. Probably the second event has further decreased the HCl volume mixing ratio, especially at lower altitudes because of the higher energies involved in the SEP event of 20 January as to 17.

Therefore an increment of reactive Cl molecules due to Reaction (4.1) should be present. The ClO_x catalytic cycle is one of the most effective O_3 loss cycle at about 40 km (see Lary, 1997):

$$Cl + O_3 \rightarrow ClO + O_2$$
$$ClO + O(^3P) \rightarrow Cl + O_2$$
$$\text{Net: } O + O_3 \rightarrow 2O_2 \qquad (2.34)$$

Even if the lack of solar light prevents the $O(^3P)$ formation, the first part of the cycle should be at work. A short term O_3 depletion and ClO raise could occur by:

$$Cl + O_3 \rightarrow ClO + O_2 \qquad (4.2)$$

at least until the period subjected to SEP events (see von Clarmann et al., 2005).

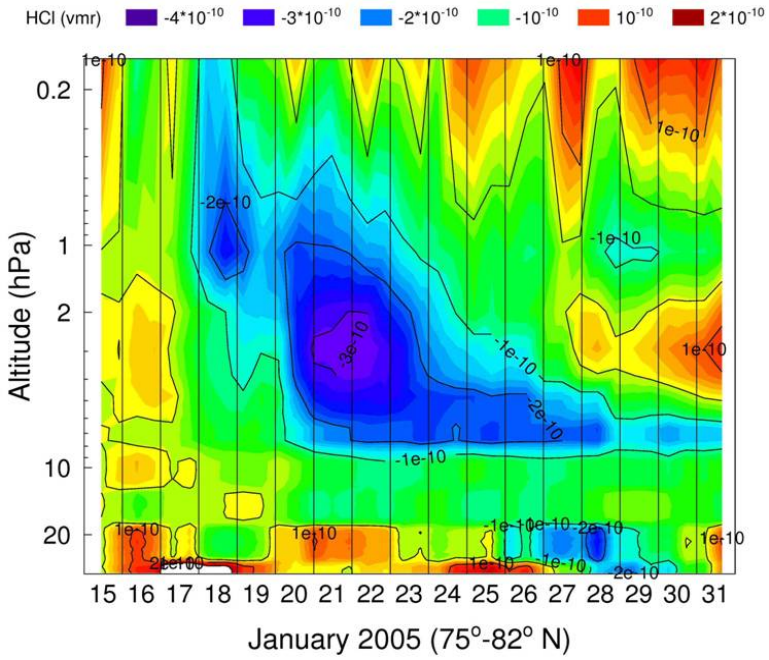

Fig. 4.5 - *Contours of HCl volume mixing ratio during the second part of January 2005 at ~ 75°-82° N. The values are reported as difference regards January 15 average.*

The Fig. 4.3 shows a weak trend of the O_3 decrease around about 2 hPa, but is not possible to assert that it depends on Cl molecules. To solve the problem related to the creation of atomic chlorine from HCl and no contemporary O_3 destruction the following pathway, increased by the presence of HO_2 radicals produced by SEPs, could be formulate:

$$Cl + HO_2 \rightarrow ClO + OH \qquad (4.3)$$

The final result is the creation of ClO with no contemporary ozone loss (see Brasseur and Solomon, 2005, pp. 364-372). The low quality of ClO data recorded by MLS instrument in January 2005 night hemisphere hides its real behavior. Anyway it is possible to single out a sudden decrease of ClO between about 1 and 3 hPa (here not shown) after each SEP event investigated. It is particularly evident on 18-19 and 21-22 January (on 20 January there is a weak ClO recovery).

The decrease of ClO at about 2 hPa (~ 40 km) and the contemporary increase of HOCl (see Fig. 4.6) seem to suggest the following pathway:

$$ClO + HO_2 \rightarrow HOCl + O_2 \qquad (4.4)$$

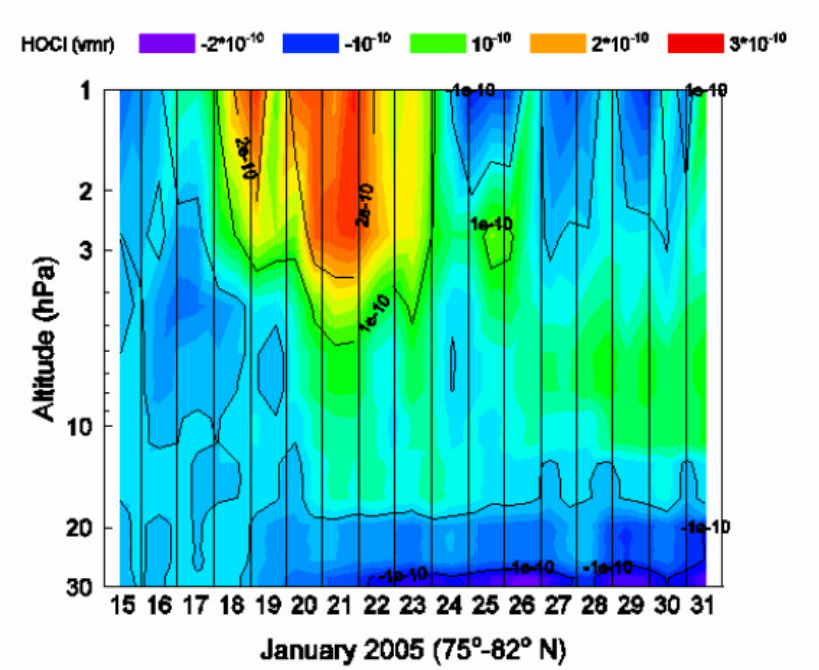

Fig. 4.6 - *Contours of HOCl volume mixing ratio during the second part of January 2005 at ~ 75°-82° N. The values are reported as difference regards January 15 average.*

The raise of HO_x species makes possible the transformation of Cl molecules from inactive to active species (HCl → Cl → ClO, the last one via O_3 and/or HO_2 path) and from active to inactive (ClO → HOCl) with HOCl peak on the day after the SEPs occurring. Moreover, the ClO decrease coincides with the peak values of HOCl (~0.2-0.3 ppbv). even if the amount of ClO lossed (not shown) is lower than the amount of HOCl increased. In addition the HOCl peaks at 1 hPa and 3 hPa on 18 and 21 January respectively, correspond to lower values of HCl (Fig. 4.5).

Finally the increase of HOCl arises from the contemporary decrease of HCl and ClO, even if it is not clear how the Cl molecules of hydrogen chloride (HCl) could add to the hypochlorous acid (HOCl) without evident rise of chlorine monoxide.

Moreover, the further increase of HOCl at lower altitudes (below 2-3 hPa, where not ClO decrease seems to be documented) could be possible through reaction of $ClONO_2$ with hydrogen radicals (see Brasseur and Solomon, 2005, pp. 364-372):

$$ClONO_2 + OH \rightarrow HOCl + NO_3 \qquad (4.5)$$

4.2 - May 2005

4.2.1 Overview

The influence on the polar atmospheric chemistry of the solar proton event of May 2005 was investigated only by MLS instrument. Its flux for the channel with energies > 10 MeV is comparable to the one for the SEPs registered during January 2005,

even if its spectrum does not reach relativistic energies.

Figure 4.7 shows the time-intensity profiles of the soft X- ray and the proton fluxes, in the three energy intervals available from GOES series, for the May 2005 SEP event.

The onset time of the SEP event was observed on 14 May 2005 at 05:25 UT, with a peak value of $1.90 \cdot 10^3$ pfu (hourly data of channel > 10 MeV) on 15 May at 03:30 UT, following the CME shock arrival. It was associated with the M8.5 flare occurred on 13 May at 16:57 UT, produced in the active region NOAA 759 along with type II and Type IV radio sweeps as well as a bright full halo CME. Nevertheless, the contribution of the most energetic protons is very small, with maximum flux values of 0.58 and 0.14 at > 50 MeV and > 100 MeV, respectively.

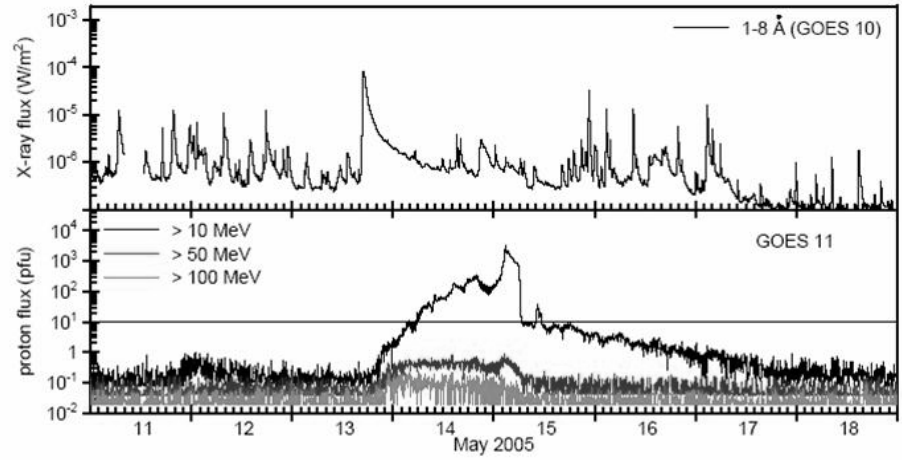

Fig. 4.7 - *Time-intensity profiles of the soft X- ray (upper panel) and the proton fluxes (lower panel), in the three considered energy intervals, for May 2005 SEP event.*

4.2.2 Chemical variability

In the night hemisphere (South side, SZA > 99°) the presence of the third ozone peak can be seen in Figure 2 reported by DAM07 (middle panel) just before the SEP event occurrence. After the arrival of the solar protons into the Earth's atmosphere and the starting of HO_x catalytic cycles, the third ozone peak is destroyed at least during 16 May and much of 15 and 17 May 2005. No EOS MLS data were available for 18 May but we note the reformation of a less intense ozone peak starting from 19 May. In the stratosphere a feeble ozone depletion can be noted at altitudes of about 50 km, although the May 2005 SEP event was not so intense as other SEPs studied in the past and the darkness of the Southern hemisphere may suggest no effectiveness of the NO_x catalytic cycle for the ozone destruction.

The trend of the ozone during the investigated period can be highlighted as follows: the first one, in the mesosphere (already described) and the second one, in

the stratosphere, that starts on 14 May and lasts up to few days after the recovery of the mesospheric depletion. The latter does not seem to be related to the HO_x rise (see Fig. 3.10 for the OH variation in the mesosphere) because of the low altitude and the difference relative to the mesospheric depletion. As pointed out by Lary (1997) the effectiveness of the NO_x catalytic cycle is maximum at about 45 km and, for this reason, it is possible to distinguish a different trend of depletion roughly above and below 50 km (see also Rohen et al., 2005). In the day hemisphere (65º<SZA<80º) no effects on the ozone layer can be detected.

Figure 4 by DAM07 shows the response of the hydroxyl radical for the May 2005 SEP event. The Northern hemisphere is shown on the left side and the Southern one on the right. After the SEP event of 14 May the odd hydrogen species exhibit some changes. In the darker hemisphere the OH variations are not as large as in January but are still strong enough to destroy the third ozone maximum (see Fig. 2, middle panel, by DAM07). Moreover, the increase seems to involve only the mesosphere. The reason maybe twofold: i) the considered SEP event has a very low content of high energy particles that results in a smaller perturbation of the lower atmospheric layers; ii) at low energies the fluence is smaller in comparison to the other analysed SEP events, even if the peak value is similar.

The OH background mixing ratio for the Southern hemisphere is roughly 1 ppbv (below 75 km), similar to that observed during January 2005 at the North side, but the maximum rise is only about 8 ppbv (at 80 km) instead of 12 ppbv. The effects of the solar protons on the odd hydrogen species are moderated in the summer hemisphere and the maximum rise happens roughly on 15 May for both hemispheres.

4.3 - September 2005

4.3.1 Overview

The influence on the polar atmospheric chemistry of the SEP registered during September 2005 was investigated only by using data from MLS instrument. The SEP flux for energies > 10 MeV (~$1.88 \cdot 10^3$ pfu, hourly data) is comparable to the one observed during January 2005 SEPs. During September 2005 the SZA of the MLS data have intermediate solar light condition.

NOAA region 808 produced a major X17 flare, peaking at 17:40 UT on 07 September. Strong type II and IV radio sweeps and a very large and fast CME were recorded; the intense proton storm at >10 MeV started at Earth on 8 September at 02:15 UT with a maximum on 11 September at 04:30 UT. The SEP intensification includes also high energy protons up to >100 MeV (peak value 7.63 pfu) despite the location of the solar source (89°E). As a matter of fact, it is extremely rare to see 100

MeV protons from a source on or near the east limb. However, we should note that the period with enhanced particle flux contains a large series of X-class bursts, which were not separated (see Fig. 4.8).

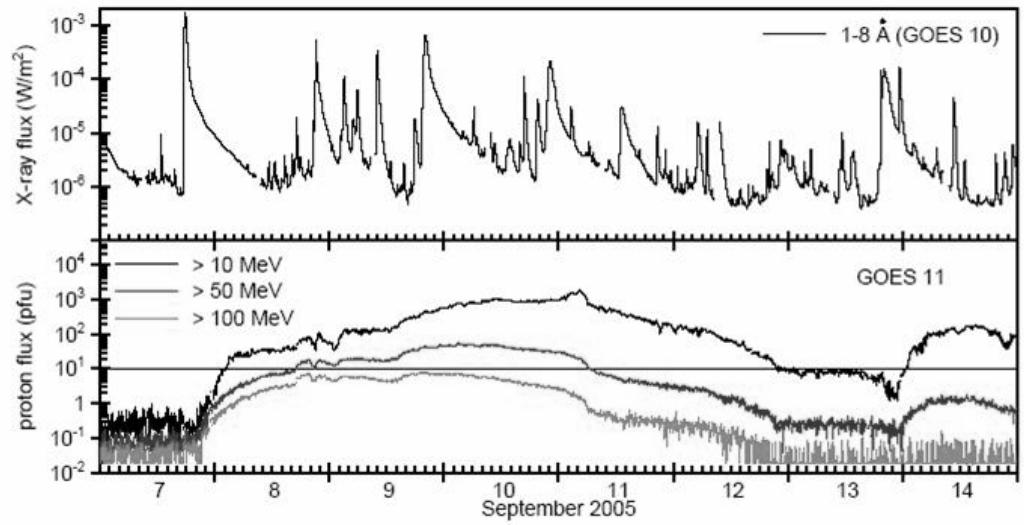

Fig. 4.8 - *Time-intensity profiles of the soft X- ray (upper panel) and the proton fluxes (lower panel), in the three considered energy intervals, for September 2005 SEP event.*

4.3.2 Chemical variability

In September, the background of the mesospheric ozone mixing ratio in the Southern hemisphere [springtime] seems to be higher than the one for the Northern hemisphere.

The ozone temporal evolutions reported in Fig. 4.9 are related to the 8 September 2005 SEP event; they seem to confirm the interpretation of the previous SEP effects.

The September sun light is fairly similar in both hemispheres. Particularly, the solar zenith angle of the satellite's measurements is: 68º<SZA<94º for the north side and 85º<SZA<111º for the south; that is the reason of the roughly similar atmospheric response to solar protons.

However for the darker hemisphere (South) the mesospheric ozone depletion is more evident since the ozone mixing ratio, before the SEP event, is more elevated than for the Northern hemisphere.

Also in the stratosphere the depletion is more evident and long lasting in the Southern hemisphere. The maximum ozone decrease occurs on 10 September in both hemispheres.

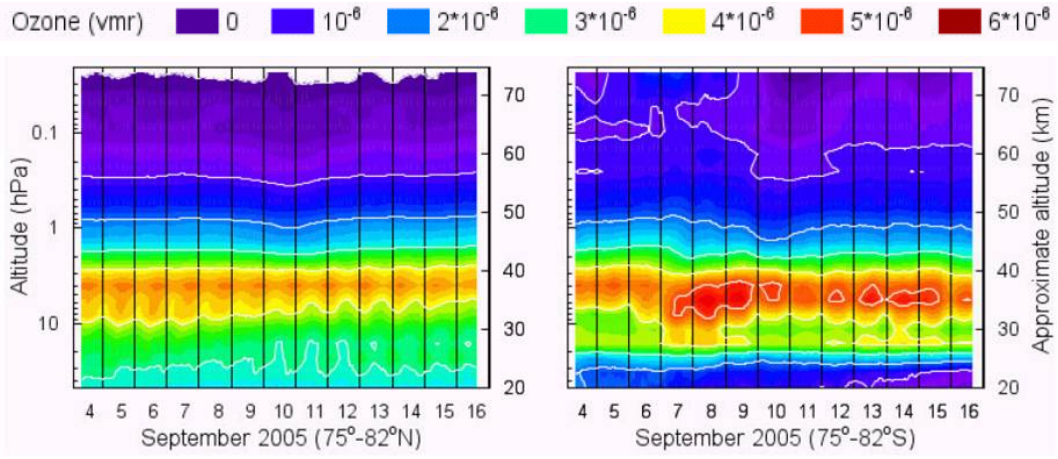

Fig. 4.9 – *Temporal evolution of averaged values (75°–82° N and S) of atmospheric O_3 volume mixing ratio (vmr) for the investigated September 2005 SEP events (North 68°<SZA<94° and South 85°<SZA<111°). The left side reports the Northern Hemisphere and the right the Southern Hemisphere. Adapted from DAM07.*

Figure 5 by DAM07 shows the response of the hydroxyl radical to the September 2005 SEP event (the Northern hemisphere is shown on the left side and the Southern one on the right). The time history of the data refers to two different altitude ranges for each hemisphere (roughly 40-60 km at the top and 60-80 km at the bottom), since there is a difference of about an order of magnitude on the OH mixing ratio between the mesosphere and the upper stratosphere (note the different OH colour scale).

The 8 September 2005 SEP occurs in a different seasonal condition if compared with previous events. In fact, the inter-hemispheric variation of the solar illumination is not very large like for the previous SEP events. The background of the mesospheric (stratospheric) OH mixing ratio is few ppbv (< 0.1 ppbv) for both hemispheres. Its variability is more evident in the darker hemisphere (South) where, above 75 km, it is also discernible a small rise due to a new moderate increase of the proton flux on 14 and 15 September. In addition the increase of odd hydrogen species, represented by the OH proxy, is apparent also in the stratosphere at least up to 50 km, where it becomes less evident since it is masked by the seasonal trend.

4.4 - December 2006

4.4.1 Overview

The used atmospheric data come from the MLS instrument of Aura satellite. Even if with minor flux intensity, the pair SEP + GLE of December 2006 is similar to January 2005 ones and it is interesting to make some comparisons.

An elevated solar activity is recorded during December 2006 even if the solar cycle 23 is approaching its end. From the active region NOAA/USAF 10930 four flares of X class and two SEPs occurred between 5 and 14 December 2006. The first

SEP event (E > 10 MeV) began at 06/1555 UTC and reached a flux maximum of 1980 pfu at 07/1930 UTC; the second one began at 13/0310 UTC and reached a flux maximum of 698 pfu at 13/0925 UTC (see Fig. 4.10). Moreover, the last event produced relativistic energies and it was recorded as the GLE n. 70 by the world wide network of neutron monitors.

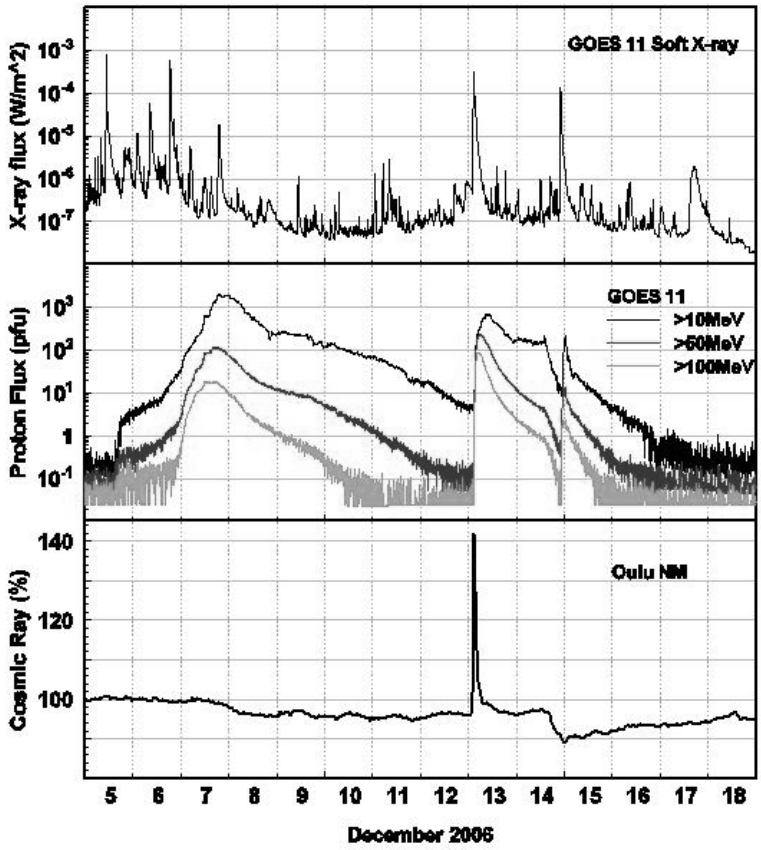

Fig. 4.10 – *From the top to the bottom: soft X ray, proton flux at different energies (>100, >50, >10 MeV) from GOES 11 and cosmic rays (%) from Oulu neutron monitor.*

4.4.2 Chemical variability

The 7 December 2006 SEP induced the ozone depletion in the mesosphere mainly through HO_x molecules. The second SEP event (13 December 2006) produced limited effects in the mesosphere, because of the minor flux and fluence at lower energies. The O_3 decrease is most intense in the night hemisphere (see Fig. 4.11).

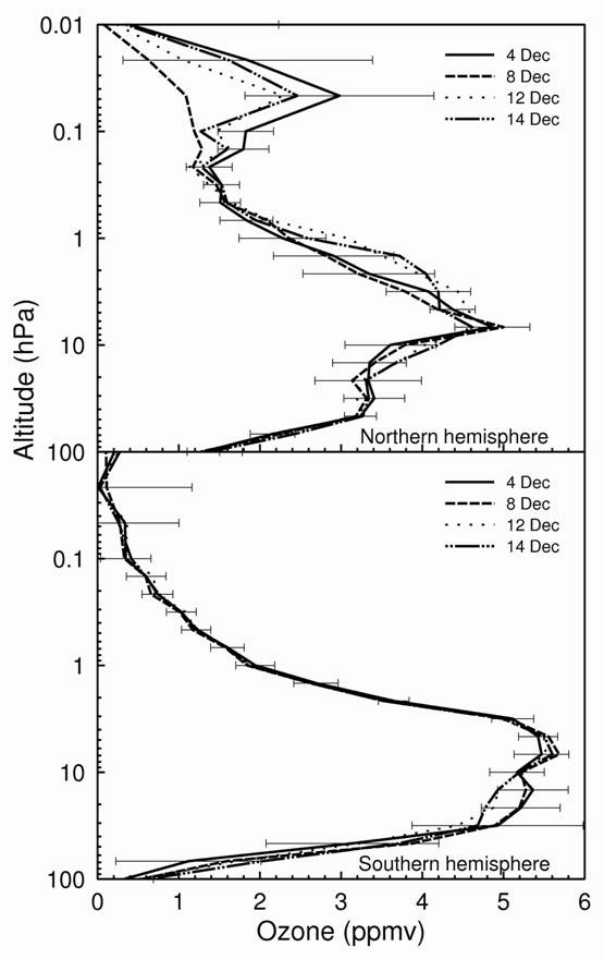

Fig. 4.11 - *Daily vertical profile of MLS ozone volume mixing ratio at 75º-82º latitude North (upper panel) and South (bottom panel).*

The ozone decrease in the winter hemisphere is clearly visible after the 7 December 2006 SEP and much less after the 13 December SEP. On the summer hemisphere it is possible to observe only a feeble modulation. The OH rise is documented by the MLS data, but is not reported here because of its low quality.

It is interesting to note that the most intense flux at higher energies of the second SEP event seems to change the ozone concentration at stratospheric altitudes. Fig. 4.12 reports the O_3 MLS real data (not the averages) roughly between 75º-82º geographic latitude North and South in December 2006-January 2007.

Larger fluctuations are present in the Northern hemisphere (light grey) but not in the as to Southern one (dark grey). These features arise from air with different O_3 concentration which enters the polar cap region from lower latitudes.

Even if the daily average hides the ozone decrease in the stratosphere of Northern hemisphere (see Fig. 4.10, upper panel), the minima of O_3 concentration on 14 December are the lower ones of the examined two months. Further, note the descending trend from 7 to 14 December.

In addition, the HNO_3 trend has been examined. As above pointed out, the most important HNO_3 production process is:

$NO_2 + OH + M \rightarrow HNO_3 + M$.

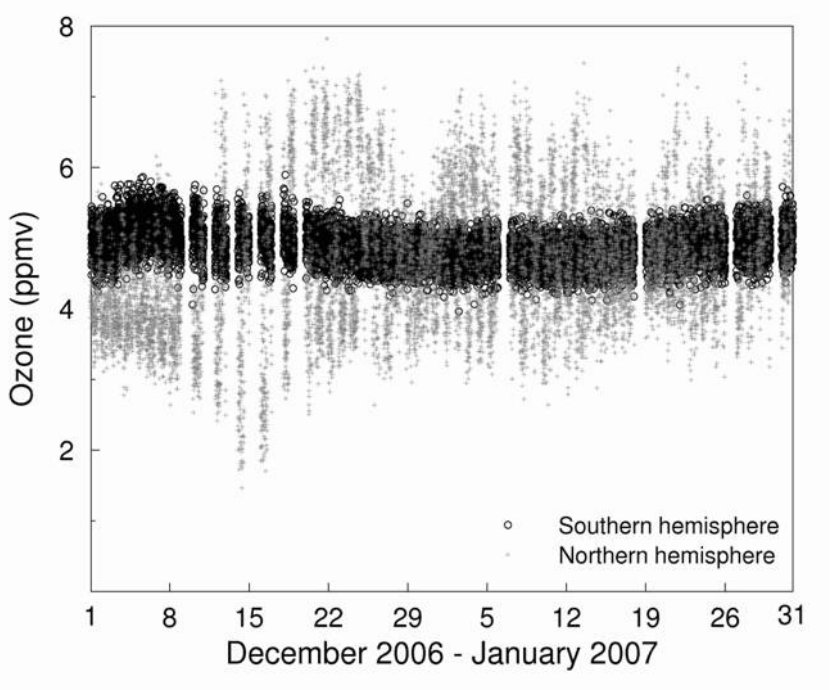

Fig. 4.12 - *December 2006-January 2007 MLS ozone (ppmv) at 3 hPa (75º-82º latitude North and South). Real data.*

Therefore the HNO_3 increase can result from the OH and/or NO_2 raise. The second one is related to ion chemistry and may be important since it is active also during night time (i.e., the winter hemisphere at elevate latitudes). Through reaction of water cluster ions with NO_3 the nitric acid is able to rise.

Fig. 4.13 (left side) demonstrate no remarkable effects during the investigated period. The HNO_3 trend at 2 hPa between December 2006 and January 2007 is compared to the trend observed between December 2004 and January 2005 (right side). In both years some rises of HNO_3 are present. Nevertheless, the increases connected to the SEP events of January 2005 are superimposed over an ascendant HNO_3 trend. De Zafra and Smyshlyaev (2001) showed that sudden HNO_3 rises inside Polar Regions can occur in winter; they are probably linked to the descending air of rich of NO_x molecules from mesosphere. Therefore, the peak values of January 2005 probably are not wholly caused by SEP ionization. Therefore more detailed analyses are need.

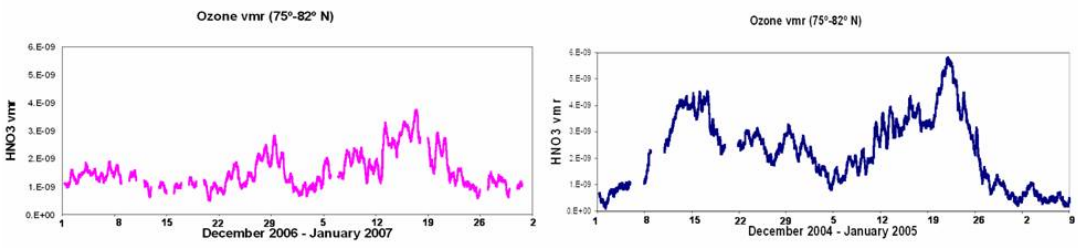

Fig. 4.13 – *December 2006 - January 2007 (left) and December 2004 - January 2005 (right) MLS HNO_3 volume mixing ratio at 2 hPa (75°-82° latitude North and South).*

4.5 - April 2002

4.5.1 Overview

The onset time of 21 April 2002 SEP event was observed at 02:25 (E > 10 MeV) with a peak value of 2520 part·cm^{-2}·s^{-1}·sr^{-1} at 23:20 UTC (see Tab. 1.1). Fig. 4.14 illustrates the temporal development of the Soft X-ray flux (top) and proton flux (bottom).

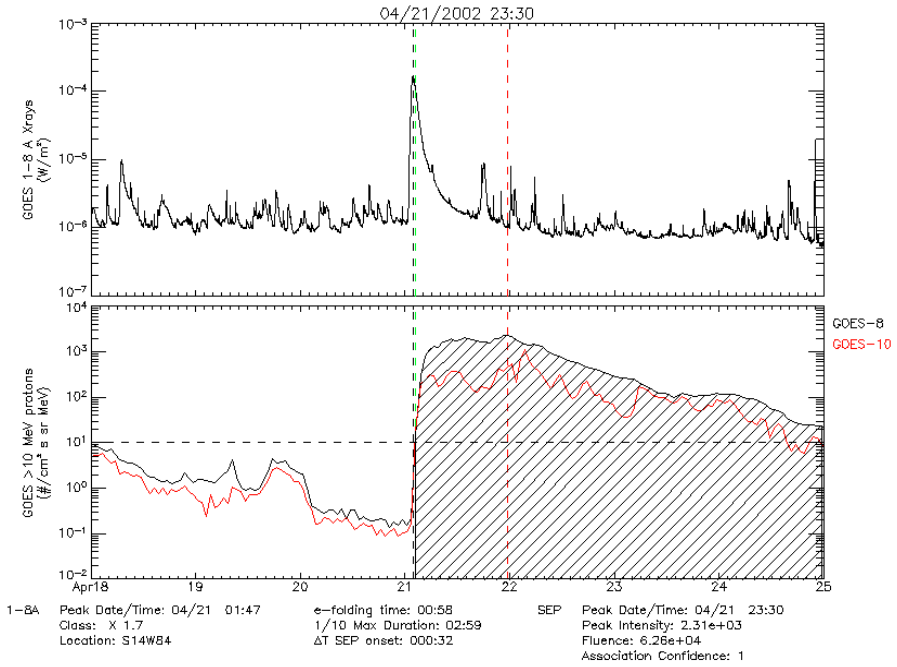

Fig. 4.14 - *Time-intensity profiles of the soft X- ray and the proton flux at > 10 MeV for April 2002 SEP event.*

SR HALOE data coming from UARS satellite between 19 and 27 April 2002 is used to investigate this SEP event. Since the UARS satellite does not have a polar orbit, the recorded data does not allow the simultaneous check of both atmospheric hemispheres. In the period here analysed the geographic latitude of the UARS data coverage is between 67ºN and 76º N. Like for the previous SEP event the data used are those coming after a 15-point running average procedure.

4.5.2 Chemical variability

The inserted panel in Fig. 4.15 (upper right) gives the mesospheric ozone variability (ppmv differences from April 20 ozone average) at diverse altitudes (52 km, 54 km, 57 km and 60 km) from April 20 to 26. It clearly shows four days of ozone depletion, with the maximum value (0.4 ppmv, over 40 %) just after the solar proton flux peak.

The mesospheric O_3 recovery seems to be very slow (four days) particularly if compared to July 2000 SEP event (two days). The reason could be the elevate particle fluence [6.26 x 10^4 particle/(cm^2 sr x 3600), hourly data] for the April 2002 SEP event that, even if lower than the one associated with July 2000 SEPs [3.63 x 10^5 particle/(cm^2 sr x 3600), hourly data], had kept elevated the protons flux value at > 10 MeV for about four days [more then ~100 particle/(cm^2 s sr MeV), hourly data].

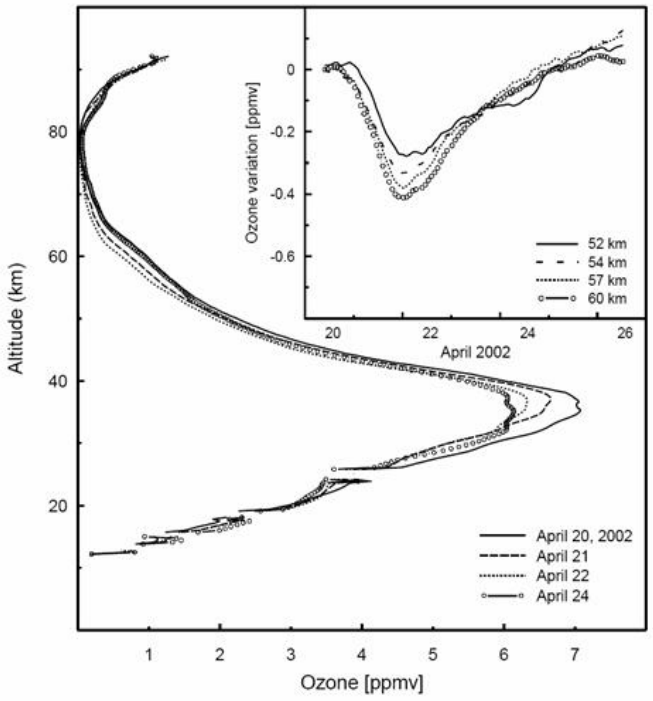

Fig. 4.15 - *Ozone variation during April 2002 monitored by HALOE on board of UARS with data coverage between 67° N and 76° N geographical latitudes. Main panel: mean daily ozone vertical profiles (see legend inside). Inserted panel: O_3 deviation of each measurement from the 20 April average concentration, at different altitudes. From DAM-S.*

Figure 4.15, in the main panel illustrates the daily ozone profile for pre (April 20, 2002) and SEP event days. Again mesospheric ozone depletions can be identified even at low altitudes during the SEPs (~ 1 ppmv) incoming. The short life of odd hydrogen cannot explain the long lasting ozone depletion, but a probably contribution from NO_x rise could lead more ozone destruction.

Indeed, an increase of about one order of magnitude in mesospheric NO HALOE data is found. Fig. 4.16, main panel, highlights the NO trend at least until April 24; it could explain the ozone decrease at similar heights. Moreover a NO_2 rise at lower altitudes peaks on day 24, as for the ozone depletion at similar altitudes.

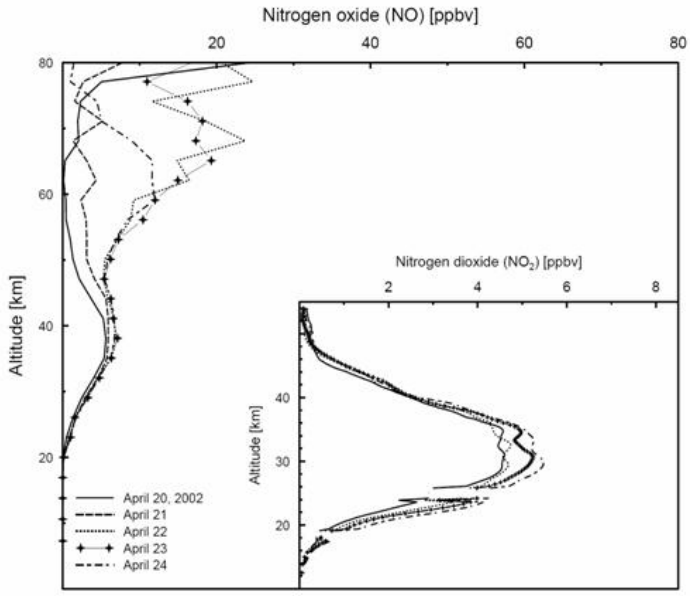

Fig. 4.16 - Vertical *profiles of nitrogen oxide (mail panel) and nitrogen dioxide (inserted panel) during the April 2002 event, monitored by HALOE on board of UARS with data coverage between 67° N and 76° N geographical latitudes. From DAM-S.*

4.6 - July 2000

4.6.1 Overview

The SEP influence on the atmospheric chemistry for July 14, 2000 event is investigated also by using HALOE data. Even if this event was already studied by other researchers (see Jackman et al., 2001; Krivolutsky et al., 2006 and references therein), we chose to analyse it again because it occurred on July, when the solar illumination is approximately inverse to the one for the January 2005 SEPs. In addition, this particle event recorded (E > 10 MeV) a peak flux of about 24000 part.cm^{-2}·s^{-}1·sr^{-1}, i.e. it is the stronger SEP event among the ones analized for the current solar activity cycle. Between July 10 and July 18, 2000 the latitude coverage of HALOE instrument is between 62° N and 66° N (with a maximum at 69° N on July 16).

4.6.2 Chemical variability

Analyses on HALOE data are conduced in similar way to the previous April 2002 SEP event. A strong mesospheric ozone variation is found (see DAM-S). At 60 km of altitude at least a 0.6 ppmv depletion (over 60 %) on ozone records are found, lasting

the depletion about two days. The maximum ozone decrease at altitudes greater than 40 km occurs during the day in which the SEP event maximizes and that stresses the quick response of the atmospheric chemistry to solar protons coming during day state.

In addition, daily NO and NO_2 profiles recorded during the investigated period highlight an outstanding NO increase above ~ 40 km and a minor NO_2 rise between 40 and 50 km is also emerging. There is a NO_2 increase at about 32-35 km, probably related to the different geographic latitudes of the data coverage for the considered days; therefore, it should not depend on the SEP occurrence but on the satellite position.

It is important to emphasize that since a strong ozone destruction was not observed after the January 2005 SEPS in the summer hemisphere (only a feeble and short depletion was pointed out) whereas it was recorded in the winter one, the intense O_3 depletion at sunlight polar latitudes of July 2000 presupposes a more intense mesospheric depletion in the night hemisphere (contrary to predictions of past models for the chemistry of the terrestrial atmosphere). Present experimental results will help to construct more reliable theoretical models.

4.7 - May 2003

Even if SEPs are able to enhance the production of nitrogen species at Polar Regions, it must be taken great attention for the evaluation of atmospheric effects especially during minor solar particle events. A huge increase of odd nitrogen species at elevated latitudes has been recorded in June and July 2003. Hauchecorne et al., 2006 underlined, from data obtained by the stellar occultation GOMOS instrument, that a sudden rise of NO_2 (proxy of NO_x) occurred in the high latitudes of the southern hemisphere during the winter. The instrument made measurements of night time NO_2 vmr from the troposphere up to 50 km from April to September 2003 but not in May. The winter downward dynamic of the vortex led to descend air with elevated NO_2 amounts toward the lower stratosphere. Peak values more than 20 ppbv between 60º and 80º S were observed above 35 km in July. This behavior has been confirmed by the solar occultation HALOE instrument.

Figure 4.17 reports the day time NO vmr (proxy of NO_x) for the last solar cycle from 1996 to 2005 at latitudes roughly between 30º S and 50º S from 30 km to 65 km in May, June, July and August (the climatology is reported in black and the 2003 in red).

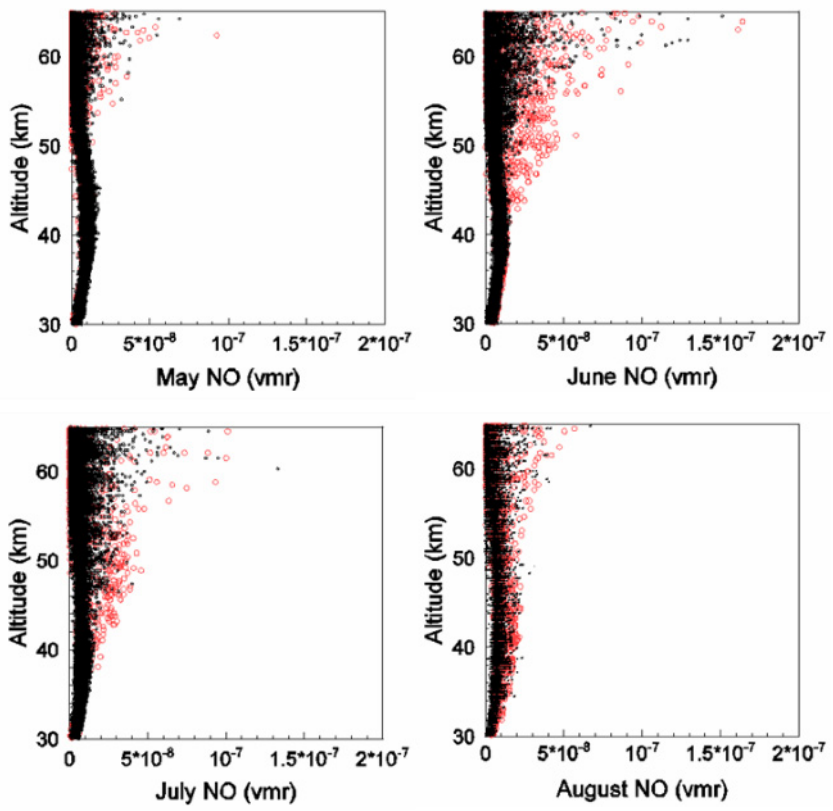

Fig. 4.17 - *NO vmr for the last solar cycle from 1996 to 2005 at latitudes roughly between 30° S and 50° S in May, June, July and August (the climatology is reported in black and the 2003 in red).*

The latitudinal coverage of the data changes a little from one year to the others, but does not exceed ~50° S (not data are recorded during the winter at elevated latitudes of southern hemisphere since there is not solar light). See the Tab. 4.1 for the latitudinal coverage of NO HALOE data used.

Tab. 4.1 – *Latitudinal coverage of the HALOE data used in Fig. 4.21.*

MONTH	LATITUDE of NO HALOE data
May	From 30° S to 50° S
June	From 30° S to 48° S
July	From 30° S to 50° S
August	From 30° S to 58° S

Fig. 4.17 suggests the sudden increase of NO vmr above 45 km in June 2003, which persists at lower altitudes in July and with a smaller amount in August. The recorded NO peak value is ~ 20-25 ppbv. In addition, a NO enhancement, larger than the one derived from climatology, seems to start in May 2003 at about 70 km.

It is important to highlight that in the polar cap ionospheric regions an additional ionization is occasionally present during the winter and it leads to NO_x production. The photodissociation by EUV and “hard” X rays (ionization source) is not possible because of the lack of solar light. The cause of the NO_x rise are the so-called Energetic Particle Precipitations (EPPs) [see Randall et al., 2007, 2006, 2005; Clilverd, 2006 and references therein], linked to the Relativistic Electron Precipitations from the radiation belts and Auroral Proton and Electron Precipitations in the sub-auroral latitudes which occur in the MLT zone during the winter. All the energetic particles above-mentioned are able to increase the ionization in the ionosphere D region. Therefore the elevate values of NO between 30º S and 50º S could come from more elevated latitudes (> 60 Sº) and altitudes (MLT zone) after the transport processes.

Hauchecorne et al., 2006 highlight that on 29 May 2003 a modest SEP event occurred. Even if it was of negligible intensity [the peak flux > 10 MeV reached 76.3 pfu and its fluence 487 part./(cm^2 sr x 3600), hourly data] they suppose that its elevate flux at low energies [peak ~$3 \cdot 10^4$ part./(cm^2 ·s·sr) in the band 0.8-4 MeV] should be able to ionize the mesosphere and increase the NO_x molecules. There the strong adiabatic descent path of the southern polar vortex moves the odd nitrogen species toward the upper stratosphere.

Anyway, HALOE data confirmed that an elevate amount of NO molecules was already present above ~ 60 km in May (not shown). Further, the utilized data refer to 3-12 and 21-28.5 May when the satellite recorded measurements inside the range 30º-50º S, therefore before the occurrence of the SEP event (the last days of May 2003, the HALOE instrument was at latitudes < 30º S, i.e. outside the main regions involved by EPP ionization).

Finally, the large amount of odd nitrogen species observed during June and July 2003 appears to be related rather than to the solar energetic protons, to other EPP like electrons (and protons in minor percents) of auroral origin that occur throughout the solar cycle. They provide a continuum (but fluctuating) source of NO_x to the lower thermosphere and mesosphere (see Randall et al., 2007, 2006; Clilverd, et al., 2006, Callis et al., 1996). Moreover, the stability of the atmospheric vortex determines if this produced NO_x can go down towards the stratosphere.

Chapter 5

RESULTS AND DISCUSSION

In order to investigate the influence of Solar Energetic Particle events on the minor components of the polar atmosphere, several SEP events have been analyzed: July 2000, April 2002, May 2003, January 2005, May 2005, September 2005 and December 2006. The considered SEP events are among the most intense events recorded in the current solar cycle (see Tab. 1.1). Except for July 2000 and May 2003 SEP events, the proton (E > 10 MeV) flux is of comparable magnitude. The event of July 2000 is the largest one (maximum flux: 24000 pfu), whereas the May 2003 event is the lighter one (121 pfu).

The 2005 and 2006 SEP events have been analyzed by using data from the limb sounder instrument (called MLS) on AURA satellite, looking for variabilities in the O_3, OH, HNO_3, H_2O (and ClO, HOCl, HCl for January 2005 only). The SEP events of 2000, 2002 and 2003 have been examined by using data from the solar occultation instrument (named HALOE) on UARS satellite and the investigated components have been the following: O_3, NO, NO_2, H_2O.

The four SEP events occurred during 2005 (in January, May and September) were investigated looking for the O_x, HO_x, NO_y and ClO_y response. In spite of their somewhat weaker particle fluxes (if compared to the previous SEP events analysed in the past; Sect. 1.5), they have been able to produce intense variations in the mesospheric chemistry and minor in the stratospheric one.

The considered 2005 SEP events present different characteristics between each other. The SEP event of 17 January has the highest flux and fluence at 10 MeV, although it has a shorter duration than the longest one registered from 11 September (2.76 d and 4.81 d, respectively). Moreover, it has a minor content of very high energies relative to the January 20 SEP (it turned to be a clear GLE), where the rise of the three different energy ranges is also simultaneous. Finally, the 15 May SEP has the shortest duration (1.05 d), low content of high energies and the smallest particle fluence.

It is proved that SEP effects on the Earth's atmosphere are different on the night and day hemisphere at the high latitudes here investigated (75°-82°). Generally, the mesospheric ozone layer of high latitudes undergoes a large decrease during the night state, while the corresponding ozone decrease is weaker in the day state. Moreover, the ozone decrease lasts more during the winter time, with feeble solar light, than during the summer, when minor short depletions can be identified (see also DAM06).

The stratospheric ozone depletion of the day hemisphere is very light in January and September, whereas is about absent in May (nevertheless, more detailed analyses are needed to distinguish the SEP effects from the ozone variability induced by the polar vortex).

The identified changes in the ozone content are different during the diverse SEP events analysed. The presence of a tertiary ozone peak in the winter mesosphere makes it easier to single out its decrease linked to the HO_x rise. The destruction of the ozone peak is very clear on 18 January 2005 and the maximum percentage of destroyed O_3 varies from ~ 25 % (at ~ 55 km) to ~ 75 % (at ~ 70 km). The slightly darker condition of the Southern hemisphere favours the presence of a similar third ozone peak (even more intense) in May and its subsequent destruction during and after the solar particle event. The weak fluence of > 10 MeV particles leads to O_3 depletion (on 16 May) at ~ 60 km (10 %) that reaches 45 % at ~70 km. The ozone depletion in the summer hemisphere is negligible for both SEP events.

The higher solar illumination in September in the Southern hemisphere induces ozone depletion also in the stratosphere. The O_3 decrease on 10 September seems to start at ~ 40 km of altitude and becomes greater than ~ 20 % at ~ 45 km. It is connected with the NO_x rise, more active in the stratosphere. Anyway, the depletion in the mesosphere is not intense as for the 17 January SEP event. In fact the MLS instrument recorded a decrease of only ~ 40 % at 70 km (more intense above this height). Note also the stratospheric ozone decrease above 40 km in the day hemisphere on 10 and 11 September. Odd nitrogen species could cause ozone

depletion again.

The EOS MLS instrument on the AURA satellite recorded mesospheric OH (proxy for the odd hydrogen species) increases, related to SEP events, for the first time during the investigated periods. No HO_x data were available before 2005 SEP events in order to check the accuracy of models related to mesospheric ozone destruction triggered by HO_x components. As expected, the response of odd hydrogen species to solar particles is very fast, almost contemporary, either in the summer or winter hemisphere. The higher mesospheric OH values under solar illumination make it difficult to detect the rise due to solar protons since the background concentration of hydrogen species depends on H_2O concentration. On the contrary, reduced solar illumination makes it easier to observe atmospheric chemistry changes due to SEPs. Moreover, the OH changes are long lasting in the winter hemisphere with respect to the summer one (because of the shorter life under solar light of OH components) but the affected altitudes are similar. Thus, the opposite terrestrial season does not influence the possibility of odd hydrogen species to trigger catalytic cycles at specific altitudes, but only the percentage of variation and the duration. The sudden and intense OH enhancement, recorded by the MLS instrument evidences the goodness of available models (e.g., Verronen et al., 2006a).

The SEP event of 17 January has the most intense flux at > 10 MeV among the analysed 2005 SEP events, whereas the 20 January SEP is approximately similar to that of May and September 2005 at the considered energy range. Nevertheless, the mesospheric OH rise during September seems to reach an order of magnitude, similar to the one of 17 January event, probably because of the comparable particle fluence for both events. The OH increase due to the May SEP event is less intense, in this case it was registered a smaller particle fluence during the event. Moreover it seems to be limited only to the mesosphere because of a minor proton flux at high energies.

It was shown that even SEP events characterised by lower particle fluxes strongly affect the mesospheric chemistry at elevated latitudes, but their impact is different if night and day hemispheres are compared. Moreover, when different SEP events have comparable maximum flux values, the most relevant SEP feature is its particle fluence. In particular, the greater the fluence at E >10 MeV, the more important are the SEP effects. Furthermore, SEP events with low content of high energy particles result in a smaller perturbation of the lower atmospheric layers. Seasonal conditions are also essential to spread SEP influence on the stratosphere.

MLS instrument cannot measure atmospheric NO_x, but it is able to retrieve nitric acid, being it a good proxy for NO_y (reservoir nitrogen). During January 2005 SEPs,

together with the ozone depletion, appears the HNO_3 increase in the winter hemisphere produced by HO_x and/or NO_x rise (see SD07). The HNO_3 peak reaches ~ 7 ppbv on 21-22 January (more than ~ 3 ppbv of January 15 level). Anyway a pre-existent nitric acid rise seems to be present in the central weeks of December 2004 and January 2005 in the Northern winter hemisphere, probably connected to the NO_y production from the upper atmosphere (see De Zafra and Smyshlyaev, 2001). No HNO_3 rise was documented during the other investigated SEP events of 2005 (during the December 2006 SEP too).

Finally also some ClO_y components were investigated in the winter hemisphere during January 2005 SEP events. An important HCl decrease (~ 0.2-0.3 ppbv) was pointed out on 18 and 21 January at 1 and 3 hPa respectively, right after the two SEP events. HO_x rise caused HCl loss on 18 January. In addition, the stronger flux at higher energies during the 20 January SEP event has further decreased HCl values, already low (because of the 17 January SEP) and has extended the effects to lower altitudes. A contemporary OHCl rise (~ 0.2 ppbv) caused by the transformation of reactive atomic Cl (coming from HCl) in non reactive species via ClO (decreased more then 0.15 ppbv at ~1-2 hPa) and/or $ClONO_2$ at lower altitudes was documented in the same days.

In addition other interesting features connected to chemistry variability arise from the study of July 2000 SEP event. The HALOE instrument recorded O_3 decrease together with NO and NO_2 increases (roughly above 40 km) in the Northern hemisphere (“day state” of the high-latitude atmosphere). The NO climatology is about few ppbv in the winter mesosphere whereas exceeded 60 ppbv during the days after the SEP event. Further the stratospheric NO_2 was increased up to 2 ppbv at about 50 km whereas the pre event day was < 0.5 ppbv. An ozone depletion greater than 60 % of the pre-event level appeared at 60 km; this depletion is almost similar to the one measured by MLS AURA for the “night state” of the atmosphere (same altitude in both events), but it is completely different to the one measured in the “day state” (Southern high latitudes) during the January 2005 SEP, when it was almost absent. Even if we are trying to compare ozone values coming from different instruments and recorded on pretty different geographic areas, it is important to stress that July 2000 SEP maximum flux was at least six time higher than the one for January 2005 SEPs. Since it is hypothesized a strong atmospheric ionization and an increased number of molecules involved in the catalytic cycles of the ozone destruction for July 2000 (not so high the number of particles present in January 2005 SEPs), it should be conclude that also in the “day state” of the ozone layer the depletion can be observed. On the other hand, the “night state” seems to preserve

the effectiveness of catalytic cycles and also to prolong and increase their effects. The Sun's light is responsible for the fast destruction of NO_x molecules. Moreover, in the "day state" there is a prompt response of the atmospheric chemistry to SEPs, if compared with the one for the "night state". During July 2000 SEP the induced effects on the atmospheric components do not appear below 40 km (the weak variations are probably caused by the latitudinal effects arising from the temporal variation of the satellite latitudes).

On the contrary, for January 2005 winter season it is possible to detect a second maximum in the ozone decrease in the ~ 45-35 km range. Reasons for this behaviour can be two; one should be connected to the atmospheric dynamics and the other to the atmospheric chemistry.

The atmospheric transport is generally upwards during summer season and the enhanced odd nitrogen cannot go down toward the lower stratosphere where the catalytic effects could be increased (Lary, 1997). Nevertheless, at the polar winter season we have the opposite: the atmospheric transport is generally downwards and the enhanced odd nitrogen, created by the first SEP event, can go down. In this case, it is possible to observe an odd nitrogen enhancement due to the superposition of two SEP effects (the same mechanism is involved in the strong HCl decrease recorded after the second SEP event of January 2005).

Moreover, the greater stability of the winter polar vortex prevents enriched NO_x air from going away and the catalytic cycle of ozone destruction can be at work.

The ozone depletion recorded in the winter lower altitudes during the days after the SEPs could arise from the long-lasting effectiveness of the catalytic cycles involving NO_x (and/or ClO_x) under night state.

Chemical variability was here pointed out also during minor SEP events i.e., April 2002 and December 2006. From results here presented, it is possible to highlight the ozone depletion (over 40 % at 60 km) and the odd nitrogen rise (mesospheric NO values reached ~ 20 ppbv whereas the pre event day was few ppbv) at high and low altitudes for April 2002 SEP (occurring in a midway condition of light and/or dynamics). Despite of April 2002 SEP was certainly weaker, when compared with July 2000 and also 17 January 2005 SEP (see Table 1.1), the ozone depletion is long-lasting after the SEP start (four days, but not more intense than for the other events).

Even if of minor intensity the pair SEP/GLE of December 2006 is similar to the January 2005 ones and it was interesting to make some comparisons. The SEP of 7 December was able to destroy the third ozone peak in the polar winter mesosphere but no appreciable variability was recorded in the polar summer hemisphere. The

GLE event of 13 December influenced lightly the mesosphere but seems to able to affect the stratospheric ozone at about 40 km. This behaviour could confirm the results found analysing January 2005 SEP events.

Finally, it is necessary to mention the 29 May 2003 SEP event, since a contemporary elevate NO concentration was recorded in the upper stratosphere at the boundary of the southern polar cap region; some researchers supposed a relationship among the two phenomena. Anyway that linkage seems to be improbable because of the poor associated SEP flux and because the NO rise appears to start in the mesosphere before the beginning of the SEP event.

Chapter 6

CONCLUSIONS

The possibility to compare chemical atmospheric data, acquired during SEP events, with the available theoretical models gave us the opportunity to check the accuracy of a large part of the reactions expected to work in the chemistry of the middle/upper stratosphere and the mesosphere.

The sudden increase of HO_x and NO_x species in the polar atmosphere occurring during such phenomena triggers a large number of chemical pathways, which can be carefully monitored. Therefore, it is possible to attend reactions that change the chemical composition of the atmosphere in few days, whereas they take usually a long time to develop.

Besides the possibility to better define the natural variability of the minor atmospheric components also in the upper atmosphere is a further important advantage arising from the present study.

In order to obtain a good time (approximately the current solar cycle), latitudinal (polar cap regions) and chemical species (O_x, HO_x, NO_y and ClO_y) coverage, data from different instruments have been utilized.

The classic solar occultation instrument allowed to investigate the response of nitrogen components and ozone in the “day” hemisphere during and after the SEP events of July 2000, April 2002, and May 2003 and these analyses have basically confirmed past results.

In addition, the real novelty of this study is the employment of the limb sounder

instrument to monitor the chemical variability associated to the solar energetic particle incoming in the terrestrial environment. Particularly, the MLS of the EOS AURA satellite has been able to measure chemical components in the “night” and “day” hemispheres, because of its polar orbit and thermal emission technique. In this way the behaviour of HO_x family, only foresaw by models until today (i.e., Reid et al. 1991 and Krivolutsky et al. 2005), has been carefully illustrated for the first time during the SEP events of 2005 (January, May and September) and 2006 (December).

Mesospheric chemical variability has mainly been investigated in this work because of the energies involved in 2005 and 2006 SEP events, even if interesting features were pointed out also in the stratospheric environment.

Further, past results have been reanalyzed in the light of the new ones and fascinating comparison among different events has been done. *It was possible to definitively highlight most intense mesospheric changes in the “night” hemisphere than in the “day” one* (being lower the background values of the chemical components there). In this way, it was easier to demonstrate the abrupt HO_x rise after the SEP events and the chemical pathways involving other species. We remark:

- The increase of OH values, starting almost at the same time in the two hemispheres, is long lasting in the “night” one, because of the negligible UV photolysis at work.

- The mesospheric OH peak at night, induced by solar proton events, is almost of the same order of magnitude as the OH values in the day hemisphere.

- The destruction of the third ozone peak in the polar latitudes by the HO_x rise has been recorded in all the considered events during the winter state of each hemisphere.

- Also solar particles peaking at ~ 2000 particles/cm^2·s·sr (at > 10 MeV) are absolutely able to influence at least the mesosphere and its effects can be further increased by elevate fluence.

- About 10 particles/cm^2·s·sr (at > 10 MeV) seems to be enough to trigger the increase of OH radicals in the night hemisphere.

Even if the main part of the effects connected to the hydrogen species rise occurs in the upper/middle atmosphere, many chemical changes happen also in the stratosphere. The destruction of stratospheric ozone after the SEPs of 2005 and 2006 was not very intense principally because the solar energetic particles flux was not so strong (at the energies reaching the lower atmosphere) as in the past events analyzed by other researchers (i.e., October 1989, July 2000 and October 2003).

Further, the fast photolysis processes in the “day” hemisphere is producing the rapid destruction of the NO_x species added by the induced effects of SEPs, and

preventing the start of the catalytic cycles for the ozone depletion. Instead, in the “night” Polar Regions the lack of atoms of oxygen prevented the evolution of the same cycles. Nevertheless, feeble processes of O_3 depletion can not be excluded and they could arise also from ClO_x variability. In fact at least during January 2005 an important HCl decrease and a contemporary OHCl rise (caused by the transformation of reactive atomic Cl in no-reactive species via ClO) was also documented just after the two SEP events.

Finally, it is necessary to emphasize that the performed work showed the relevance of interdisciplinary studies for a better understanding of the Atmosphere, especially in the Polar Regions. The exclusion of Solar-Terrestrial Relations from the terrestrial atmospheric chemistry could bring to some misleading conclusions and incomplete theoretical models. It is expected that this thesis is only a step for further work, aiming to improve the knowledge on the topic.

REFERENCES

Adriani A., Fiocco G., Gobbi G. P., and Congeduti F., Correlated behavior of the aerosol and ozone contents of the stratosphere after El Chichon eruption, J. Geophys. Res., 92 (D7), 8365-8372, 1987.

Baldwin M. P., Gray L.J., Dunkerton T.J. et al., The Quasi-Biennial Oscillation, Reviews of Geophysics, 39 (2), 179–229, 2001.

Barth C.A., Baker D.N., Manko K.D., Bailey S.M., The northern auroral region as observed in nitric oxide, Geophys. Res. Lett., 28 (8), 1463-1466, 2001.

Bates D.R. and Nicolet M., The photochemistry of the atmospheric water vapor, J. Geophys. Res., 55, 301, 1950.

Brasseur, G. P. and Solomon, S., Aeronomy of the Middle Atmosphere, Springer, Dordrecht, 3rd revised and enlarged edn., 2005.

Callis L.B., Boughner R.E., Baker D.N. et al., Precipitating electrons: Evidence for effect on mesospheric odd nitrogen, Geophys. Res. Lett., 23 (15), 1901-04, 1996.

Canty T., Pickett H. M., Salawitch R. J., Jucks K. W., Traub W. A. and Waters J. W., Stratospheric and mesospheric HOx: Results from Aura MLS and FIRS-2, Geophys. Res. Lett., 33, L12802, doi:10.1029/2006GL025964, 2006.

Chandra S., The solar UV related changes in total ozone from a solar rotation to a solar cycle, Geophys. Res. Lett., 18, 837–840, 1991.

Chapman S., A theory of upper atmospheric ozone, Mem. Royal Meteorological Society, 3, 103-125, 1930.

Clilverd M. A., Seppälä A., Rodger C. J., Verronen P. T., and Thomson N. R., Ionospheric evidence of thermosphere-to-stratosphere descent of polar NOX, Geophys. Res. Lett., 33, L19811, doi:10.1029/2006GL026727, 2006.

Cowley S.W.H., in From the Sun: Auroras, Magnetic Storms, Solar Flares, and Cosmic Rays, ed. S. T. Suess & B. T. Tsurutani (Washington, DC: AGU), 103, 1998.

Crutzen P.J., Ozone Production Rates in an Oxigen-Hydrogen-Nitrogen Oxide Atmosphere, Journal of Geophys. Res., 76 (30), 7311-7327, 1971.

Crutzen P. J., Isaksen I. S. A., and Reid G. C., Solar proton events: Stratospheric sources of nitric oxide, Science, 189, 457-458, 1975.

Crutzen P.J., Mesospheric Mysteries, Science, 277, 1951-1952, 1997.

Damiani A., Diego P., Laurenza M, Storini M., Rafanelli C., Search for the ozone variability related to SEP events during the current solar cycle, Adv. in Space Res., (submitted), Ms. Ref. No.: C21-0038-06.

Damiani A., Storini M., Laurenza M., Rafanelli C., Piervitali E. and Cordaro E.G., Southern ozone variations induced by solar particle events during 15 January–5 February 2005, JASTP, 68, 2042–2052, 2006.

Damiani A., Storini M., Laurenza M., Rafanelli C.: Solar Particle Effects on minor components of the Polar Atmosphere, Annales Geophysicae, 2007a (in press).

Damiani A., Storini M., Laurenza M., Rafanelli C., Piervitali E. and Cordaro E.G., Erratum to “Southern ozone variations induced by solar particle events during 15 January–5 February 2005”, JASTP, 69, 628–630, 2007b.

Degenstein D. A., Gattinger R. L., Lloyd N. D. et al., Observations of an extended mesospheric tertiary ozone peak, JASTP, 67, 1395-1402, 2005a.

Degenstein D.A., Lloyd N.D., Bourassa A.E. et al., Observations of mesospheric ozone depletion during the October 28, 2003 solar proton event by OSIRIS, Geophys. Res. Lett., 32, L03S11, doi:10.10129/2004GL021521, 2005b.

Dessler A.E., M.D. Burrage, J.-U. Grooss, J.R. Holton, J.L. Lean, S.T. Massie, M.R. Schoeberl, A.R. Douglass, and C.H. Jackman, Selected science highlights from the first five years of the Upper Atmosphere Research Satellite (UARS) program, Reviews of Geophysics, 36, 183-210, 1998.

De Zafra R. and Smyshlyaev S.P., On the formation of HNO3 in the Antarctic mid to upper stratosphere in winter, Journal of Geophys. Res., 106 (D19), 23.115-23.125, 2001.

Duldig M.L., Australian Cosmic Ray Modulation Research, Publications of the Astronomical Society of Australia, arXiv:astro-ph/0010147v1, 2001.

Evans W.F.J. and Llewellyn E.J., Measurements of mesospheric ozone from observations of the 1.27-micron band (Mesospheric ozone measurement for altitude profiles, comparing rocket and ground based observations of 1.27 micron emission band at twilight), Radio Science, 7, 45-50,1972.

Farman J.C., Gardiner B.G., Shanklin J.D., Large losses of total ozone in Antarctica reveal seasonal CLOx/NOx interaction, Nature, 315, 207-210, 1985.

Fadel Kh., Vashenyuk E.V., Kirillov A.S., Ozone depletion in the middle atmosphere during solar proton events in October 2003, Adv. Space Res., 38, 1881-1886, 2006.

Ferguson, E.E., Fehsenfeld, F.C. and Albritton, D.L. in Bowers, M.T. (ed.), Gas phase ion chemistry, 1, Academy Press, NY, 1979.

Forbush S. E., Three Unusual Cosmic-Ray Increases Possibly Due to Charged Particles from the Sun, Phys. Rev., 70, 771, 1946.

Forbush S.E., On the Effects in Cosmic-Ray Intensity Observed During a Recent Magnetic Storm, Phys. Rev., 51, 1108-1109, 1937.

Forbush S.E., World-Wide Cosmic Rays Variations, 1937-1952, J. Geophys. Res., 59, 525-542, 1954.

Foukal P., in From the Sun: Auroras, Magnetic Storms, Solar Flares, and Cosmic Rays, ed. S. T. Suess & B. T. Tsurutani (Washington, DC: AGU), 103, 1998.

Froidevaux, L., Livesey, N.J., Read, W.G. et al., Early Validation Analyses of Atmospheric Profiles From EOS MLS on the Aura Satellite, IEEE TGARS, 44 (5), 1106-1121, 2006.

Hauchecorne A., Bertaux J.-L., Lallement R., Impact of Solar Activity on Stratospheric Ozone and NO2 Observed by Gomos/Envisat, Space Science Reviews, 125 (1-4), 393-402, 2006.

Heath, D.F., Krueger, A.J., Crutzen, P.J. Solar proton event: influence on stratospheric ozone, Science, 1987, 886-889, 1977.

Hervig M., Mchugh M., Summers M., Water vapour enhancement in the polar summer mesosphere and its relationship to polar mesospheric clouds, Geophys. Res. Lett., 30 (20), ASC5.1-ASC5.5, 2003.

Hessler V.P., Polar Ionospheric Reaseach, Arctic, 22 (3), 200-213, 1969

Jackman C.H., Douglass A.R., Rood R.B., McPeters R.D., and Meade P.E., Effect of solar proton events on the middle atmosphere during the past two solar cycles as computed using a two-dimensional model, J. Geophys. Res., 95, 7417-7428, 1990.

Jackman C.H., Cerniglia M.C., Nielsen J.E., et al., Two-dimensional and three-dimensional model simulations, measurements, and interpretation of the October 1989 solar proton events on the middle atmosphere, J. Geophys. Res., 100, 11641–11660, 1995.

Jackman C.H., Fleming E.L., Vitt F.M., and Considine D.B., The influence of solar proton events on the ozone layer, Adv. Space Res., 24 (5), 625-630, 1999.

Jackman C.H., McPeters R.D., Labow G.J., et al., Northern Hemisphere atmospheric effects due to the July 2000 solar proton event, Geophys. Res. Lett., 28, 2883-2886, 2001.

Jackman C.H. and McPeters R.D., The effect of solar proton events on ozone and other constituents. In: Pap, J.M. and Fox, P. (Eds.), Solar Variability and its Effects on Climate, AGU, Washington DC, Geophysical Monograph Series, 141, 305-319, 2004.

Jackman C. H., DeLand M.T., Labow G.J., et al., Neutral atmospheric influences of the solar proton events in October–November 2003, J. Geophys. Res., 110, A09S27, doi:10.1029/2004JA010888, 2005.

Johnson C.Y., Ionospheric composition and density from 90 to 1200 kilometers at solar minimum, J. Geophys. Res., 71, 330-332, 1966.

Johnson F.S., ed. 1965, Satellite environment handbook, 2nd Ed. Stanford, Stanford University Press., 193, 1965.

Krivolutsky A.A., History of cosmic ray influence on ozone layer-key steps, Adv. Space Res., 31(9), 2127-2138, 2003.

Krivolutsky A.A., Kuminov A., Vyushkova T., Ionization of the atmosphere caused by solar protons and its influence on ozonosphere of the Earth during 1994-2003, JASTP, 67, 105-117, 2005.

Krivolutsky A.A., Klyuchnikova A.V., Zakharov G..R., et al.: Dynamical response of the middle atmosphere to solar proton event of July 2000: Three-dimensional model simulations, Adv. Space Res., 37, 1602-1613, 2006.

Kudela K. and Langer R., Ground Level Events Recorded at Lomnicky Stit Neutron Monitor, Proceeding of 30th International Cosmic Ray conference, 2007.

Lary D.J., Catalytic destruction of stratospheric ozone, J. Geophys. Res., 102, 21515-21526, 1997.

Laurenza M., Hewitt J., Storini M., et. al., Solar energetic proton events and soft X-ray flares, Proceeding ECRS2006, 2007 (in press).

Livesey N. J., Read W. G., Filipiak M. J. et al., Earth Observing System (EOS) Microwave Limb Sounder (MLS) Version 1.5 Level 2 data quality and description document, JPL D-

32381, Version 1.51, Jet Propulsion Laboratory, California Institute of Technology, Pasadena, California, 2005.

López-Puertas M., Funke B., Gil-López S., et al., Observation of NO_x enhancement and ozone depletion in the Northern and Southern Hemispheres after the October–November 2003 solar proton events, J. Geophys. Res., 110, A09S43, doi:10.1029/2005JA011050, 2005a.

López-Puertas M., Funke B., Gil-López S., et al., HNO_3, N_2O_5, and $ClONO_2$ enhancements after the October–November 2003 solar proton events, J. Geophys. Res., 110, A09S44, doi:10.1029/2005JA011051, 2005b.

Maeda K. and Heath D.F., Stratospheric ozone response to a solar proton event: Hemispheric asymmetries, PAGEOPH, 119, 1-8, 1980.

Marsh D., Smith A., Brasseur G. et al., The existence of a tertiary ozone maximum in the high-latitude middle mesosphere, Geophys. Res. Lett., 28, 4531-4534, 2001.

Marsh D. R., Skinner W. R., Marshall A. R., Hays P. B., Ortland D. A., and Yee J.-H., High Resolution Doppler Imager observations of ozone in the mesosphere and lower thermosphere, J. Geophys. Res., 107(D19), 4390, doi:10.1029/2001JD001505, 2002.

Marsh D., Smith A., Noble E., Mesospheric ozone response to changes in water vapor, J. Geophys. Res., 108 (D3), 4109, doi: 10.1029/2002JD002705, 2003.

McEwan M.J. and Phillips L.F., Chemistry of the atmosphere, Edward Arnold, London, 1975.

McPeters R.D., Jackman C.H., Stassinopoulos E.G., Observations of ozone depletion associated with solar proton events, J. Geophys. Res., 86, 12071-12081, 1981.

Molina M.J. and Rowland F.S., Stratospheric Sink for Chlorofluoromethanes: Chlorine Atom-Catalysed Destruction of Ozone, Nature, 249, 810-814, 1974.

Mursula K. and Usoskin I., Heliospheric Physics and Cosmic Rays, Lecture notes Fall term 2003 University of Oulu, 2003.

Nevison C.D., Solomon S, Russell III J.M., Nighttime formation of N_2O_5 inferred from the Halogen Occultation Experiment sunset/sunrise NO_x ratios, J. Gophys. Res., 101 (D3), 6741-6748, 1996.

Nicolet M., On the production of nitric oxide by cosmic rays in the mesosphere and stratosphere, Planet. Space Sci., 23 (4), 637–649, 1975.

Orsolini Y. J., Manney G. L., Santee M. L., Randall C. E., An upper stratospheric layer of enhanced HNO3 following exceptional solar storms, Geophys. Res. Lett., 32, L12S01, doi:10.1029/2004GL021588, 2005.

Pickett H. M., Drouin B. J., Canty T. et al., Validation of Aura MLS HOx measurements with remote-sensing balloon instruments, Geophys. Res. Lett., 33, L01808, doi: 10.1029/2005GL024442, 2006.

Pickett H.M., Microwave Limb Sounder THz Module on Aura, IEEE TGARS, 44 (5), 1122-1130, 2006.

Porter H.S., Jackman C.H., Green A.E.S., Efficiencies for production of atomic nitrogen and oxygen by relativistic proton impact in air, J. Chem. Phys., 65 (1), 154-167, 1976.

Randall C. E., Harvey V. L., Singleton C. S., et al., Enhanced NOx in 2006 linked to strong upper stratospheric Arctic vortex, Geophys. Res. Lett., 33, L18811, doi: 10.1029/2006GL027160, 2006.

Randall C. E., Harvey V. L., Singleton C. S., et al., Energetic particle precipitation effects on the Southern Hemisphere stratosphere in 1992–2005, J. Geophys. Res., 112, D08308, doi:10.1029/2006JD007696, 2007.

Reames D.V., Particle acceleration at the sun and in the heliosphere, Space Science Revs., 90 (413), 1-76, 1999.

Reagan J.B., Meyerott R.E., Nightingale R.W. et al., Effects of the August 1972 solar particle events on stratospheric ozone, J. Geophys. Res., 86, 1473-1494, 1981.

Reid G.C., Solar energetic particles and their effects on the terrestrial environment, in STURROCK, PA, HOLZER, TE, MIHALAS, DM and ULRICH, R.K. (eds.), Physics of the Sun, D. Reidel Publishing Company, Dordrecht, 1986.

Reid G. C., Solomon S., and Garcia R. R., Response of the middle atmosphere to the solar proton events of August-December, 1989, Geophys. Res. Lett., 18 , 1019–1022, 1991.

Rohen G., von Savigny C., Sinnhuber M., et al., Ozone depletion during the solar proton events of October/November 2003 as seen by SCIAMACHY, J. Geophys. Res. 110, A09S39, doi:10.1029/2004JA010984, 2005.

Rusch D.W., Gérard J.-C., Solomon S., Crutzen P.J. and Reid G.C., The effect of particle precipitation events on the neutral and ion chemistry of the middle atmosphere, 1, Odd nitrogen, Planet. Space Sci., 29, 767-774, 1981.

Russell J. M. III, Gordley L. L., Park J. H. et al,. The Halogen Occultation Experiment, J. Geophys. Res., 98 (D6), 10, 777-797, 1993.

Schoeberl M.R., Douglass A.R., Hilsenrath E. et al., Overview of the EOS aura mission, IEEE TGARS, 44 (5), 1066-1074, 2006.

Seele C. and Hartogh P., Water vapor of the polar middle atmosphere: Annual variation and summer mesosphere conditions as observed by ground-based microwave spectroscopy, Geophys. Res. Lett., 26 (11), 1517-1520, 1999.

Seppälä A., Verronen P.T., Kyrölä E., et al., Solar proton events of October-November 2003: Ozone depletion in the Northern Hemisphere polar winter as seen by GOMOS/Envisat, Geophys. Res. Lett., 31, L19107, doi:10.1029/2004GL021042, 2004.

Seppälä A., Verronen P.T., Sofieva V. F. et al., Destruction of the tertiary ozone maximum during a solar proton event, Geophys. Res. Lett., 33, L07804, doi: 10.1029/2005 GL025571, 2006.

Smith A. and Marsh D, Processes that account for the ozone maximum at the mesopause, J. Geophys. Res., 110, D23305, doi: 10.1029/2005JD006298, 2005.

Solomon S.C., Barth C. A., Bailey S.M., Auroral production of nitric oxide measured by the SNOE satellite, Geophys. Res. Lett., 26 (9), 1259–1262, 1999

Solomon S., Rusch D.V., Gérard J.-C. et al., The effect of particle precipitation events on the neutral and ion chemistry of the middle atmosphere: II odd hydrogen, Planet. Space Sci., 29, 885-892, 1981a.

Solomon S., Crutzen P.J., Analysis of the August 1972 solar proton event including chlorine chemistry, J. Geophys. Res., 86, 1140-1146, 1981b.

Solomon S., Crutzen P.J., Roble R.G., Photochemical Coupling Between the Thermosphere and the Lower Atmosphere 1. Odd Nitrogen From 50 to 120 km, J. Geophys. Res., 87 (C9), 7206-7220, 1982a

Solomon S., Reid G.C., Roble R.G., Crutzen P.J., Photochemical Coupling Between the Thermosphere and the Lower Atmosphere 2. D Region Ion Chemistry and the Winter Anomaly, J. Geophys. Res., 87 (C9), 7221-7227, 1982b.

Solomon S., Reid G.C., Rusch D.W., Thomas R.J., Mesospheric ozone depletion during the solar proton event of July 13, 1982, 2, Comparison between theory and measurements, Geophys. Res. Lett., 10, 257-260, 1983.

Solomon S., Stratospheric ozone depletion a review of concepts and history, Review of Geophysics, 37 (3), 275-316, 1999.

Sonnemann G.R., Grygalashvyly M., Hartogh P., et al., Behavior of mesospheric ozone under polar night condition, Adv. Space Res., 38, 2402-2407, 2006.

Storini M., Kudela K., Cordaro E.G., Massetti S., Ground-level enhancement during solar cycle 23: results from SVIRCO, LOMNICKY STIT and LARC neutron monitors, Adv. Space Res., 35, 416-420, 2005.

Storini M., Damiani A., Effects of the January 2005 GLE/SEP Events on Minor Atmospheric Components", Proceedings 30th International Cosmic Ray Conference, 2007.

Stolarsky R. and Cicerone R. J., Stratospheric Chlorine - Possible Sink for Ozone, Can. J. Chem., 52 (8), 1610–1615, 1974.

Thrush B.A., The chemistry of the stratosphere, Rep. Prog. Phys., 51, 1341-1371, 1988.

Verronen P.T., Seppälä A., Clilverd M.A. et al., Diurnal variation of ozone depletion during the October–November 2003 solar proton events, J. Geophys. Res. 110, A09S32, doi:10.1029/2004JA010932, 2005.

Verronen P.T., Seppälä A., Kyrölä E. et. al., Production of odd hydrogen in the mesosphere during the January 2005 solar proton event, Geophys. Res. Lett., 33, L24811, doi:10.1029/2006GL028115, 2006a.

Verronen P.T., Ionosphere-atmosphere interaction during solar proton events, Phd Thesis, 2006b.

Vitt F. M., and C. H. Jackman, A comparison of sources of odd nitrogen production from 1974 through 1993 in the Earth's middle atmosphere as calculated using a twodimensional model, J. Geophys. Res., 101, 6729-6739, 1996.

von Clarmann T., Glatthor N., Höpfner M., et al., Experimental evidence of perturbed odd hydrogen and chlorine chemistry after the October 2003 solar proton events, J. Geophys. Res., 110, A09S45, doi:10.1029/2005JA011053, 2005.

Waters J. W., Froidevaux L., Harwood R. S. et al., The Earth Observing System Microwave Limb Sounder (EOS MLS) on the Aura satellite, IEEE TGARS, 44, 1075-1092, 2006.

Wayne R.P., Chemistry of the Atmospheres (Third Edition), Oxford University Press, 2000.

Weeks L.H., CuiKay R.S., Corbin J.R., Ozone measurements in the mesosphere during the solar proton event of November 2, 1969, J. Atm. Sci., 29, 1138-1142, 1972.

Zeller E.J., Dreschhoff G.A.M., Laird C.M., Nitrate flux on the Ross Ice Shelf, Antarctica and its relation to solar cosmic rays, Geophys. Res. Lett., 13, 1264-1267, 1986.

APPENDIX

Tab.1 - GLE LIST (source : Bartol Reseach Institute, http://neutronm.bartol.udel.edu/)

EVENT #	EVENT DATE	BASELINE DATE (YYMMDD)	RECOMMENDED BASELINE TIME START - END (UT)	
001	28 February 1942	420228		
002	07 March 1942	420307		
003	25 July 1946	460725		
004	19 November 1949	491119		
005	23 February 1956	560223	020000 - 030000	
006	31 August 1956	560831	110000 - 120000	
007	17 July 1959	590716	220000 - 240000	(-1)
008	04 May 1960	600504	090000 - 100000	
009	03 September 1960	600902	230000 - 240000	(-1)
010	12 November 1960	601112	120000 - 130000	
011	15 November 1960	601115	010000 - 020000	
012	20 November 1960	601120	190000 - 200000	
013	18 July 1961	610718	090000 - 100000	
014	20 July 1961	610720	150000 - 160000	
015	07 July 1966	660706	230000 - 240000	(-1)
016	28 January 1967	670128	010000 - 020000	
017	28 January 1967	670128	060000 - 070000	
018	29 September 1968	680929	150000 - 160000	
019	18 November 1968	681118	090000 - 100000	
020	25 February 1969	690225	080000 - 090000	
021	30 March 1969	690330	020000 - 030000	
022	24 January 1971	710124	220000 - 230000	
023	01 September 1971	710901	180000 - 190000	
024	04 August 1972	720804	110000 - 120000	
025	07 August 1972	720807	140000 - 150000	
026	29 April 1973	730429	200000 - 210000	
027	30 April 1976	760430	200000 - 210000	
028	19 September 1977	770919	090000 - 100000	
029	24 September 1977	770924	050000 - 060000	
030	22 November 1977	771122	090000 - 100000	
031	07 May 1978	780507	020000 - 030000	
032	23 September 1978	780923	090000 - 100000	
033	21 August 1979	790821	050000 - 060000	
034	10 April 1981	810410	150000 - 160000	
035	10 May 1981	810510	060000 - 070000	
036	12 October 1981	811012	050000 - 060000	
037	26 November 1982	821126	020000 - 030000	
038	07 December 1982	821207	220000 - 230000	
039	16 February 1984	840216	080000 - 090000	
040	25 July 1989	890725	070000 - 080000	
041	16 August 1989	890815	230000 - 240000	(-1)
042	29 September 1989	890929	100000 - 110000	
043	19 October 1989	891019	110000 - 120000	
044	22 October 1989	891022	160000 - 170000	
045	24 October 1989	891024	160000 - 170000	
046	15 November 1989	891115	050000 - 060000	
047	21 May 1990	900521	210000 - 220000	
048	24 May 1990	900524	190000 - 200000	
049	26 May 1990	900526	190000 - 200000	
050	28 May 1990	900528	030000 - 040000	
051	11 June 1991	910611	000000 - 010000	
052	15 June 1991	910615	070000 - 080000	
053	25 June 1992	920625	180000 - 190000	
054	02 November 1992	921102	020000 - 030000	
055	06 November 1997	971106	110000 - 120000	
056	02 May 1998	980502	110000 - 120000	
057	06 May 1998	980506	070000 - 080000	
058	24 August 1998	980824	190000 - 200000	
059	14 July 2000	000714	090000 - 100000	
060	15 April 2001	010415	110000 - 120000	
061	18 April 2001	010418	010000 - 020000	
062	04 November 2001	011104	150000 - 160000	
063	26 December 2001	011226	040000 - 050000	
064	24 August 2002	020824	010000 - 020000	
065	28 October 2003	031028	100000 - 110000	
066	29 October 2003	031029	190000 - 200000	

067	02 November	2003	031102	160000	-	170000
068	17 January	2005	050117	090000	-	100000
069	20 January	2005	050120	053000	-	063000
070	13 December	2006	061213	010000	-	020000